DISSERTATION

EROSION DYNAMICS OF A STEPWISE SMALL DAM REMOVAL, BREWSTER CREEK DAM NEAR ST. CHARLES, ILLINOIS

Submitted by

Timothy D. Straub

Civil and Environmental Engineering Department

In partial fulfillment of the requirements

For the Degree of Doctor of Philosophy

Colorado State University

Fort Collins, Colorado

Summer 2007

COLORADO STATE UNIVERSITY

June 22, 2007

WE HEREBY RECOMMEND THAT THE DISSERTATION PREPARED UNDER OUR SUPERVISION BY TIMOTHY D. STRAUB ENTITLED EROSION DYNAMICS OF A STEPWISE SMALL DAM REMOVAL, BREWSTER CREEK DAM NEAR ST. CHARLES, ILLINOIS BE ACCEPTED AS FULFILLING IN PART REQUIREMENTS FOR THE DEGREE OF DOCTOR OF PHILOSOPHY.

Committee on Graduate Work

Dr. Brian P. Bledsoe

Dr. Robert R. Holmes

Dr. Pierre Y. Julien

Dr. Ellen E. Wohl

Dr. Chester C. Watson (Adviser)

Dr. Luis Garcia (Department Head)

ABSTRACT OF DISSERTATION

EROSION DYNAMICS OF A STEPWISE SMALL DAM REMOVAL, BREWSTER CREEK DAM NEAR ST. CHARLES, ILLINOIS

A stepwise dam-removal project, consisting of cutting five 12- to 18-in. notches in the dam, was completed from June 2003 through February 2004. The study area included Willow Lake on Brewster Creek near St. Charles, Illinois. The dam was 8-ft high and had a 30-ft wide crest. In 2002, the lake had a surface area of 3.96 acres and had filled with sediment to an average water depth of less than 1 ft, sediment volume equaling 14.47 acre-ft, and average sediment thickness of 3.7 ft. The deposited sediments consisted of 67 to 99 percent silts and clays. The stream channel downstream of the dam consisted primarily of sand, gravel, and cobble.

The total sediment eroded during and after dam removal was approximately 13 percent of the lake sediment. The downstream normalized sediment yield (sediment yield divided by the mean-daily flow) during the notchings and the first 7 months after the notchings (June 15, 2003, through September 30, 2004) was 14 tons/mi^2-yr-ft^3/s. From October 1, 2004, through September 30, 2006, the downstream normalized sediment yield (6.5 tons/mi^2-yr-ft^3/s) was within 17 percent of the upstream normalized sediment yield (5.4 tons/mi^2-yr-ft^3/s).

During and after dam removal, a knickpoint established and developed upstream of the dam. A flow model was applied to determine the shear stress acting upon the

knickpoint for five surveyed conditions. The maximum knickpoint shear stress for each condition was always a result of flow between 50 ft^3/s and the 1.5-yr streamflow (139 ft^3/s). The backwater effects caused by the remnant abutments and embankments limited the shear stresses acting on the knickpoints for the two higher streamflows modeled (10- and 100-yr streamflows, 477 ft^3/s and 920 ft^3/s, respectively). Empirical equations were determined to relate the knickpoint shear stress with eroded sediment for sixteen storms from November 2003 through February 2005.

A Cohesive Knickpoint Parallel Retreat method was developed utilizing the erosion-rate equation determined in this research from the cohesive-erosion laboratory testing results. The method was applied to the Brewster Creek study and predicted the eroded volume, knickpoint height, and migration length within 17, 20, and 6 percent, respectively, of measured values.

Timothy D. Straub
Civil and Environmental Engineering Department
Colorado State University
Fort Collins, CO 80523
Summer 2007

ACKNOWLEDGMENTS

Bruce Yurdin, Scott Ristau, Amy Walkenbach (of the IEPA), Tim Harbaugh, Karen Kosky (of the KCDEM), and Holly Hudson (of the NIPC) supported the format of this study and use of advanced methodologies. Overall project funding for the research, feasibility study, and actual dam removal was from the following agencies and programs: the USEPA Nonpoint Source Water Pollution Control Program; the IDNR, C2000 Ecosystems Project; the Kane County Riverboat Grant Fund; the USFWS; the YWCA of Elgin; and the USGS. IDNR-OWR completed an initial conditions cross-sectional survey of the lake and stream channel upstream and downstream of the dam. Steve Pescitelli (of the IDNR) led the monitoring of stream fisheries, Jeff Mengler (of the USFWS) monitored and analyzed the vegetation, and Roger Klocek (of the SAC) led an initial conditions mussel survey. Technical assistance was provided by the following USGS employees and volunteers: Don Roseboom, Gary Johnson, Dave Schrader, Elizabeth Murphy, Christopher Hamblen, Jay Angel, Shawn Cutshaw, Tom Wicker, King Kwok, Dave Straub, and Angel Martin. Brett Jordan (of CSU) assisted in flume and torvane testing, analysis, and summary writing. IDOT completed Erosion Function Apparatus and soil properties testing. Final editing and formatting of the report were completed by Gloria Garza (of CSU). Dr. Chester Watson (of CSU) advised in overall project research. Technical reviews were completed by Dr. Pierre Julien, Dr. Brian Bledsoe, Dr. Ellen Wohl (of CSU), and Dr. Robert Holmes (of the USGS).

TABLE OF CONTENTS

ABSTRACT OF DISSERTATION ..... **iii**

ACKNOWLEDGMENTS ..... **v**

LIST OF FIGURES ..... **ix**

LIST OF TABLES ..... **xv**

LIST OF SYMBOLS, UNITS, AND ABBREVIATIONS ..... **xx**

CHAPTER 1 INTRODUCTION **1**

1.1 Objective and Scope 4

1.2 Description of the Study Area and Watershed 4

CHAPTER 2 LITERATURE REVIEW **15**

2.1 Dam Removal 15

2.1.1 Geomorphic Response 20

2.1.2 Ecological Response 26

2.2 Knickpoint Theory and Laboratory Studies 27

2.3 Knickpoint and Cohesive Erosion Field Studies 31

2.4 Cohesive Erosion Laboratory Tests and Modeling 32

CHAPTER 3 METHODS OF INVESTIGATION **34**

3.1 Streamflow, Sediment, and Channel Geometry Data 35

3.2 Cohesive-erosion Laboratory Testing 39

3.2.1 Erosion Function Apparatus 41

3.2.2 Flume and Torvane 43

CHAPTER 4 EROSION DYNAMICS OF A STEPWISE SMALL DAM REMOVAL.....45

4.1 Sediment Erosion 45

4.2 Stream-channel Evolution 53

4.2.1 Knickpoint Shear Calculations 65

4.2.2 Knickpoint Shear Stress and Sediment Erosion Relation 68

4.2.3 Cohesive-erosion Testing Results 72

4.2.4 Knickpoint Migration Method 85

4.2.5 Notching Assessment 90

4.3 Stream-channel Stability 94

4.3.1 Streambed 97

4.3.2 Streambank 107

CHAPTER 5 SUMMARY, CONCLUSIONS, AND RECOMMENDATIONS.....112

5.1 Summary and Conclusions 112

5.2 Recommended Analytical Techniques for Dam-removal Assessment 114

5.2.1 Step 1 – Determine the amount of deposited sediment and estimate potential amount to be eroded after dam removal 115

5.2.2 Step 2 – Establish physical properties of the deposited sediment and pre-dam stream substrate 115

5.2.3 Step 3 – Develop a model to simulate erosion rates, channel evolution, and final channel stability after dam removal 116

5.2.4 Step 4 – Conduct a sediment balance of sediment passing upstream of the pool, in the pool, and downstream of the dam before and after dam removal 117

CHAPTER 6 REFERENCES 118

APPENDIX A NOTCHING DISSOLVED OXYGEN DATA.....132

APPENDIX B BIOTIC RESPONSE.....134

APPENDIX C SEDIMENT VOLUME SUMMARIES.....141

APPENDIX D KNICKPOINT SHEAR CALCULATIONS.....148

APPENDIX E COHESIVE EROSION TESTING PARTICLE SIZE 150

APPENDIX F ATTERBERG LIMITS.....155

APPENDIX G EROSION FUNCTION APPARATUS AND FLUME RESULTS 157

LIST OF FIGURES

Figure 1.1. Location of Brewster Creek watershed and the U. S. Geological Survey (USGS) streamflow and sediment stations near St. Charles, Illinois. 2

Figure 1.2. Aerial photographs of the study area including Brewster Creek Dam on Willow Lake in 1939, 1967, and 1998. 5

Figure 1.3. Location of the study area (2002, 2004, and 2005) including Brewster Creek dam on Willow Lake and the USGS streamflow and sediment stations on Brewster Creek near St. Charles, Illinois. 6

Figure 1.4. Approximate shorelines and stream boundaries in 1939, 2002, 2004, and 2005 determined from the aerial photographs shown in Figure 1.2 and Figure 1.3. 7

Figure 1.5. Brewster Creek dam before removal (views looking upstream). 7

Figure 1.6. Valley slopes (in ft/ft) of Brewster Creek from a 1993 USGS 7.5-minute topographic map. 9

Figure 1.7. Topography for the Brewster Creek study area. 9

Figure 1.8. Physiography for Brewster Creek study region. 10

Figure 1.9. Glacial drift thickness for the Brewster Creek study region. 11

Figure 1.10. Soil types for the Brewster Creek study region. 12

Figure 1.11. Land cover for the Brewster Creek study region. 13

Figure 2.1. A conceptual outline for dam-removal decisions and analysis from Heinz Center (2002).....17

Figure 2.2. Indicators for dam-removal decisions and analysis from Heinz Center (2002). 18

Figure 2.3. Channel Evolution Model Upstream of Dams (modified from MacBroom (2005)). 22

Figure 2.4. Conceptual channel evolution model upstream of dam removal (from Doyle *et al*. (2003a) and modified from Schumm *et al*. (1984); Simon and Hupp (1986)).....23

Figure 2.5. Speculative relations among the height of a reservoir sediment fill, the dominant grain size of the fill, and different processes of incision. Erosion of gravel depends on high-flow events; therefore, these incision processes are "event-driven." Incision of sand and of silt and clay do not depend on high-flow events, but rather on the mechanism of incision; therefore, removal of fills of sand and of silt and clay are "process-driven" (from Pizzuto (2002)).....25

Figure 2.6. Conceptual framework for ecosystem recovery following removal of a small dam (modified from Doyle and Stanley (2005)).....27

Figure 2.7. Models of knickpoint evolution for various types of bed material. τ_c is the critical bottom shear stress needed to initiate erosion. τ_o is the actual bottom shear stress (from Gardner (1983)). 29

Figure 2.8. Variation in (a) bottom shear stress and (b) channel bed along a knickpoint reach for a model run (modified from Gardner (1983)). 29

Figure 3.1. Cross-section and thalweg surveys completed throughout the study. 38

Figure 3.2. Cohesive-sediment sampling instrumentation. 39

Figure 3.3. Illinois Department of Transportation, Erosion Function Apparatus. 40

Figure 3.4. Erosion Function Apparatus conceptual diagram (modified from Briaud *et al*. (2003)).....40

Figure 3.5. Colorado State University testing flume, measurement layout, and top view of bed readings (brown dots), and velocity and shear reading (yellow dot) of sample area.....41

Figure 4.1. Sediment yield for each time period presented in Table 4.2.....49

Figure 4.2. Mean-daily flows for the four time periods during the study. 54

Figure 4.3. Repeated photographs taken from the footbridge 15 ft downstream of the old dam looking upstream. 57

Figure 4.4. Repeated photographs taken from the footbridge 15 ft downstream the old dam looking upstream. 58

Figure 4.5. Repeated photographs taken from the footbridge 15 ft downstream the old dam looking upstream. 59

Figure 4.6. Diagram of a knickpoint (modified from Schumm *et al*. (1984)).....61

Figure 4.7. Knickpoint progression after stepwise dam removal of Brewster Creek dam near St. Charles, Illinois. 62

Figure 4.8. Primary knickpoint location throughout the study and selected cross-section locations. 63

Figure 4.9. Knickpoint on October 18, 2006 after stepwise dam removal of Brewster Creek dam near St. Charles, Illinois (view looking upstream).....63

Figure 4.10. Surveyed top of deposited sediment and assumed pre-dam streambed in 2002, and thalweg and knickpoint locations surveyed at various times throughout the study. 64

Figure 4.11. Knickpoint shear-stress parameter diagram. 66

Figure 4.12. Variation in shear stress, flow, and knickpoint location and survey date. 67

Figure 4.13. Knickpoint shear stress and knickpoint location and thalweg distance upstream of old dam. 68

Figure 4.14. Sediment erosion from channel evolution and knickpoint shear stress.....71

Figure 4.15. Locations along Brewster Creek where cohesive-sediment samples were obtained for EFA and flume testing. 73

Figure 4.16. Summary of particle-size analysis on cohesive-streambed samples.....75

Figure 4.17. Summary of Atterberg Limits on cohesive-streambed samples. 76

Figure 4.18. EFA results showing shear stress and erosion rate. 78

Figure 4.19. Erosion rate at three sample locations for EFA-measured results and computed values as a function of shear stress, plasticity index, and percent finer that 0.063. 81

Figure 4.20. Erosion Function Apparatus (EFA) and flume (FL) erosion rate and specific stream power results for similar sites and materials at Brewster Creek.....82

Figure 4.21. Highest and lowest torvane-measured samples presented by erosion rate and specific stream power flume (FL) sample tests.....84

Figure 4.22. The average erosion rates and shear values for jet-test apparatus (Hanson and Simon, 2001) and the EFA erosion rate and shear values. 85

Figure 4.23. Conceptual diagram of the CKPR method.....86

Figure 4.24. Impact of optimized notching on the conceptual CEM upstream of the dam-removal site (modified from Doyle *et al*. (2003a); Schumm *et al*. (1984); Simon and Hupp (1986)). 92

Figure 4.25. Selected cross-section locations. The cross sections are identified as the cross-section thalweg distance above the old dam for October 2006 conditions. 95

Figure 4.26. Selected cross-sectional surveys at selected times throughout the study period. The plots are labeled as the cross section thalweg distance above the old dam for October 2006 conditions. The cross-section plots only show the main channel, not the full floodplain. The locations of the cross sections are shown in Figure 5.25.....96

Figure 4.27. Riffle and pool locations for bed-material sampling. 103

Figure 4.28. Median particle size of samples at various riffle locations in 2004 and 2006. 104
Figure 4.29. Particle-size distribution of samples at various riffle and pool locations in 2003 and 2004. 104
Figure 4.30. Particle-size distribution of samples at various riffle locations in 2006. 105
Figure 4.31. Particle-size distribution of samples at various riffle locations in 2004 and 2006. 105
Figure 4.32. Location of Shelby tube samples taken to determine stability of banks. 108
Figure 4.33. Particle-size distribution for streambank and streambed samples. 110
Figure A.1. Dissolved-oxygen concentrations during notching events at the downstream station on Brewster Creek near St. Charles, Illinois. 133
Figure B.1. Stream fish-survey locations and corresponding species (SPP) and IBI. 135
Figure B.2. Photographs taken on August 24, 2005 show that low flows have allowed dense revegetation of lower banks and point bars throughout the channel that has evolved in the old lake bed (view looking downstream). 139
Figure E.1. Particle-size distribution for samples used in the flume. 151
Figure E.2. Particle-size distribution for samples used in the EFA. 152
Figure E.3. Particle-size distribution for samples used in the EFA and flume. 154

LIST OF TABLES

Table 1.1. Percent of Brewster Creek watershed for various land-cover categories. 14

Table 2.1. Dam-removal monitoring protocol (from Stewart and Grant (2005)).....19

Table 2.2. Stream monitoring and remediation parameters (from Bushaw-Newton *et al*. (2002)).....20

Table 2.3. Range of critical shear values for cohesive materials (adapted from Briaud *et al*. (2003)).....33

Table 3.1. Streamflow and sediment stations used in the study and corresponding drainage areas, Brewster Creek near St. Charles, Illinois. 35

Table 4.1. Time line of events during the study period. 46

Table 4.2. Sediment loads and yields, and mean-daily streamflows upstream and downstream of Brewster Creek dam near St. Charles, Illinois. 47

Table 4.3. Sediment loads eroded from the lake by channel evolution determined from upstream and downstream station data and survey data downstream of the dam. 50

Table 4.4. Total sediment deposited in October 2002 and sediment volumes eroded from the lake by channel evolution determined from survey data upstream of the dam. 51

Table 4.5. Highest seven mean daily and peak flows for each of the four time periods during the study. 55

Table 4.6. Recurrence interval and corresponding streamflow values for Brewster Creek.....56

Table 4.7. Annual peak streamflows for the current study time period and station location, and historical values from a crest gage at Illinois Route 25 (Figure 1.3). 56

Table 4.8. Knickpoint height and migration lengths between observations or surveys. 65

Table 4.9. Shear stress for various flows across the surveyed knickpoints. 67

Table 4.10. Sediment load, streamflow, and knickpoint characteristics for each of the largest storms during and after notching. 69

Table 4.11. Summary of particle-size analysis on cohesive-streambed samples assuming the sand-silt break is at 0.063 mm. 74

Table 4.12. Summary of Atterberg Limits on cohesive-streambed samples. 76

Table 4.13. Summary of specific weight and moisture content on cohesive-streambed samples. 77

Table 4.14. Critical shear values for EFA samples. 78

Table 4.15. Soil properties, flow conditions, and erosion rates for the EFA samples. 79

Table 4.16. Coefficient of determination and standard error for logarithmic data in the equations for estimating erosion rate for the three sample locations at Brewster Creek. 80

Table 4.17. Mechanical shear strength of flume samples measured with a torvane. 83

Table 4.18. Approximate duration of the storm hydrograph rising limb and peak for each storm modeled. Note that some storm time periods have multiple peaks (Figure 4.2). 89

Table 4.19. CKPR method results and measured values for erosion dynamics at Brewster Creek. 90

Table 4.20. Parameters and results for alternative three stepwise notches modeled with the CKPR method for approximately 1 yr (using the first thirteen storm knickpoint shear stresses and durations in Tables 4.10 and 4.18, respectively). 93

Table 4.21. Channel and reach characteristics including width-to-depth and entrenchment ratio and friction slope. 98

Table 4.22. Main-channel shear stress, channel velocity, specific stream power, estimated particle size moved at the given shear stress, and size of bed material in the riffle or nearby cohesive material (summarized in Section 4.2.3, *Cohesive-erosion Testing Results*). 101

Table 4.23. Summary of water content, specific weight Atterberg Limits, particle size, and type of geotechnical tests completed on streambank and streambed samples. 109

Table 4.24. Bank-stability model results. 110

Table B.1. Surveyed stream fishes and corresponding IBI for each control section and the new channel. 136

Table B.2. Plant survey on June 24, 2004 in the old lakebed by Jeff Mengler, U. S. Fish and Wildlife Service Botanist (italic green text indicates native species). 138

Table B.3. Results of mussel survey. 140

Table C.1. Pre-dam removal (October 2002) lake cross section and reach summary. 143

Table C.2. October 2002 – downstream main-channel cross section and reach summary. 144

Table C.3. September 15, 2003 – main-channel cross section and reach summary. 144

Table C.4. April 4, 2004 – main-channel cross section and reach summary. 145

Table C.5. November 2, 2004 – upstream main-channel cross section and reach summary. 145

Table C.6. November 2, 2004 – downstream main-channel cross section and reach summary. 146

Table C.7. October 8, 2006 – main-channel cross section and reach summary. 147

Table D.1. Knickpoint shear calculations. 149

Table E.1. Particle-size distribution for samples used in the flume. 151

Table E.2. Particle-size distribution and summary characteristics for samples used in the EFA. 153

Table F.1. Soil group symbols and typical names for cohesive soils as established in the USC (Casagrande, 1948) for soils found in the St. Louis Metro East region in Illinois. 156

Table G.1. EFA summary: Sample B1-EFA (0 - 177.8 mm). 158

Table G.2. EFA summary: Sample B2B-EFA (0 - 76.2 and 76.3 - 279.4 mm). 159

Table G.3. EFA summary: Sample B3-EFA (0 - 101.6 mm). 160

Table G.4. Flume testing results. 161

LIST OF SYMBOLS, UNITS, AND ABBREVIATIONS

Symbols

a	flume height
b	flume width
A	flume area
AE	longitudinal area eroded (m^2)
B	wetted width of streambed
CA	cross-section area
ch	main-channel
D	circular pipe diameter or hydraulic diameter for a rectangular flume equal to the circular pipe diameter
D_{50}	median particle size
D_n	aspect ratio of knickpoint drop height
e	erosion-rate constant
EI	erosion index
ER	erosion rate
f	friction factor obtained from the Moody Chart
F	function of Froude number
FS	factor of safety
h	elevation of the pre-dam streambed (m)
h_n	normal depth
HD	hydraulic depth

HD_{ch}	main-channel hydraulic depth
HDC	main-channel hydraulic depth upstream of the knickpoint
l	length of soil sample eroded in a time t
LL	liquid limit
LR	lake reach
LSA	lake surface area
LVBS	lake volume to bottom of sediment
LVTS	lake volume to top of sediment
MDF	mean-daily flow
MMDF	maximum mean-daily flow
P	flume perimeter
PF	percentage of sediment sample finer than 0.063 mm
PI	plasticity index
PL	plastic limit
q_t	volume total sediment transport rate per unit stream width
Q1.5	1.5-yr streamflow
Q10	10-yr streamflow
Q100	100-yr streamflow
R^2	coefficient of determination
Re	Reynold's number
RV	reach volume
S_b	slope of the pre-dam streambed (m/m) ($S_b = \tan \theta$)
S_f	average reach friction slope
Sf_{ac}	friction slope across the knickpoint = (*EGE-US* – *EGE-DS*) / D_{ac}
SD	sediment load downstream

SE	sediment eroded
ST	sediment thickness (m)
SU	sediment load upstream
SV	sediment value
SY	sediment yield
t	time
TW	top width
TW/HD	top-width and hydraulic-depth ratio
v	mean flow velocity (m/s)
V_{ch}	main-channel velocity
Vol	volume eroded (m^3)
W	representative channel width (m)
W/D	width-to-depth ratio
x	streamwise distance (m)
$\dot{Z}$	erosion rate
γ	specific weight of water
ε	rate constant (Parchure and Mehta, 1985)
ε	surface roughness (Briaud *et al*., 2003)
ε/D	pipe relative roughness
ε_f	floc erosion rate
η	level of the sand above an arbitrary datum
θ	bottom slope
λ_p	bed porosity
ν	kinematic viscosity of water ($10^{-6} m^2/s$ at 20°C)
ρ	mass density of water (1,000 kg/m^3)

σ_1	major principal stress
σ_3	confining or chamber pressure
τ	shear stress
τ_b	bed shear stress
τ_c	critical shear stress
τ_{ch}	main-channel shear stress
τ_{kn}	shear stress across the knickpoint
τ_o	bottom shear stress (Gardner, 1983)
τV	specific stream power
ω_{ch}	main-channel specific stream power

Units

°C	degrees Celsius
°F	degrees Fahrenheit
acre/ft	acre per foot
CFS	cubic feet per second
ft	feet
ft^2	square feet
ft/day	feet per day
ft^3/s	cubic feet per second
ft/ft	feet per foot
in.	inch(es)
kg/cm^2	kilogram(s) per square centimeter
kg/m^3	kilogram(s) per cubic meter
km^2	square kilometer(s)

kPa	kiloPascal(s)
lb	pound(s)
lbs/ft^3	pounds per cubic foot
m	meter(s)
m/m	meter(s) per meter
m/s	meter(s) per second
m^2/s	square meter(s) per second
m^3	cubic meter(s)
m^3/s	cubic meter(s) per second
mg/L	milligram(s) per liter
mi^2	square mile(s)
mm	millimeter(s)
mm/hr	millimeter(s) per hour
N/m^2	Newton(s) per square meter
Pa	Pascal(s)
psf	pound(s) per square foot
tons/day	ton(s) per day
$tons/(ft^3/s)$	ton(s) per cubic feet per second
$tons/mi^2$-yr	ton(s) per square mile per year
$tons/mi^2$-yr-ft^3/s	ton(s) per square mile per year per cubic foot per second
W/m^2	Watt(s) per square meter
yr(s)	year(s)

Abbreviations

ADV	Acoustic Doppler Velocity
ASTM	American Society for Testing and Materials

CEMs	channel evolution models
CEMUD	Channel Evolution Model Upstream of Dam
Cd	cadmium
CH	classification for inorganic clay of high plasticity, fat clay
CKPR	Cohesive Knickpoint Parallel Retreat
CL	classification for inorganic clays of low to medium plasticity, gravelly clays, sandy clays, silty clays, lean clays
Cr	chromium
CSU	Colorado State University
Cu	copper
D/S	downstream
EFA	Erosion Function Apparatus
FL	flume
GPS	global positioning system
HEC-RAS	Hydrologic Engineering Center, River Analysis System
IBI	Index of Biotic Integrity
IEPA	Illinois Environmental Protection Agency
IDNR	Illinois Department of Natural Resources
IDNR-OWR	Illinois Department of Natural Resources, Office of Water Resources
IDOT	Illinois Department of Transportation
KCDEM	Kane County Division of Environmental Management
MH	classification for inorganic silts, micaceous or diatomaceous fine sands or silts, elastic silts
ML	classification for inorganic silt and very fine sand, silty or clayey fine sand, or clayey silt with low plasticity
N	nitrogen

NAVD 88	North American Vertical Datum of 1988
Ni	nickel
NIPC	Northeastern Illinois Planning Commission
NP	non-plastic
OH	classification for organic clay of medium to high plasticity
OL	classification for organic silt and organic silty clay of low plasticity
PAHs	Polycyclic Aromatic Hydrocarbons
Pb	palladium
PCBs	Polychlorinated Biphenyls
SAC	Shedd Aquarium in Chicago
SPP	species
TSS	total suspended solids
USACE	U. S. Army Corps of Engineers
USC	Unified Soil Classification
USEPA	U. S. Environmental Protection Agency
USFWS	U. S. Fish and Wildlife Service
USFWS-CIFO	U. S. Fish and Wildlife Service, Chicago Illinois Field Office
USGS	U. S. Geological Survey
USGS-IWSC	U. S. Geological Survey, Illinois Water Science Center
UU	unconsolidated-undrained triaxial compression test
YWCA	Young Women's Christian Association
Zn	zinc

CHAPTER 1

INTRODUCTION

For a growing number of small dams (dams with impounded reservoirs less than 100 acre-ft (Heinz Center, 2002)), physical deterioration, risk of failure, and a loss of economic viability have created a financial liability for owners, such that removal is often less expensive than continued maintenance and operation (Born *et al*., 1998; Doyle and Harbor, 2003). A small dam, built in 1929, on Brewster Creek near St. Charles, Illinois (Figure 1.1), was declared a Class I structure, having a high probability of causing loss of life and/or substantial economic loss in the event of a catastrophic failure by the Illinois Department of Natural Resources, Office of Water Resources (IDNR-OWR) (Kane County Environmental Management, 2006). Costs were prohibitive to repair the dam; therefore, the owners decided to remove the dam. Possible environmental effects and costs of removing dams, and managing or removing the impounded sediment can be substantial. In Illinois, State regulations require complete sediment containment during any construction project. Project engineers developed a first design for the total removal of Brewster Creek dam that complied with these regulations. The projected construction, oversight, and restoration costs under this first design were $1.17 million and exceeded available funds (Kane County Environmental Management, 2006).

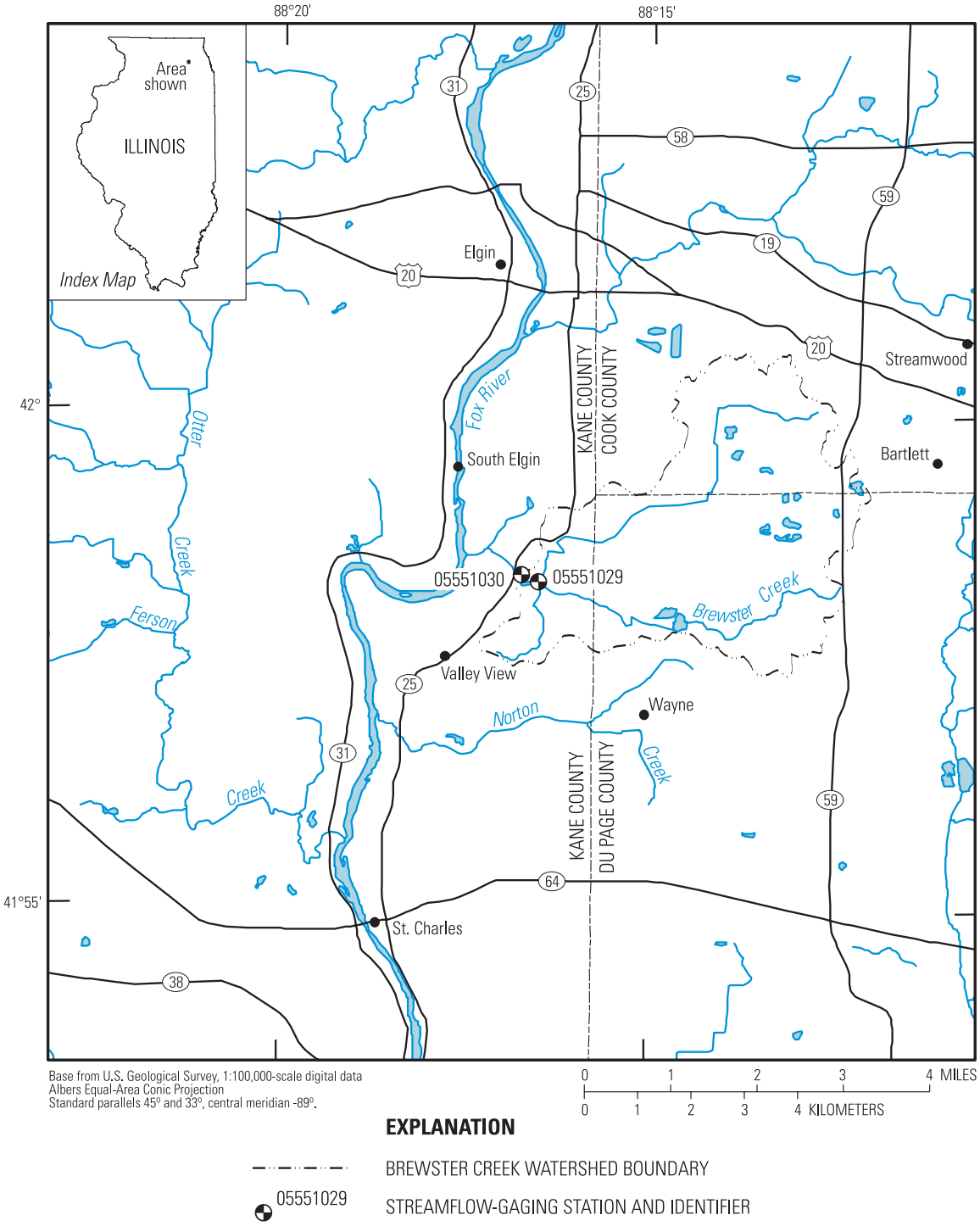

Figure 1.1. Location of Brewster Creek watershed and the U. S. Geological Survey (USGS) streamflow and sediment stations near St. Charles, Illinois.

The Illinois Environmental Protection Agency (IEPA) granted permission for a pilot stepwise dam-removal project, consisting of cutting five 12- to 18-in. notches, across the length of the dam (or some portion of the length), completed from June 2003 through February 2004. The projected construction, oversight, and restoration cost for the stepwise removal was $330,000 (Kane County Environmental Management, 2006). The benefits of removing the dam in steps included reducing the removal cost and reducing possible environmental effects by allowing the impounded sediment to slowly move downstream, and a stable stream and re-vegetated floodplain to form upstream (Graber *et al*., 2001).

In 2002, an investigation began to monitor, analyze, and interpret erosion dynamics before, during, and after stepwise removal of a dam on Brewster Creek near St. Charles, Illinois. The USGS-IWSC has monitored and analyzed streamflow and sediment data. The USGS-IWSC and Colorado State University (CSU) monitored and analyzed stream-channel geometry, and stream and lake substrate. IDNR-OWR completed an initial conditions cross-sectional survey of the lake and stream channel upstream and downstream of the dam.

The USGS-IWSC monitored dissolved oxygen concentrations before, during, and after each notching event (Appendix A). Biotic data were collected by various agencies (Appendix B). The Illinois Department of Natural Resources (IDNR) and the Shedd Aquarium in Chicago (SAC) monitored and analyzed aquatic organisms. The U. S. Fish and Wildlife Service, Chicago Illinois Field Office (USFWS-CIFO) monitored and analyzed the vegetation in the exposed lake-bed and stream riparian area.

1.1 Objective and Scope

The objectives of this research were to evaluate erosion dynamics of a stepwise small dam removal on Brewster Creek near St. Charles, Illinois, and develop analytical techniques for future application on small dams similar to the Brewster Creek dam. Sediment erosion and stream-channel evolution and stability were analyzed utilizing data collected on streamflow, sediment transport, knickpoint migration, and stream-channel geometry and substrate. A Cohesive Knickpoint Parallel Retreat method and empirical equations developed in this study may be applicable to future stepwise small dam-removal projects with similar dams, sediments, lakes, and watersheds.

1.2 Description of the Study Area and Watershed

The study area included Willow Lake on Brewster Creek near St. Charles, Illinois (Figures 1.2 and 1.3). The shorelines and stream boundaries for 1939, 2002, 2004, and 2005 are presented in Figure 1.4. The dam was approximately 8-ft high and had a 30-ft wide crest in the shape of an arc (Figure 1.5). The abutments for the footbridge downstream of the dam are approximately 24 ft apart. In 2002, the lake had a surface area of 3.96 acres and sediment accumulation had continued until the average water depth was less than 1 ft, sediment volume equaling 14.47 acre-ft, and average sediment thickness of 3.7 ft determined from an October 2002 survey of the lake by IDNR-OWR (Appendix C). Quantities of various potential undocumented dredging throughout the life of the impoundment inhibit an accurate estimation of sediment yield from the existing sediment impounded in the lake. Also, the sediment deposited in the area above the lake (Figures 1.2 and 1.3) has not been documented. The deposited sediments

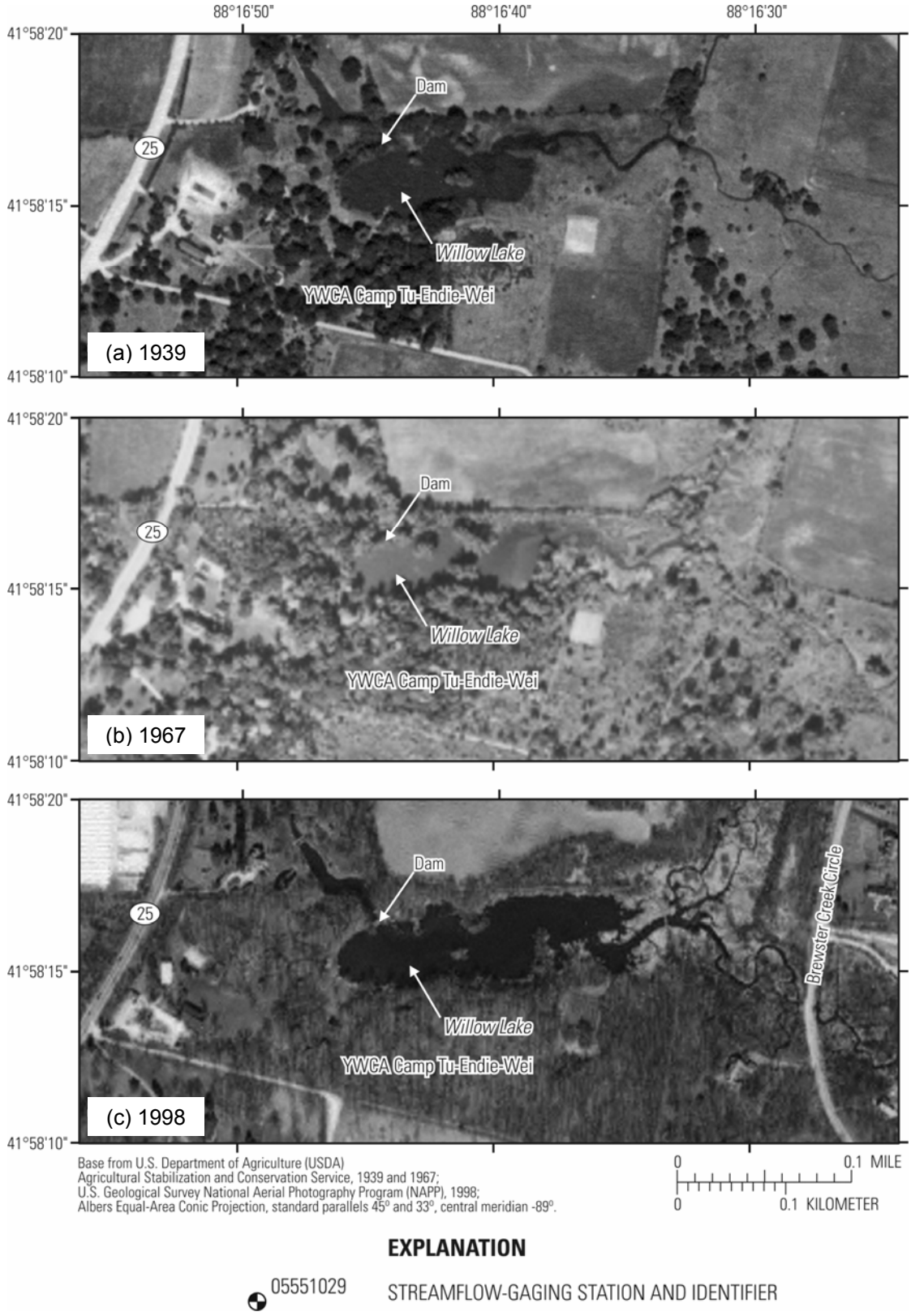

Figure 1.2. Aerial photographs of the study area including Brewster Creek Dam on Willow Lake in 1939, 1967, and 1998.

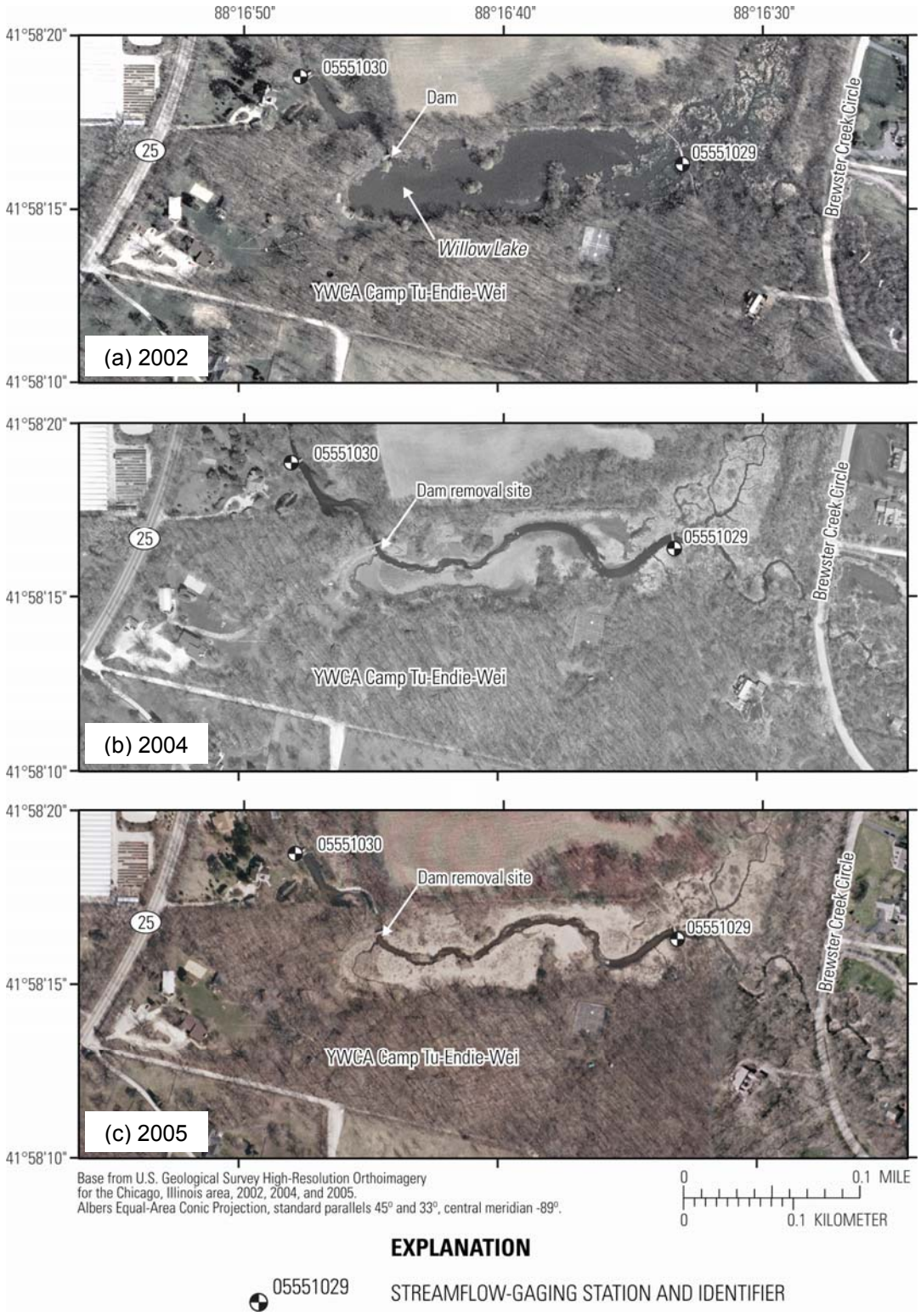

Figure 1.3. Location of the study area (2002, 2004, and 2005) including Brewster Creek dam on Willow Lake and the USGS streamflow and sediment stations on Brewster Creek near St. Charles, Illinois.

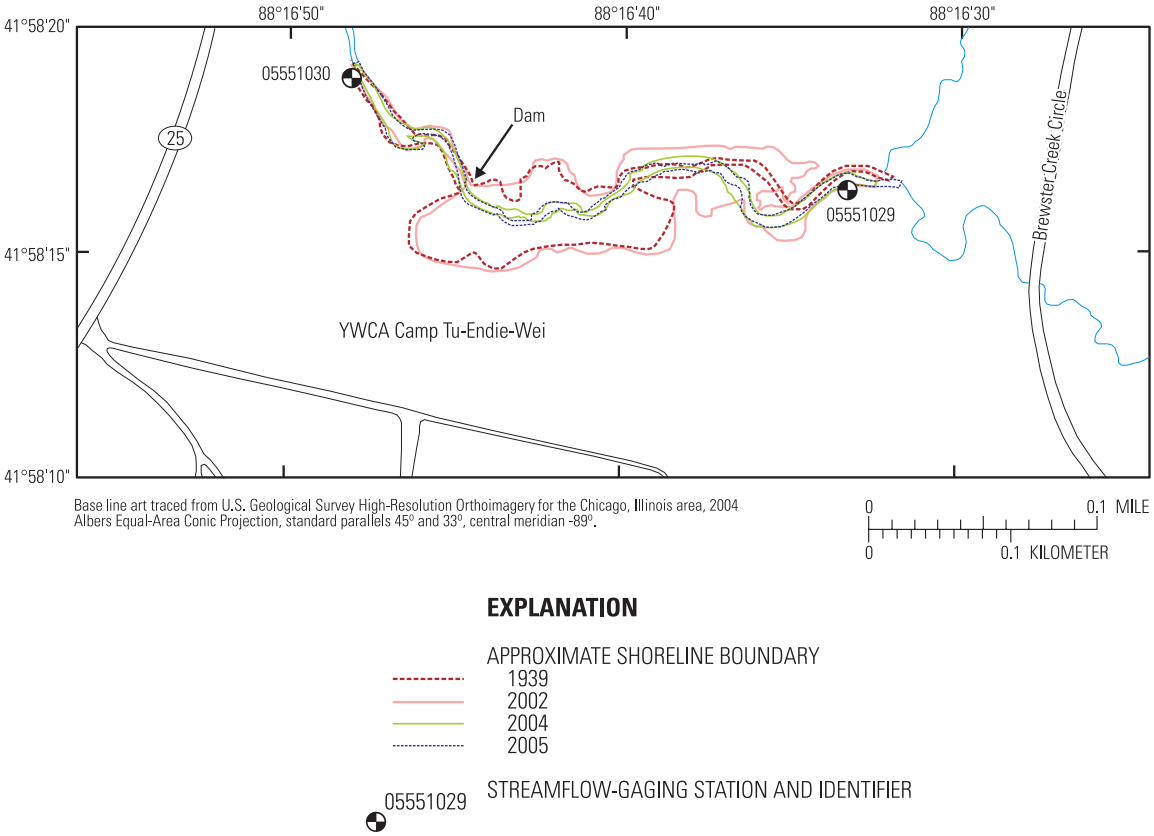

Figure 1.4. Approximate shorelines and stream boundaries in 1939, 2002, 2004, and 2005 determined from the aerial photographs shown in Figure 1.2 and Figure 1.3.

(a) (b)

Credit: Figure 1.5(a) photograph taken by Karen Kosky, KCDEM, and Figure 1.5(b) photograph taken by Mitch Harris, USGS

Figure 1.5. Brewster Creek dam before removal (views looking upstream).

consisted of 67 to 99 percent silts and clays based on samples analyzed in this study. The stream channel below the dam consisted primarily of sand, gravel, and cobble. These coarse materials, along with intermittent areas of stiff clay, are present in the streambed that evolved after stepwise dam removal. The valley slopes immediately upstream and downstream of Willow Lake range from 0.0043 to 0.0092 (Figure 1.6). The topography for the watershed and surrounding area is shown in Figure 1.7. The climate of northeastern Illinois is humid continental with a long-term average annual precipitation of 37 in. and the long-term mean temperature of approximately 49°F at Elgin, Illinois (Figure 1.1), for 57 yrs of data (U. S. Department of Commerce, National Oceanic Atmospheric Administration, 2006).

The Brewster Creek watershed is within the Wheaton Morainal Country (Figure 1.8) (Leighton *et al*., 1948). The Wheaton Morainal Country is characterized by rugged glacial topography, with several morainal ridges, lakes, and swamps (Leighton *et al*., 1948). Regionally thick drift over the bedrock surface is present in the northeastern portions of the State and range from 60 to 200 ft in the Brewster Creek watershed (Figure 1.9). The soils in Brewster Creek are predominantly hydrologic soil Groups B and C (Figure 1.10) (U. S. Department of Agriculture, Natural Resources Conservation Service, 1994). Group B soils are silt loam or loam and Group C soils are sandy clay loam (U. S. Department of Agriculture, Soil Conservation Service, 1986). The land cover in Brewster Creek is presented in Figure 1.11 and Table 1.1. The two highest land covers are row crops (38 percent) and the combination of residential and urban (26 percent).

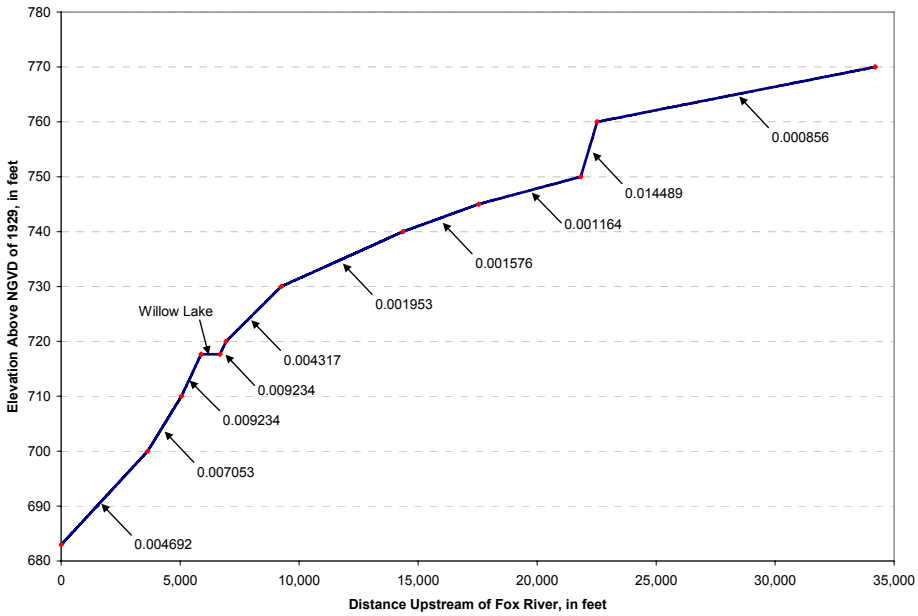

Figure 1.6. Valley slopes (in ft/ft) of Brewster Creek from a 1993 USGS 7.5-minute topographic map.

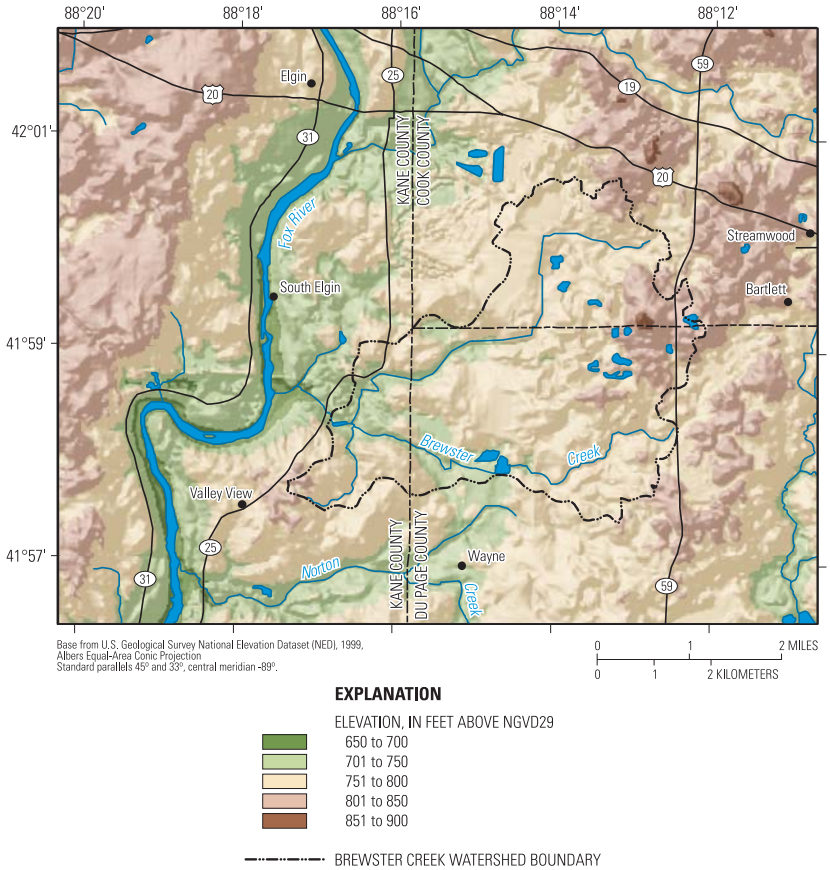

Figure 1.7. Topography for the Brewster Creek study area.

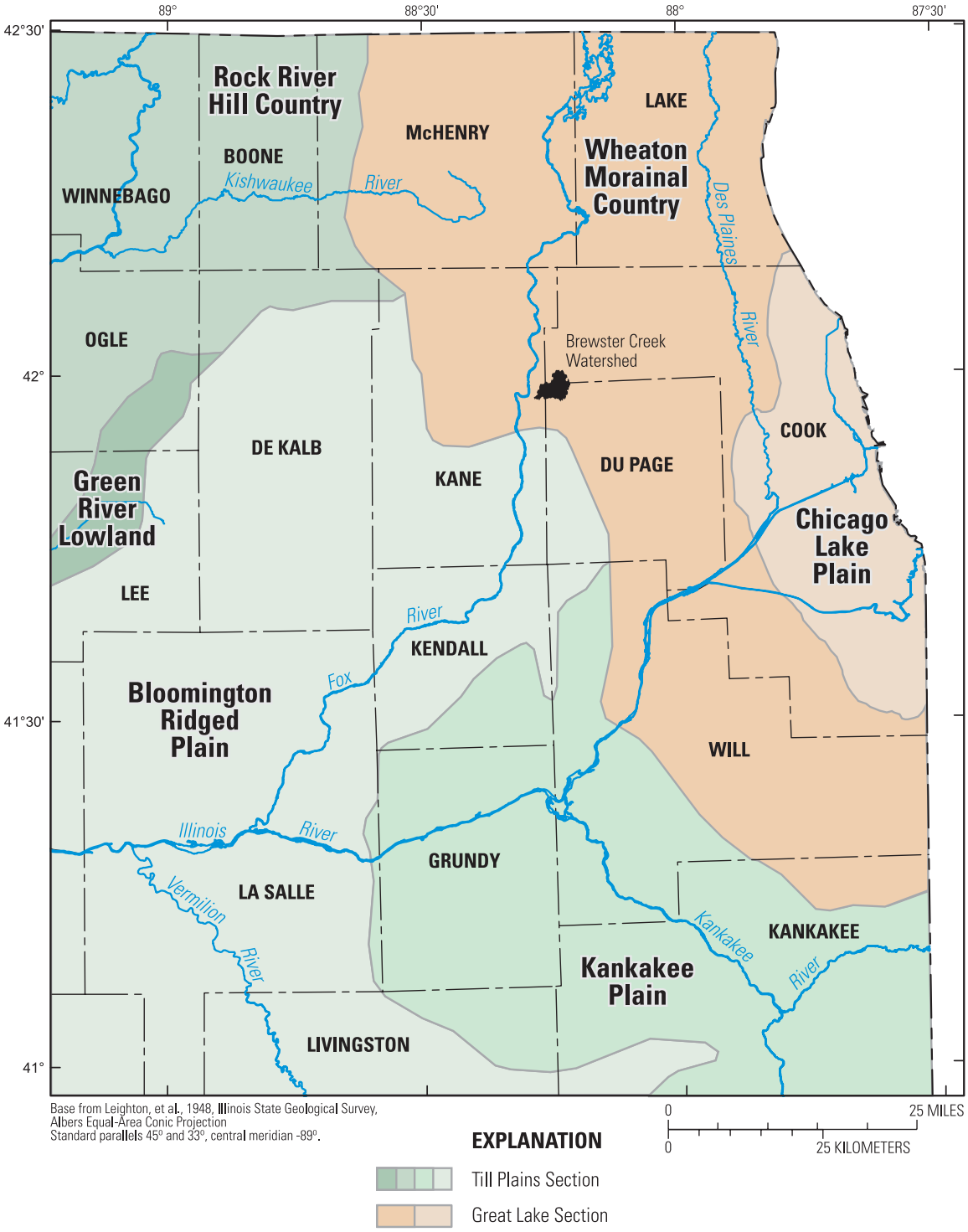

Figure 1.8. Physiography for Brewster Creek study region.

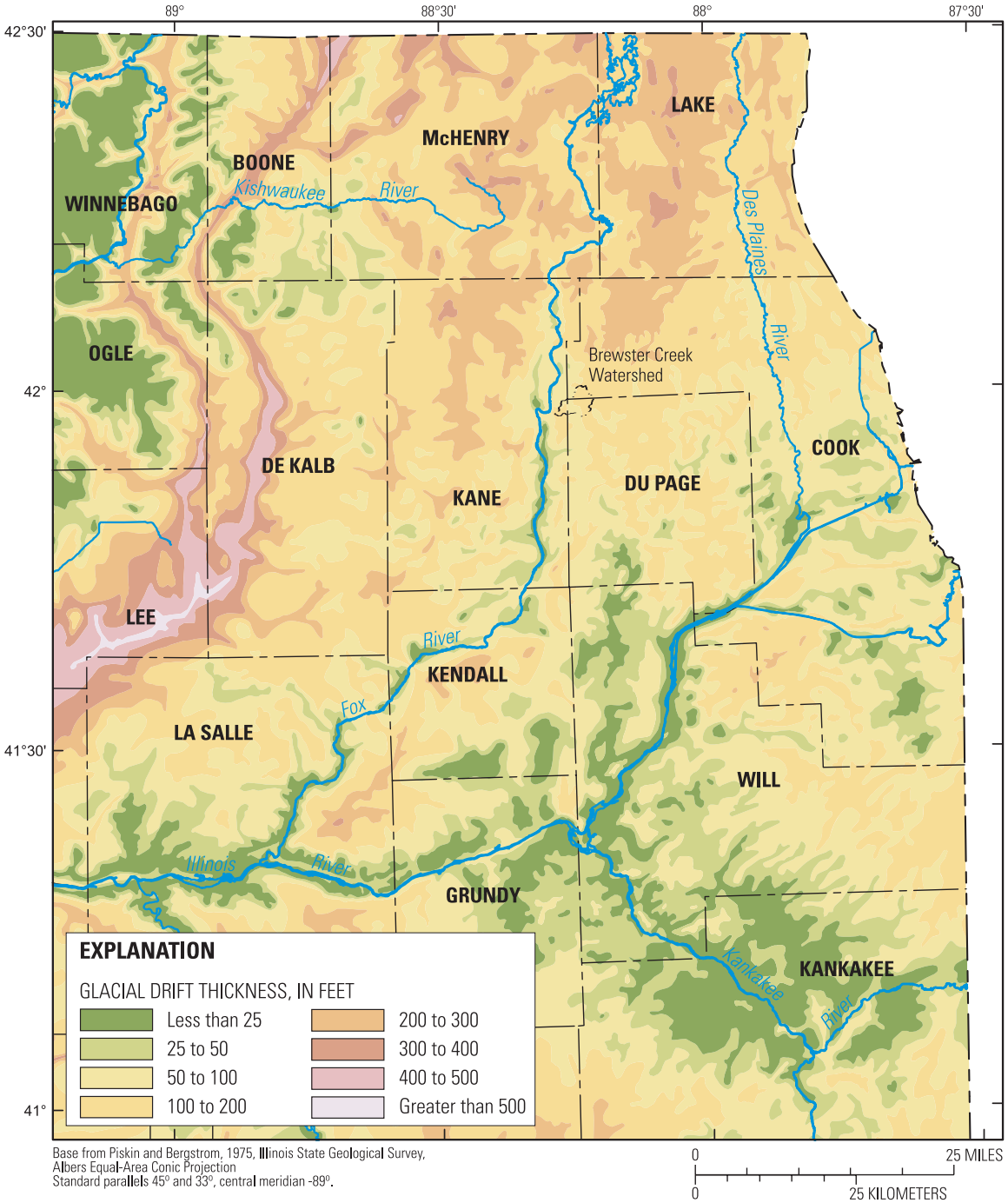

Figure 1.9. Glacial drift thickness for the Brewster Creek study region.

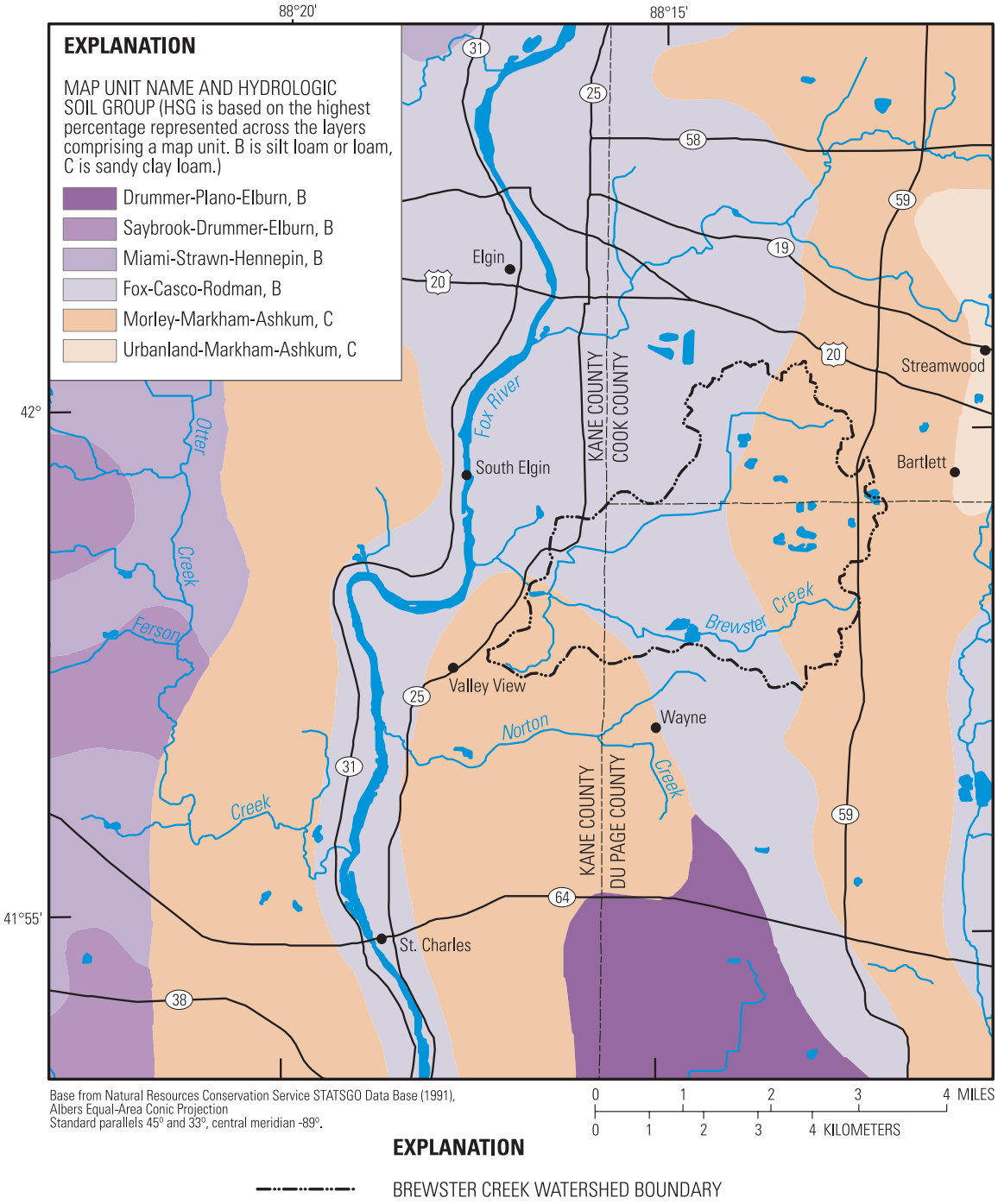

Figure 1.10. Soil types for the Brewster Creek study region.

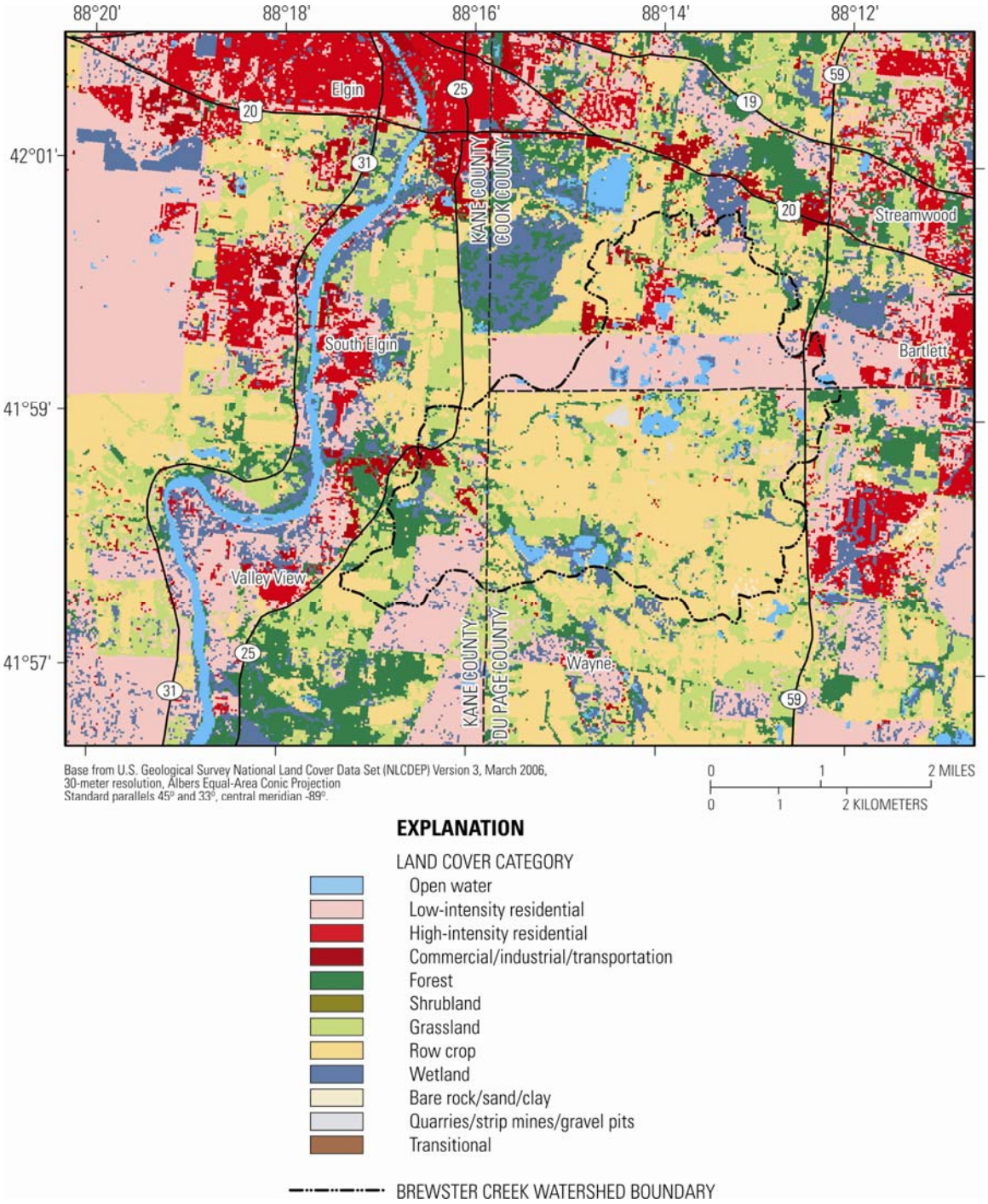

Figure 1.11. Land cover for the Brewster Creek study region.

Table 1.1. Percent of Brewster Creek watershed for various land-cover categories.

Land-cover Category	Percent of Watershed
Open Water	3.1
Low-intensity Residential	6.8
High-intensity Residential	2.7
Commercial/Industrial/Transportation	2.6
Residential without Trees	8.3
Forested Residential	5.2
Bare Rock/Sand/Clay	0.2
Quarries/Strip Mines/Gravel Pits	0.3
Deciduous Forest	8.9
Evergreen Forest	0.3
Mixed Forest	0.0
Grasslands/Herbaceous	2.1
Pasture/Hay	13.7
Row Crops	38.9
Small Grains	0.0
Urban/Recreational Grasses	4.1
Woody Wetlands	1.8
Emergent Herbaceous Wetlands	1.0

CHAPTER 2

LITERATURE REVIEW

This literature review summarizes the broad range of considerations and data needs related to dam removal, and the studies of the geomorphic and ecological response of dam removal. Also, literature specific to understanding the erosion dynamics of dam removal in cohesive soils is summarized. The related topics include laboratory, field, and theoretical knickpoint migration and cohesive erosion rate testing.

2.1 Dam Removal

The American Rivers (2005) organization provides a list of dams removed and slated for removal. It is important to address the broad range of considerations and data needs associated with dam removal. Also, it is important to learn from past removals and determine the best ways to monitor future removals.

> "When managed thoughtfully, removing a small dam can significantly and cost-effectively improve aquatic habitat and water quality. No matter how well a small dam removal project is designed and implemented, there may be some negative short-term impacts to the environment. Restoration of aquatic communities is not an immediate process; stabilization of the stream channel and habitat improvements may take several years as the complex interactions of sediment and flowing water approach an equilibrium." (Graber *et al*., 2001)

Graf (2002) and the Heinz Center (2002) provide a qualitative background on dam removal. Although not exhaustive, the following list of issues to be considered for dam-

removal projects was developed from these two references and the American Society of Civil Engineers (2005):

- Public Safety (dams in disrepair; public water supply and quality)
- Social-cultural Perspectives (aesthetics; recreation)
- Economic Impacts (removal or modification costs; hydroelectric; tourism)
- Regulatory Requirements (standard permitting; potential variances in permitting)
- Removal and Modification Criteria Development (assessment of pilot projects)
- Sediment (upstream management; downstream hazards)
- Geomorphic (upstream channel formation; downstream channel deposition)
- Hydrologic (upstream flood storage; downstream flood hazards)
- Ecologic (upstream habitat creation; downstream channel deposition)
- Fish Passage (structure design; hydraulic conditions)
- Water Quality

> "The underlying science of dam removal is relatively undeveloped and most agencies faced with dam removal lack a coherent purpose for removing dams. These shortcomings can be overcome by the implementation of two policies by agencies faced with dam removal: (1) the development and adoption of a prioritization scheme for what constitutes an important dam removal, and (2) the establishment of minimum levels of analysis prior to decision-making about a dam removal" (Doyle and Harbor, 2003).

A conceptual outline and list of indicators for dam-removal decisions and analysis are presented in *Dam Removal: Science and Decision Making* (Heinz Center, 2002) as shown in Figures 2.1 and 2.2.

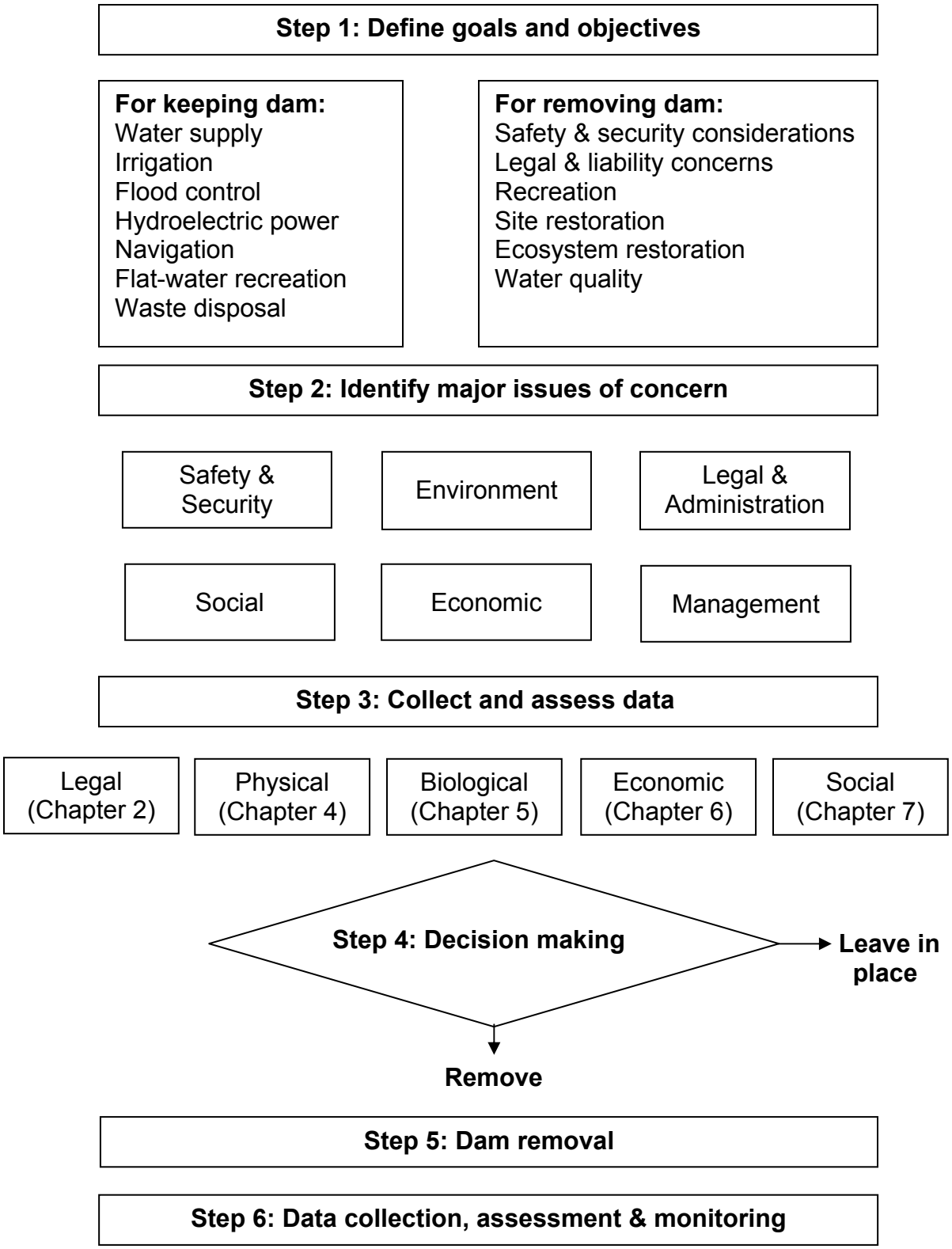

Figure 2.1. A conceptual outline for dam-removal decisions and analysis from Heinz Center (2002).

Key Indicators for Dam-removal Decisions

Physical
- River network segmentation
- Watershed fragmentation
- Downstream hydrology
- Downstream sediment system
- Downstream channel geomorphology
- Floodplain geomorphology
- Reservoir geomorphology
- Upstream geomorphology

Chemical
- Water quality
- Sediment quality (reservoir area and downstream)
- Air quality

Ecological
- Aquatic ecosystems
- Riparian ecosystems
- Fishes
- Birds
- Terrestrial animals

Economic
- Dam-site economics
- Economic values, river reach
- Regional economic values

Social
- Safety and security
- Aesthetic and cultural values
- Non-majority considerations

Note: Ideally, these indicators would be used to measure or estimate today's conditions and forecast conditions one year, five years, and a decade or two into the future.

Figure 2.2. Indicators for dam-removal decisions and analysis from Heinz Center (2002).

> "Although more than 500 dams have been removed in the United States in the last century, surprisingly little documented research exists on the ecological and geomorphic changes that occur following dam removal or on the techniques for managing these projects to achieve desirable results." (Graber *et al*., 2001)

The majority of dams in this country, and almost all dams removed thus far, are small (Heinz Center, 2002). A consistent set of monitoring protocols are required to develop a comprehensive understanding of dam-removal effects (Stewart and Grant, 2005). From the study dam removals, Stewart and Grant (2005) and Bushaw-Newton *et al*. (2002) (Tables 2.1 and 2.2, respectively) offer the beginning of a dam-removal monitoring protocol where an empirical set of data can be built with which to test more rigorous dam-removal models.

Table 2.1. Dam-removal monitoring protocol (from Stewart and Grant (2005)).

Physical Measurements	When to Collect	What they Inform
Monumented photographs	Before, during, after	Process, volume, timing, geometry
Topographic surveys	Before, during, after	Process, volume, timing
Discharge	During, after	Process controls
Surface and subsurface grain size	Before, after	Process controls
Sediment properties (e.g., cohesiveness)	After	Process controls

Table 2.2. Stream monitoring and remediation parameters (from Bushaw-Newton *et al*. (2002)).

Stream Parameters
Longitudinal Profiles Channel Cross-sectional Profiles Grain Size (Wentworth Scale) In-stream Temperature
Polycyclic Aromatic Hydrocarbons (PAHs) Polychlorinated Biphenyls (PCBs) Trace Metals (Cd, Cu, Cr, Ni, Pb, Zn)
Dissolved Nutrients (inorganic and organic N species, phosphorus species) Dissolved Organic Carbon Total Suspended Solids (TSS) Biological Oxygen Demand Conductivity, pH, Dissolved Oxygen
Algal Biomass (*chl a*) and Ash Free Dry Mass Species Composition and Abundance: - diatoms and algae - freshwater bivalves - benthic macroinvertebrates - fish species
Stabilization and Replanting Alleviation of Erosion Problem Elimination of Small Stagnant Pond

Cd = cadmium; Cr = chromium; Cu = copper; N = nitrogen; Ni = nickel; Pb = palladium; Zn = zinc

2.1.1 Geomorphic Response

Given the limited understanding and empirical studies documenting geomorphic changes associated with dam removal, geomorphic analogies of dam removal offer some basis for qualitative predictions (Doyle *et al*., 2003a). The Channel Evolution Model Upstream of Dam (CEMUD) sites were developed to determine geomorphic response based upon observations of dam-removal projects, dam failures, reservoir drawdowns, at post-glacial lakes and dams, along with available records and literature (MacBroom, 2005). A flow chart of the model identifies a series of potential channel-evolution trends and provides examples of each (Figure 2.3). Several parameters are used to help identify

potential dam-removal impacts. The parameters include the presence of sediment, presence or absence of a well-defined thalweg across the pool bed, type of sediment deposit, sediment gradation, and the ratio between the pool width versus the anticipated pre-dam channel width (MacBroom, 2005). The case where a reservoir is predominantly filled with fine sediment is conceptually shown in Figure 2.4 (Doyle *et al*., 2003a) and is similar to alluvial channel incision responding to base-level lowering (Schumm *et al*., 1984; Simon and Hupp, 1986).

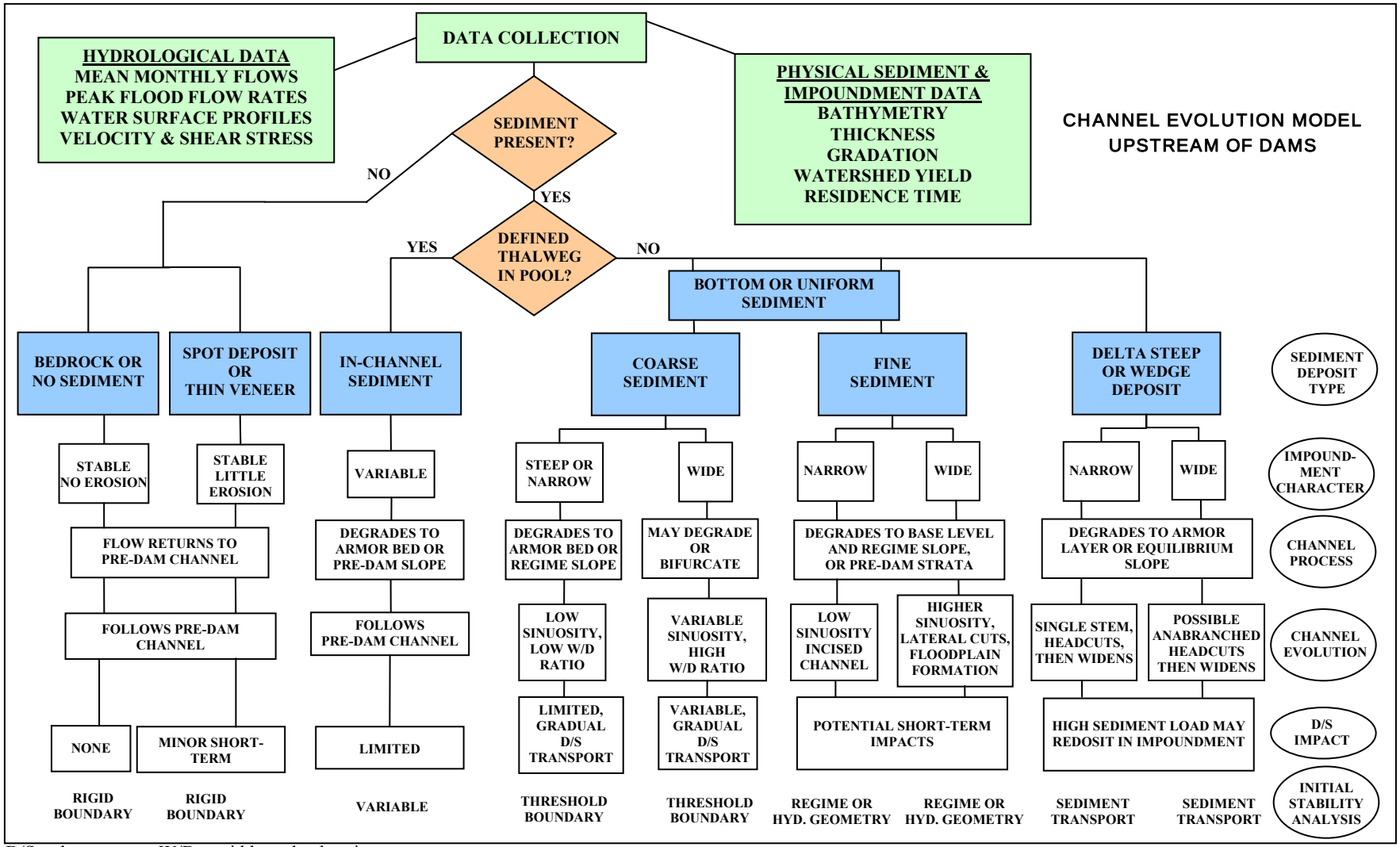

D/S = downstream; W/D = width-to-depth ratio

Figure 2.3. Channel Evolution Model Upstream of Dams (modified from MacBroom (2005)).

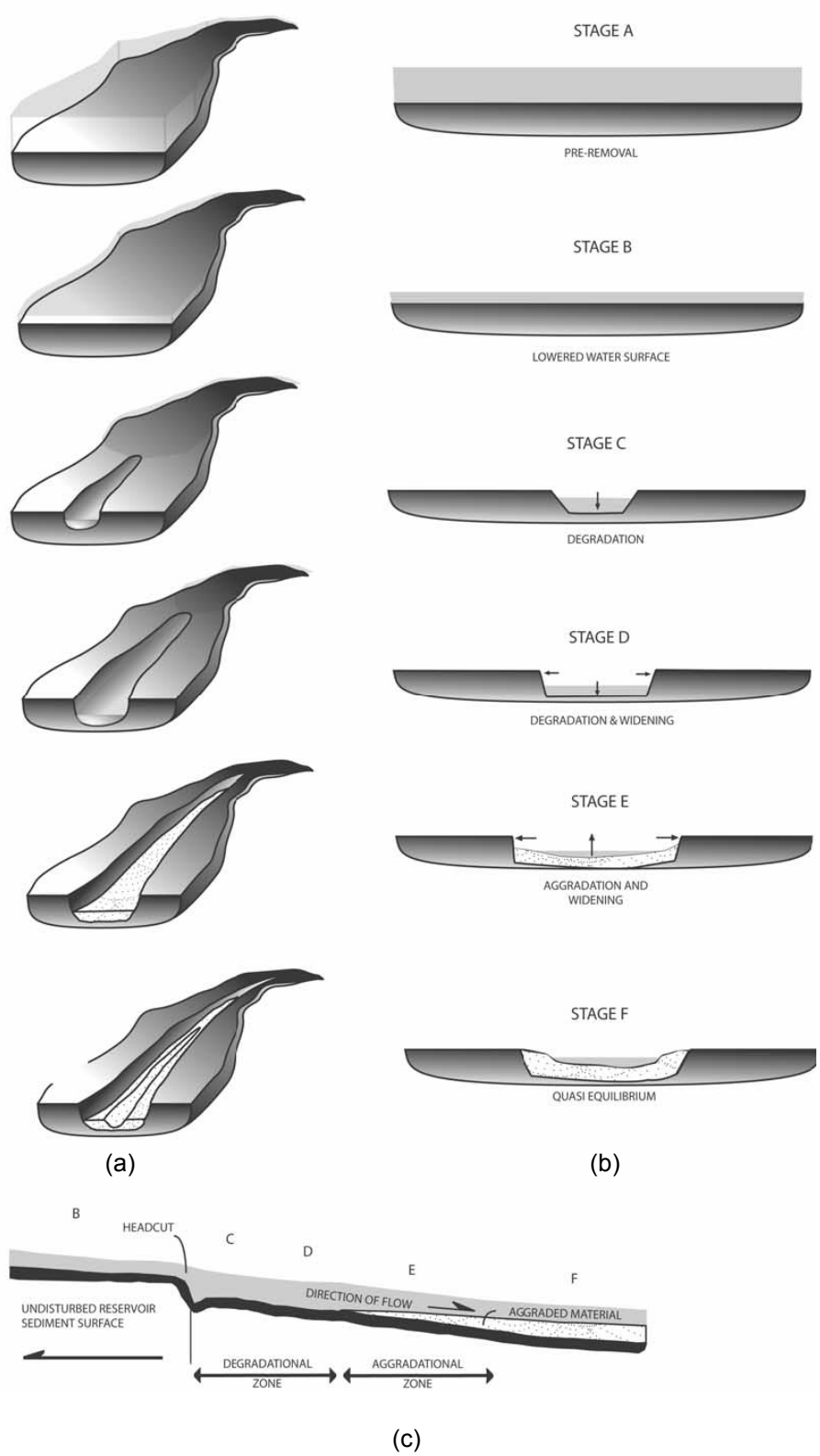

Figure 2.4. Conceptual channel evolution model upstream of dam removal (from Doyle *et al*. (2003a) and modified from Schumm *et al*. (1984); Simon and Hupp (1986)).

The following are two case studies in Wisconsin from Doyle *et al*. (2003a) explaining the geomorphic response to dam removal studied over a 14-month time period: 1) The response on the Koshkonong River at the Rockdale Dam (approximately 360 km^2 drainage area in the low-relief, glaciated region of south-central Wisconsin) is applicable to the Brewster Creek study; and 2) The Baraboo at the LaValle Dam (approximately 575 km^2 drainage area in the high-relief, unglaciated area of southwestern Wisconsin) gives a contrasting response given the differences in sediment between the two sites.

The Koshkonong River site had a distinct difference between the deposited surface sediment (36 percent sand, 45 percent silt, 19 percent clay) and the underlying coarser sediment (gravel with D_{50} greater than 3 mm) interpreted as the pre-dam channel substrate. The D_{50} is the median particle size of which 50 percent of the material is finer. At this site, headcut migration governed channel adjustments as a deep, narrow channel formed downstream of the headcut, with negligible changes upstream of the headcut. "There was little downstream sedimentation through time due to limited reservoir sediment erosion." (Doyle *et al*., 2003a)

The Baraboo River study reach contained a relatively uniform mixture of fine sand and silt with no gravel.

> "Upstream changes were rapid and included bed degradation, minimal bank erosion, and sediment deposition on channel margins and new floodplain. Sand was transported through the former impoundment and temporarily deposited downstream." (Doyle *et al*., 2003a)

> "These contrasting results highlight the potential role of head-cut migration on controlling rates of both upstream erosion and corresponding downstream sedimentation." (Doyle *et al*., 2003a)

The observations and conclusions of Doyle *et al*. (2003a) at the Koshkonong River site were that "staged drawdown of a reservoir and establishing vegetation following dam removal can reduce the quantity of sediment eroded from a reservoir."

Additional explanation of channel-incision processes related to dam removal were presented by Pizzuto (2002) and depended on the height and grain sizes of the sediment fill (Figure 2.5). In cohesive silt and clay sediments, a vertical headcut (an eroding vertical face in the streambed) is likely to migrate upstream through the fill (Pizzuto, 2002).

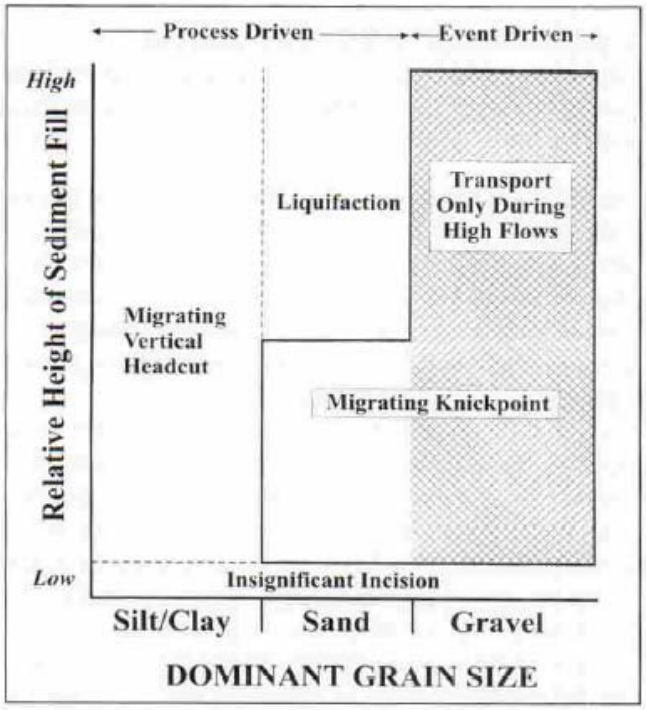

Figure 2.5. Speculative relations among the height of a reservoir sediment fill, the dominant grain size of the fill, and different processes of incision. Erosion of gravel depends on high-flow events; therefore, these incision processes are "event-driven." Incision of sand and of silt and clay do not depend on high-flow events, but rather on the mechanism of incision; therefore, removal of fills of sand and of silt and clay are "process-driven" (from Pizzuto (2002)).

Three studies conducted on streams in the mid-Atlantic region of the United States predict general trends regarding the effect of dam removal on mid-Atlantic streams (Skalak and Pizzuto, 2005). Major changes were determined to include significant aggradation or degradation of the bed, slope adjustments, channel width adjustments, changes in channel planform, formation of stable channel bars, and changes in stream type. Minor changes were determined to include textural adjustments of the bed, slight modifications of slope and width, and the formation of ephemeral bars.

"In some cases, the release of sediment during dam removal may be similar to what mobilizes naturally during a flood event." (Graber *et al*., 2001) An example is summarized by (Graber *et al*., 2001) of the

> "South Batavia Dam on the Fox River in Illinois found 19,000 cubic yards of fine grain sediment in the impoundment, but this amount was only 38 percent of the total annual sediment yield. Consequently, the release of this sediment or a portion thereof after dam removal was determined to have a minimal impact downstream, similar to natural flow events."

Retirement of dams nationwide were researched to develop insight into the actual retirement process (American Society of Civil Engineers, 1997). Case studies were reviewed objectively and sediment control was an issue common to all of the case studies.

2.1.2 Ecological Response

Full and partial ecosystem recovery through time are assumed asymptotic toward an equilibrium or steady-state after dam removal, although alternative recovery trajectories are possible (Figure 2.6) (Doyle and Stanley, 2005). The mussels have the slowest recovery in both recovery schemes. Transport and deposition of sediments were

found to likely contribute mussel mortality in a study by Sethi *et al*. (2004). Plants established in the first growing season, although if native species are desired, plans must be made to minimize the establishment of aggressive invading species (Orr and Stanley, 2006).

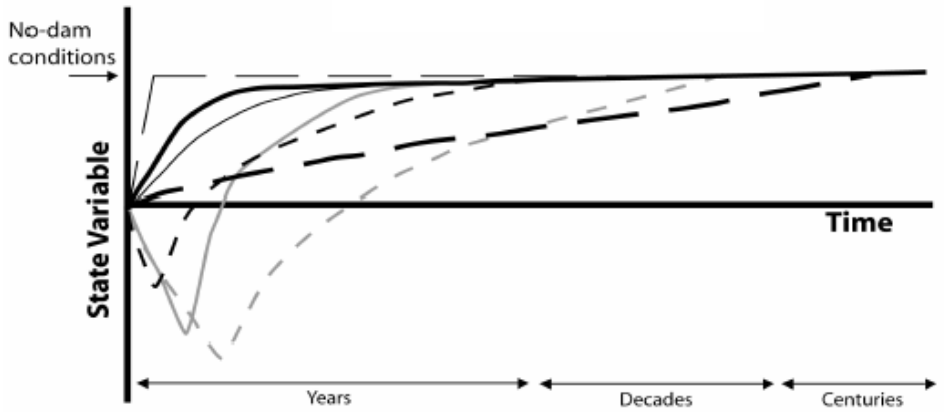

(a) Ecosystem full recovery

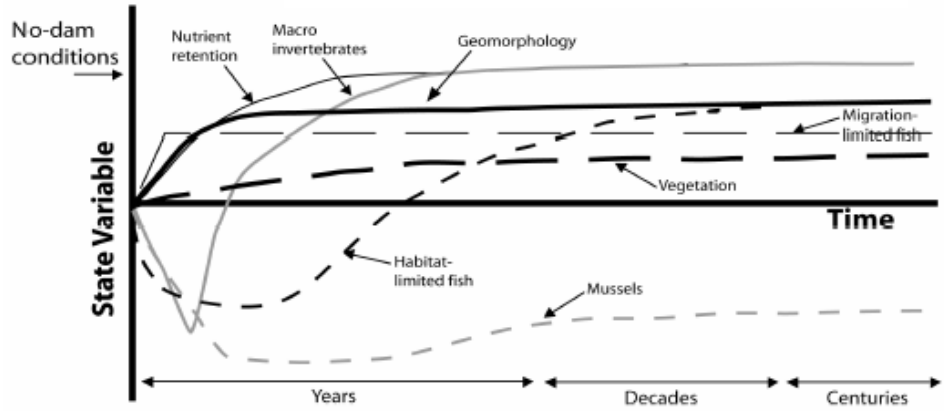

(b) Ecosystem partial recovery

Figure 2.6. Conceptual framework for ecosystem recovery following removal of a small dam (modified from Doyle and Stanley (2005)).

2.2 Knickpoint Theory and Laboratory Studies

A knickpoint or headcut is an oversteepened reach of a stream or old lake bed where erosion can occur if the eroding forces of the flow are greater than the resisting

forces of bed material (Schumm *et al*., 1984). Difficulties are present in examining actively migrating headcuts and limit the information available on the mechanics of headcut and knickpoint migration (Bennett *et al*., 2000a).

The Exner (1925) equation for bed sediment conservation, describes the level of sand that forms in the river bottom:

$$(1-\lambda_p)\frac{\partial \eta}{\partial t} = -\frac{\partial q_t}{\partial x} \qquad \textbf{Equation (2.1)}$$

where

λ_p = bed porosity;

η = level of the sand above an arbitrary datum;

t = time;

x = streamwise distance; and

q_t = volume total sediment transport rate per unit stream width.

Fredsoe (1978) provides a solution of the Exner equation that can be used for knickpoint migration fitting the uniformly nonresistant inclination category conceptualized by Gardner (1983) (Figure 2.7), where degradation and aggradation occur upstream and downstream of a fixed fulcrum. Gardner (1983) characterizes knickpoint evolution by three general models: 1) parallel retreat, 2) replacement, and 3) inclination. These models are primarily based on the relation between bottom shear stress (τ_o) and critical shear stress needed to initiate motion (τ_c). Bottom shear stress (τ_o) and erosion attain maximum values at the knickpoint lip (Figure 2.8), caused by incision along the channel thalweg, which decreases the channel width but increases flow depth and velocity towards the lip (Gardner, 1983).

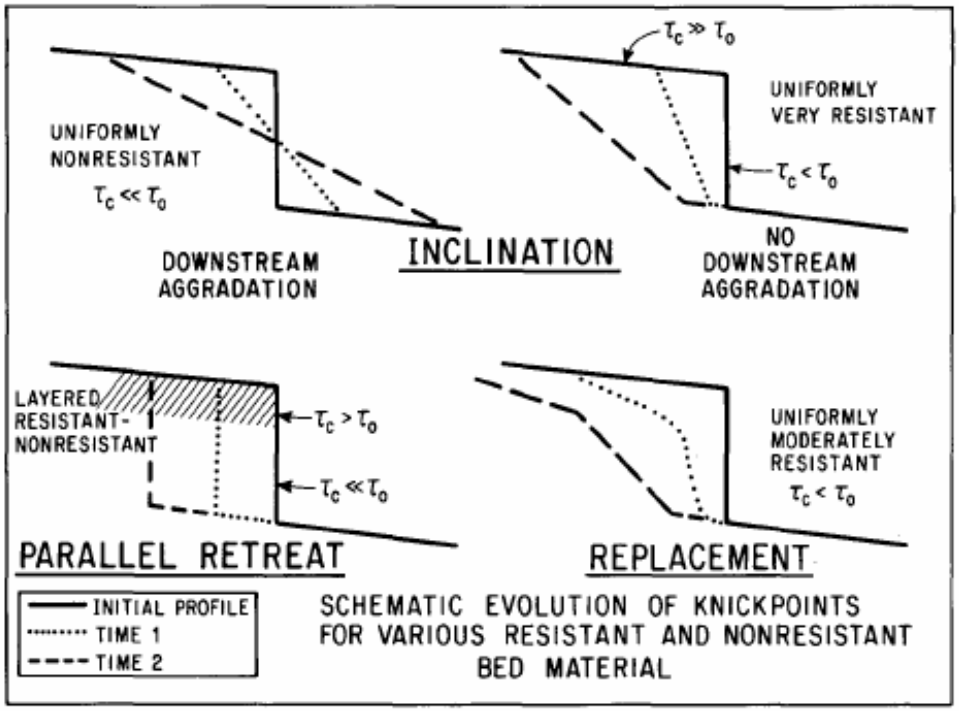

Figure 2.7. Models of knickpoint evolution for various types of bed material. τ_c is the critical bottom shear stress needed to initiate erosion. τ_o is the actual bottom shear stress (from Gardner (1983)).

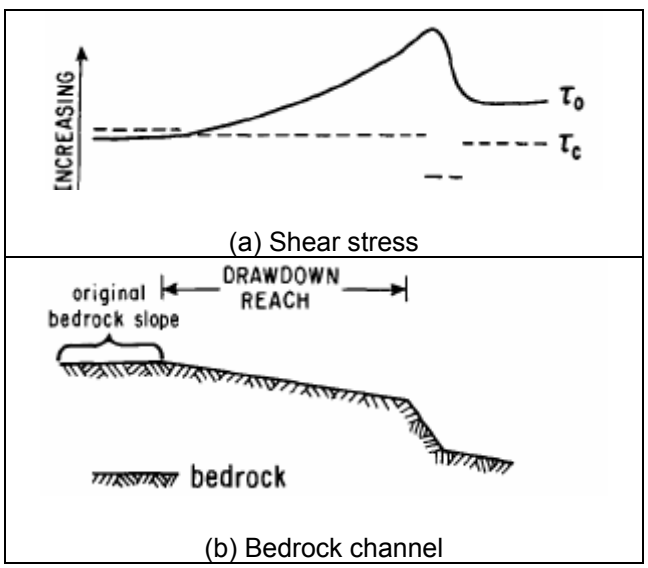

Figure 2.8. Variation in (a) bottom shear stress and (b) channel bed along a knickpoint reach for a model run (modified from Gardner (1983)).

In a study by Stein and Julien (1993), mode of headcut migration for homogeneous cohesive material was found to be a function of Froude number (F), and the aspect ratio of knickpoint drop height (D_n) to the normal depth (h_n) upstream of the knickpoint. The critical aspect ratio was defined by the following function of the Froude number (Stein and Julien, 1993):

$$\left.\frac{D_n}{h_n}\right|_C = 1.5\left(\frac{F^2 + 0.4}{F}\right)^2 \qquad \textbf{Equation (2.2)}$$

For an aspect ratio greater than the function, the headcuts migrated in a stepped (parallel retreat) mode. For an aspect ratio less than the function, the headcuts migrated in a rotational mode.

Although the shape and rate of bed adjustment differs for cohesive and noncohesive material, the process described in Gardner (1983) for cohesive material is similar to that described in noncohesive studies (Cantelli *et al*., 2004, 2006). Rapid and substantial narrowing occurs during the initial period of incision and is followed by a phase of slow widening (Cantelli *et al*., 2004, 2006). Large amounts of sediment are transported during the narrowing (Cantelli *et al*., 2004, 2006). In base-level lowering flume tests on cohesive soils, Begin *et al*. (1980) found similar time-dependent sediment transport with a power function decay of sediment discharge with time. In flume testing of cohesive soils, Aberle *et al*. (2004) found that once the critical threshold of erosion was exceeded, erosion increases sharply at the onset of each velocity level and then ceases. Aberle *et al*. (2004) developed an equation with an exponential decay of erosion rate with time.

Headcut development and migration in upland areas on sandy loam to sandy clay loam soil beds were studied by Bennett (1999a) and Bennett *et al*. (2000a).

> "During overland flow, soil erosion occurred exclusively at the headcut, and after a short period of time, a steady state condition was reached where the headcut migrated at a constant rate, the scour hole morphology remained unchanged, and sediment yield remained constant." (Bennett *et al*., 2000a)

2.3 Knickpoint and Cohesive Erosion Field Studies

Shear stress was found to be the primary factor for cohesive bed erosion in a study of a stream in eastern Nebraska (Hotchkiss and McClenathan, 1997). Other important factors affecting erosion included fluctuations in the flow, amount of clay, stress history, surface roughness, channel avulsion, surface discontinuities, vegetation, and effects from animals (Hotchkiss and McClenathan, 1997). The fluctuations in flow increased erosion showing the potential need for additional analysis of the more frequent flows in modeling and erosion prediction (Hotchkiss and McClenathan, 1997). In the Yalobusha River in Mississippi, Bennett *et al*. (2000b) postulated that the knickpoints become destabilized at the more frequent flows and when the height of the water downstream of the knickpoint was low.

An in-situ, jet-test device has been used to determine critical shear stresses and erosion rates of cohesive materials (Hanson and Simon, 2001; Simon and Thomas, 2002; Hanson and Cook, 2003; Hanson *et al*., 2004). This device has been used in various rivers including the Yalobusha River in Mississippi, where resistant clay beds have controlled advancement of knickpoints (Simon and Thomas, 2002). Knickpoint migration over a 10-yr period governed new channel development following the avulsion of Little Grassy Creek, Illinois (Ritter *et al*., 1999).

2.4 Cohesive Erosion Laboratory Tests and Modeling

The Erosion Function Apparatus (EFA) (Briaud *et al*., 2003) and other flume tests have been used to predict erosion rates and critical shear (Table 2.3) of cohesive sediments.

> "The transport, deposition, and erosion processes of cohesive sediments are extremely complex due to their highly varying properties and, therefore, behavior when their environment changes." (Langendoen, 2000)

The CONCEPTS model (Langendoen, 2000; Langendoen *et al*., 2000, 2001, 2002, 2005; Langendoen and Wells, 2006) uses the following equations to determine rates of erosion:

$$E = eB\left(\frac{\tau_b}{\tau_c} - 1\right) \qquad \textbf{Equation (2.3)}$$

Equation (2.3) is from Ariathurai and Arulanandan (1978), where e is erosion-rate constant, B is wetted width of the streambed, τ_b is bed shear stress, and τ_c is shear strength of the bed material. Sediment type, water content, total salt concentration, ionic species in the water, pH, and temperature will affect the erosion-rate constant (Mehta *et al*., 1989).

For soft (water content well above 100 percent), partially consolidated beds, $E = \varepsilon_f B \exp\left(\varepsilon\sqrt{\tau_b - \tau_c}\right)$. This equation from Parchure and Mehta (1985) is used where ε_f is floc erosion rate and ε is a rate constant. "When the excess shear stress becomes large, the bed may fail at some plane below the surface and clumps of material are mass eroded." (Langendoen, 2000)

Table 2.3. Range of critical shear values for cohesive materials (adapted from Briaud *et al*. (2003)).

Study	Critical Shear Stress Range τ_c (Pa)
Dunn (1959)	2 – 25
Enger *et al*. (1968)	15 – 100
Raudkivi (1976)	1 – 20
Lyle and Smerdon (1965)	0.35 – 2.25
Smerdon and Beasley (1959)	0.75 – 5
Arulanandan *et al*. (1975)	0.1 – 4
Arulanandan (1975)	0.2 – 2.7
Kelly and Gularte (1981)	0.02 – 0.4
Briaud *et al*. (1999)	0.18 – 2.7

CHAPTER 3

METHODS OF INVESTIGATION

Sediment erosion and stream-channel evolution and stability were analyzed utilizing data collected on streamflow, sediment transport, knickpoint migration, and stream-channel geometry and substrate. The dynamics of stream-channel evolution were analyzed by modeling the knickpoint shear stress for the stream-channel surveys and various streamflows. The knickpoint shear stresses were then related to sediment erosion providing a method to simulate erosion given varying physical and hydraulic conditions. Another prediction model was developed using the results from cohesive erosion testing on samples obtained from the lake bed, and conceptual and theoretical information regarding knickpoint migration.

The stability of the stream channel that evolved was assessed using stability indicators at six locations during and after removal. Two indicators of entrenchment were used. These indicators included the width-to-depth ratio using the main-channel top width and main-channel hydraulic depth at the 1.5-yr return period streamflow and the ratio of top width (*TW*) at the 100-yr return period by the main-channel *TW* at the 1.5-yr return period streamflow. The channel and valley slope calculated from survey data, and the energy slope for the 1.5- and 100-yr return period streamflow were compared to see if the channel slope was significantly steeper and, hence, possibly unstable. The average main-channel velocity and shear stress were calculated to determine the size of bed

material moved at the 1.5- and 100-yr return period streamflow. The measured D_{50} locations were then compared with the bed-material size moved to determine stability. The critical shear and erosion rates of cohesive bed material were determined from laboratory tests and were also compared to the shear stresses at the 1.5- and 100-yr return period streamflow.

3.1 Streamflow, Sediment, and Channel Geometry Data

Knowing the properties of streamflow is important when quantifying sediment erosion, and stream-channel evolution and stability. Automated streamflow gaging equipment was installed and operated by the USGS-IWSC at two stations (one upstream and one downstream of the dam) in June 2002 (Figures 1.1 and 1.3, and Table 3.1). At the downstream station, both streamflow and stage were determined at 5-minute time steps. At the upstream station, only stage was determined at 5-minute time steps and miscellaneous streamflow measurements were made during selected storm events. Measurements of discharge were made with current meters and acoustical flow meters. The methods of streamflow measurement and computation are described in Rantz *et al*. (1982) and Cutshaw *et al*. (2004).

Table 3.1. Streamflow and sediment stations used in the study and corresponding drainage areas, Brewster Creek near St. Charles, Illinois.

Station (Figures 1.1 and 1.3)	Station Number	Drainage Area (mi^2)
Downstream	05551030	14.00
Upstream	05551029	13.88

Sediment data are useful in quantifying the sediment yield into and out of Willow Lake on Brewster Creek. Sediment data are also useful in the analysis of stream-channel evolution and stability. Suspended-sediment gaging equipment was installed and operated by the USGS-IWSC at two stations (one upstream and one downstream of the dam) in June 2002 (Figures 1.1 and 1.3, and Table 3.1). At these continuous-record sediment stations, suspended-sediment concentrations were determined from samples collected with automatic water samplers collecting samples from a fixed point. Stage-weighted event, suspended-sediment samples were collected by electronically connecting the automatic suspended-sediment collector to the streamflow station. Periodic cross sections were obtained at various verticals with depth-integrating, isokinetic samplers to compare to and adjust the fixed-point samples for computing the mean suspended-sediment concentration at the cross section. All suspended-sediment samples were collected following protocols outlined in Edwards and Glysson (1999).

Methods used in the computation of sediment records are described in Guy (1970) and Porterfield (1972). During periods of rapidly changing flow, samples are collected more frequently (generally, multiple times on the rising and falling limbs of the storm hydrograph). Certain streamflow conditions cause the shear stress to be higher on the rising limb than on the falling limb of the hydrograph, causing larger sediment transport on the rising limb than on the falling limb for a given flow depth (Julien, 2002; Straub *et al*., 2006). Also, mass bank failures can occur on the falling limbs in flashy streams. The slump material may stay near the bank and then be transported downstream on the next rising limb of a storm, causing increased sediment concentrations on the rising limb as compared to the falling limb. Also, during low-flow periods, sediment can be deposited

in the stream channel and then again be transported during the rising limb of the next storm. Lastly, in general, the higher the flood peak, the higher the peak sediment concentration at a given location.

The computed sediment discharges for days of rapidly changing flow or concentration were computed by the subdivided-day method (time-discharge weighted average) (Guy, 1970; Porterfield, 1972). Therefore, for those days when the published sediment discharge value differs from the value computed as streamflow (ft^3/s) times mean suspended-sediment concentration (mg/L) times 0.0027 (conversion factor to tons/day), the sediment discharge for that day was computed by the subdivided-day method. For periods when no samples were collected, daily discharges of suspended sediment were estimated on the basis of streamflow, suspended-sediment concentrations observed immediately before and after the periods, and suspended-sediment concentrations for other periods of similar streamflow. The sediment load for a given day was calculated by the product of the sediment discharge and 1 day. The daily suspended-sediment loads for a year were then summed and divided by the number of days in a year and by the drainage area of the watershed to obtain the suspended-sediment yield. Note that the sediment loads at the downstream station were adjusted for some deposition that occurred between the station and the dam-removal site during the notching period as outlined in Appendix C.

The stream-channel assessments were completed to evaluate the conveyance, slope, and stability along the emerging profile of the new channel upstream of the dam. Cross-section and thalweg surveys were completed seven different times during the study. The timing and extent of the surveys are presented in Figure 3.1. The surveys

were completed with a combination of Trimble Global Positioning System (GPS) and Robotic Total Station equipment.

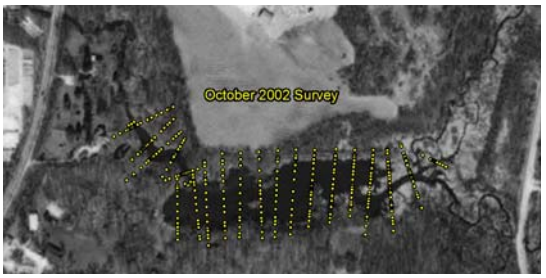

(a) October 2002 survey

(b) September 2003 survey

(c) April 2004 survey

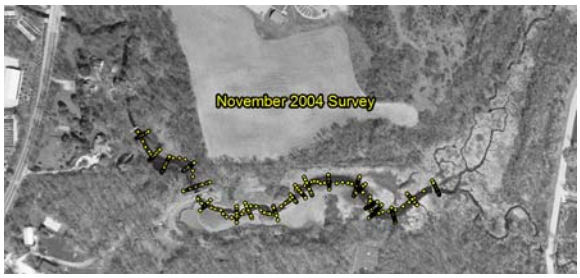

(d) November 2004 survey

(e) March 2005 survey

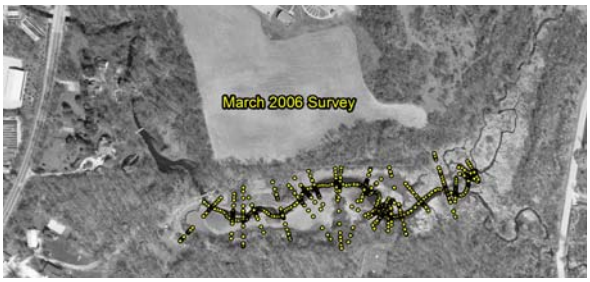

(f) March 2006 survey

(g) October 2006 survey

Figure 3.1. Cross-section and thalweg surveys completed throughout the study.

3.2 Cohesive-erosion Laboratory Testing

Laboratory tests on undisturbed cohesive sediment samples were completed to test erosive response to increasing velocity, shear stress, and specific stream power. Two types of samples were collected and tested in two different laboratory tests. The first sample type was collected with a standard Shelby tube with a 76.2-mm outside diameter (American Society for Testing and Materials (ASTM), 2007; Standard D1587) and tested in the Illinois Department of Transportation's Erosion Function Apparatus (Figures 3.2, 3.3, and 3.4). The second sample type was collected with a 508 mm x 215.9 mm. x 127 mm box-cutter sampler and tested in a flume at the Engineering Research Center at Colorado State University (Figures 3.2 and 3.5). Various soil properties were tested on the samples and used in the development of an empirical equation to relate soil properties, flow conditions, and erosion rates. The soil properties included particle-size distribution, Atterberg Limits, specific weight, moisture content, and torvane tests. The torvane tests were only completed on the flume samples.

The results from the cohesive-erosion testing were used in the prediction of knickpoint migration and the assessment of streambed stability.

(a) Shelby tube and box cutter

(b) Box cutter on the streambed

Credit: Photographs taken by Don Roseboom, USGS

Figure 3.2. Cohesive-sediment sampling instrumentation.

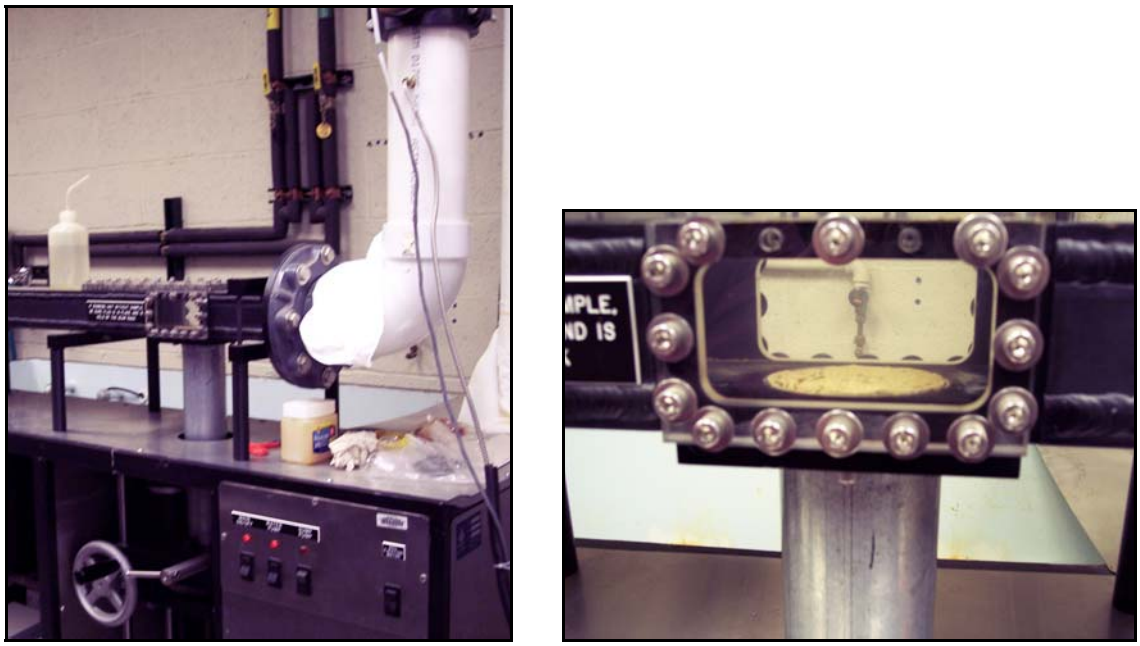

(a) (b)

Figure 3.3. Illinois Department of Transportation, Erosion Function Apparatus.

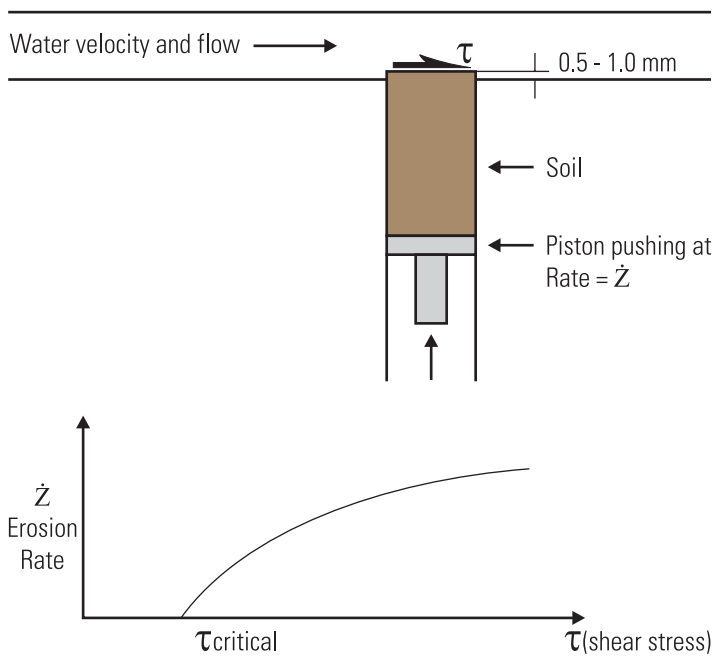

Figure 3.4. Erosion Function Apparatus conceptual diagram (modified from Briaud *et al*. (2003)).

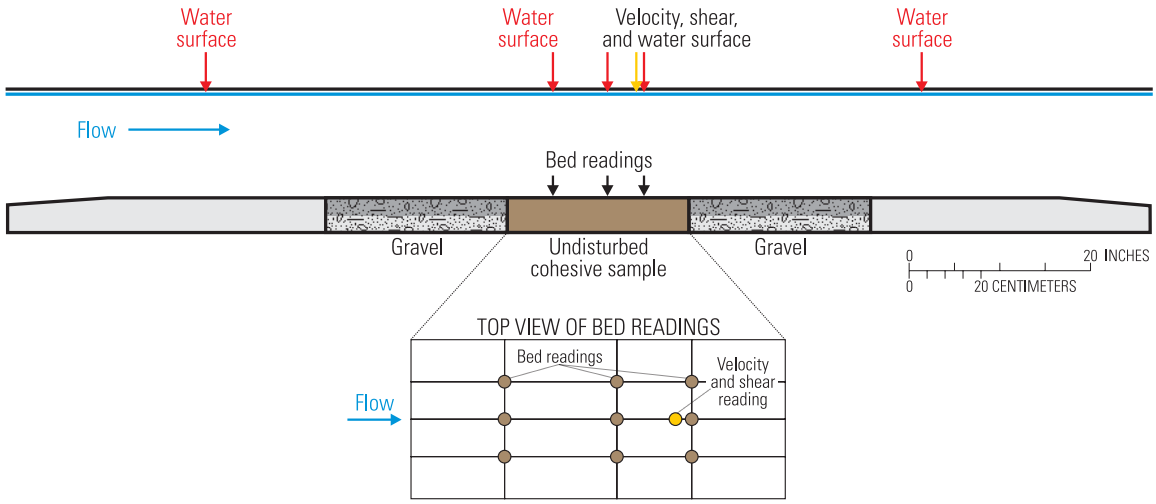

Figure 3.5. Colorado State University testing flume, measurement layout, and top view of bed readings (brown dots), and velocity and shear reading (yellow dot) of sample area.

3.2.1 Erosion Function Apparatus

Methods, description, and studies for the EFA are described in Briaud *et al*. (1999, 2002, 2003) and Kwak *et al*. (2001), and the methods are summarized in the following paragraphs.

A Shelby tube is placed through a circular opening in the bottom of a rectangular conduit (1.22-m long by 101.6-mm wide by 50.8-mm high) (Figure 3.4). A piston pushes the soil until it protrudes 0.5 to 1.0 mm into the rectangular conduit to be eroded by the flowing water (Figure 3.4). The erosion rate ($\dot{Z}$) for each flow velocity is determined by:

$$\dot{Z} = \frac{l}{t} \qquad \textbf{Equation (3.1)}$$

where l is the length of soil sample eroded in time t.

After several attempts at measuring the shear stress (τ) in the apparatus, the developers found that the best way to obtain τ was by using the Moody Chart (Moody, 1944) for pipe flows given as:

$$\tau = \frac{1}{8} f \rho v^2 \qquad \textbf{Equation (3.2)}$$

where

τ = shear stress on the sample;

f = friction factor obtained from the Moody Chart;

ρ = mass density of water (1,000 kg/m^3); and

v = mean flow velocity (m/s).

Each sample was subjected to velocities ranging from 0.6 to 5 m/s. The resulting bed shear stresses ranged from 1 to 43.8 Pa.

The friction factor (f) is a function of the pipe Reynold's number (Re) and the pipe relative roughness (ε/D). The Reynold's number is $(\nu D)/v$, where D is the pipe diameter and ν is the kinematic viscosity of water (10^{-6} m^2/s at 20°C). To ensure that the hydraulic diameter is equal to the diameter for a circular pipe (D) the following formula is used:

$$D = 2ab/(a+b) \qquad \textbf{Equation (3.3)}$$

where

a = height of the rectangular flume; and

b = width of the rectangular flume.

The average height of the surface roughness (ε) is assumed to be half the D_{50}, where D_{50} is the median grain size for the soil. Half the D_{50} is used because it is assumed that only half the particle protrudes into the flow, while the bottom half is buried.

3.2.2 Flume and Torvane

A 203-mm wide re-circulating flume with adjustable slope and tailwater conditions was used for erosion testing of the box-cutter samples. Each sample was tested at flow conditions that included three increasing discharges (0.0085, 0.014, 0.028 m^3/s) at a slope of 0.01 (m/m) followed by the maximum flow rate (0.028 to 0.042 m^3/s) at slopes up to 0.025 (m/m). The resulting bed shear stresses ranged from 3.97 to 37.8 Pa. Each sample was placed in the test section (Figure 3.5) and surrounded upstream and downstream with approximately 20-mm gravel. The gravel was used to control the elevation of the test approach section as the cohesive sample eroded. A large gravel size was needed due to the magnitude of shear stress produced during the testing. There is a variation in the hydraulic roughness from the approach section to the sample section; however, the benefit of lowering the test section was determined to be more important than equivalent roughness conditions. Water-surface and bed elevations were recorded at two stations upstream and downstream of the test section as well as at three stations in the test section (Figure 3.5). A velocity profile at 10, 20, 30, 40, and 80 percent of depth was also recorded at the sample section with a Son Tek Acoustic Doppler Velocity (ADV) meter.

Bed elevations of the cohesive sample were recorded with a point gage accurate to a thousandth of a foot for the initial conditions and after approximately 1-hr duration

for each flow regime. The bed elevations were recorded at nine locations on the sample mass (Figure 3.5).

The erosion rate, calculated as the average elevation change among all the bed readings, was measured at each velocity/shear stress above the critical shear/stream power threshold. The combination of hydraulic measurements coupled with bed-elevation measurements resulted in reasonable estimates of cohesive bed erosion as a function of bed shear, specific stream power, and unit stream power.

A hand-held torvane, Soil Test CL 600A device, was used to measure the shear-strength characteristics of the cohesive samples after the hydraulic-flume testing. The torvane device consists of a 25-mm diameter vane head with 5-mm blades that are pushed into the soil. The device is torsionally rotated in the soil until the soil mechanically fails within 5 to 10 seconds. The torvane spring is calibrated and a shear-strength reading between 0.01 and 1 (kg/cm^2) registers on the dial. The torvane device has been shown to provide reliable estimates of undrained shear strength in cohesive sediment samples ranging from soft to stiff clays (Papanicolaou, 2001; Das, 2002). Six readings were taken on each sample after testing. Readings taken after the hydraulic-flume testing represent fully-saturated conditions that are most likely present in a streambed during a flood event.

CHAPTER 4

EROSION DYNAMICS OF A STEPWISE SMALL DAM REMOVAL

The evaluation of erosion dynamics upstream of Brewster Creek dam was based on sediment erosion, stream-channel evolution, and stability analyses. These analyses utilized data collected on streamflow, sediment transport, knickpoint migration, and stream-channel geometry and substrate.

4.1 Sediment Erosion

Sediment erosion data were collected from June 2002 through September 2006. A summary of sediment loads for four time periods (Table 4.1) (pre-notching, notching, and two post-notching periods) are presented in Table 4.2. The time between notches was variable as the goal was to have at least one storm occur after a notch to allow sediment to erode before taking out another notch. A storm occurred between all notches except between Notches 1 and 2. The last notch was completed in February 2004, and the first storm after this notch is included in the "notching" time period.

Table 4.1. Time line of events during the study period.

Time Period	Event Type and Notch Height (ft)	Event Dates	Survey Date
Pre-notching 06/15/2002 - 06/14/2003	Storm	07/08/2002 - 07/15/2002	
	Storm	08/03/2002 - 08/10/2002	
	Storm	08/12/2002 - 08/16/2002	
	Storm	08/21/2002 - 08/29/2002	
			10/2002
	Storm	04/29/2003 - 05/03/2003	
	Storm	05/04/2003 - 05/12/2003	
	Storm	05/13/2003 - 05/22/2003	
Notching 06/15/2003 - 03/09/2004	**Notch 1 (1.5)**	06/19/2003 - 06/22/2003	
	Notch 2 (1.5)	07/14/2003 - 07/19/2003	
	Storm	07/30/2003 - 08/07/2003	
	Notch 3 (1.5)	08/19/2003 - 08/24/2003	
			09/15/2003
	Storm	11/01/2003 - 11/08/2003	
	Notch 4 (1.5) & Storm	11/17/2003 - 11/28/2003	
	Storm	12/08/2003 - 12/19/2003	
	Notch 5 (1)	02/18/2004 - 02/28/2004	
	Storm	03/03/2004 - 03/09/2004	
Post-notching 1 03/10/2004 - 09/30/2004	Storm	03/23/2004 - 04/01/2004	
			04/04/2004
	Storm	04/16/2004 - 04/27/2004	
	Storm	05/04/2004 - 05/25/2004	
	Storm	05/29/2004 - 06/07/2004	
	Storm	06/09/2004 - 06/15/2004	
	Storm	06/20/2004 - 06/23/2004	
	Storm	07/31/2004 - 08/05/2004	
	Storm	08/27/2004 - 08/29/2004	
Post-notching 2 10/01/2004 - 09/30/2006			11/02/2004
	Storm	12/05/2004 - 12/13/2004	
	Storm	01/10/2005 - 01/23/2005	
	Storm	02/02/2005 - 02/11/2005	
	Storm	02/12/2005 - 02/19/2005	
			03/31/2005
	Storm	03/31/2005 - 04/16/2005	
	Storm	01/28/2006 - 02/02/2006	
	Storm	03/06/2006 - 03/23/2006	03/10/2006
	Storm	06/09/2006 - 06/19/2006	
	Storm	09/22/2006 - 09/27/2006	
			10/08/2006

Table 4.2. Sediment loads and yields, and mean-daily streamflows upstream and downstream of Brewster Creek dam near St. Charles, Illinois.

Phase	Dates	Location	Sediment Load (tons)	Sediment Yield (*SY*) (tons/mi^2-yr)	Mean-daily Flow (*MDF*) (ft^3/s)	*SY*/*MDF* (tons/mi^2-yr-ft^3/s)
Pre-notching	06/15/2002 - 06/14/2003	Upstream	459	33	---	4.3
		Downstream	397	28	7.7	3.7
Notching	06/15/2003 - 03/09/2004	Upstream	267	26	---	5.6
		Downstream	709	69	4.7	14.6
Post-notching 1	03/10/2004 - 09/30/2004	Upstream	603	77	---	5.9
		Downstream	1,437	183	13.1	14.0
Post-notching 2	10/01/2004 - 09/30/2006	Upstream	675	27	---	5.4
		Downstream	889	32	4.9	6.5

--- = not calculated

During the pre-notching time period, the sediment load at the downstream station (397 tons) was less than at the upstream station (459 tons) (Table 4.2). The water impounded behind the dam trapped sediment in the pre-notching time period. The sediment yield at the upstream gage ranges from 26 to 77 tons/mi^2-yr (Table 4.2 and Figure 4.1), which is less than half or nearly half the expected sediment yield of 191 and 153 tons/mi^2-yr, respectively, determined from regional estimates (Bonini *et al*., 1983; Bhowmik *et al*., 1986). This low-sediment yield is likely attributable to the high-efficiency sediment trapping area upstream of the lake caused by the presence of the dam and the low gradient of the stream system (Figures 1.2 and 1.3). Whether a high sediment-retention area is present upstream of an impounded lake will help determine the number and time between notches with respect to the amount of sediment that can be released and still be within regional sediment-yield estimates.

A channel began to form in the lake-bed sediments during the notching time period. Evidence of the erosion process is apparent in the greater sediment loads at the downstream gage (709 tons) than was measured at the upstream gage (267 tons) (Table 4.2). During Notches 1 through 3, and the first storm after Notch 3, the sediment load (60 tons) is approximately six times lower than the sediment load during Notches 4 and 5, and the first storm after Notch 5 (382 tons) (Table 4.3).

The post-notching phase is broken into two time periods: 1) from March 9, 2004, through September 30, 2004, when the mean-daily flow was 13.1 ft^3/s; and 2) from October 1, 2004, through September 30, 2005, when the mean-daily flow was 4.9 ft^3/s (Table 4.2). During the first time period, the sediment yield (183 tons/mi^2-yr) (Table 4.2 and Figure 4.1) was within 20 and 4 percent of the expected regional estimate of annual

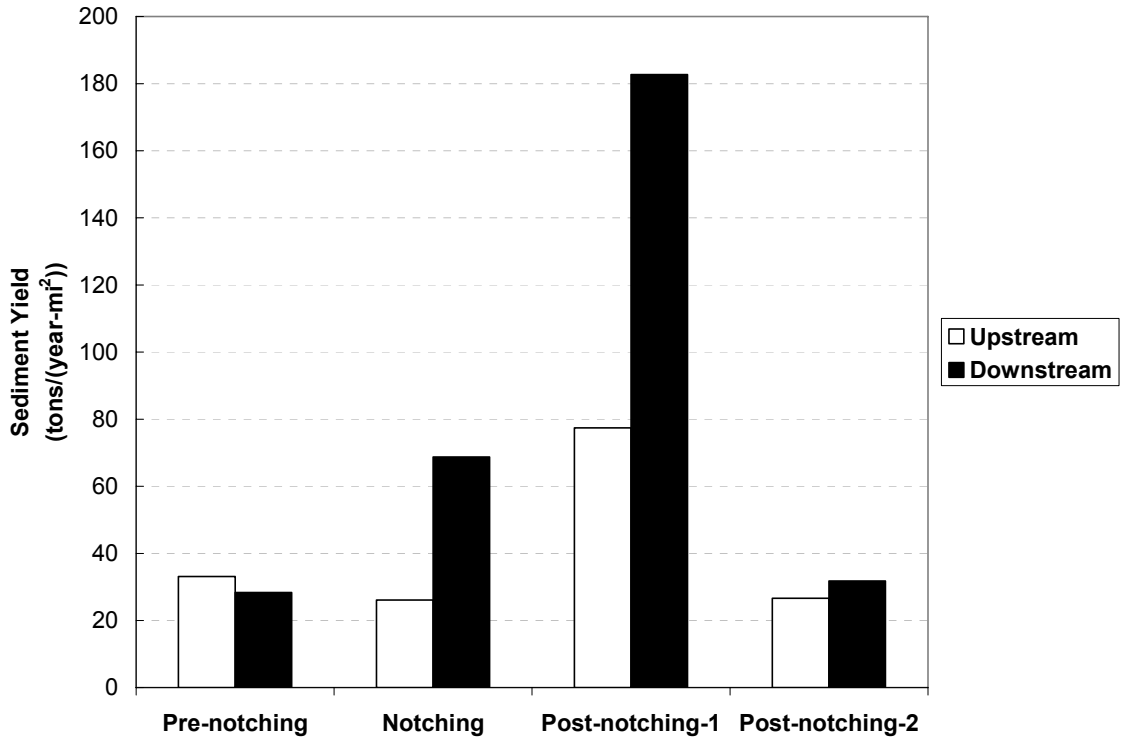

(a) Upstream and downstream sediment yields

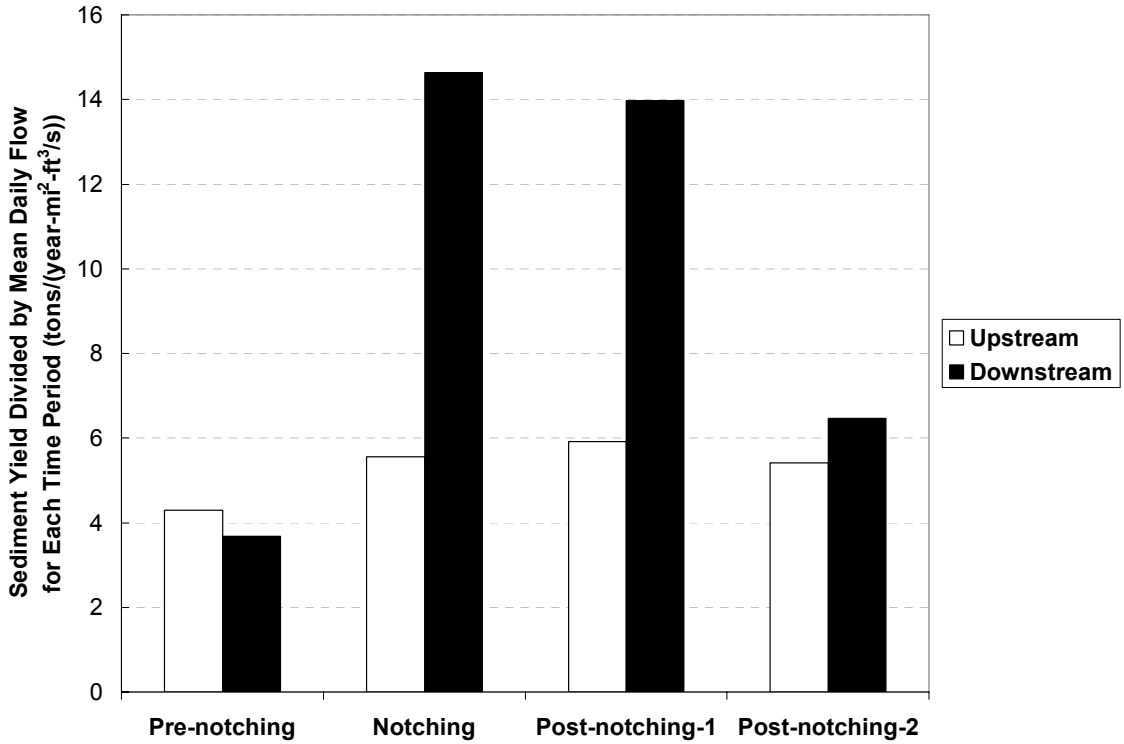

(b) Sediment yields divided by mean-daily flow

Figure 4.1. Sediment yield for each time period presented in Table 4.2.

Table 4.3. Sediment loads eroded from the lake by channel evolution determined from upstream and downstream station data and survey data downstream of the dam.

Phase	Dates	Sediment Load (tons)*	
		Time Period	Cumulative
Notches (1 - 3)	06/15/2003 - 11/16/2003	60	60
Notches (4 - 5)	11/17/2003 - 03/09/2004	382	442
Post-notching 1	03/10/2004 - 09/30/2004	834	1,276
Post-notching 2	10/01/2004 - 09/30/2006	214	1,490

*Downstream minus upstream sediment load

sediment yield of 153 and 191 tons/mi^2-yr, respectively (Bonini *et al*., 1983; Bhowmik *et al*., 1986). Erosion in the post-notching 1 time period (834 tons) accounted for 56 percent of the cumulative erosion as of September 30, 2006 (1,490 tons) (Table 4.3).

The sediment yield was normalized by dividing it by the mean-daily flow (ft^3/s) for the given time periods. The average upstream normalized sediment yield was 5.3 tons/mi^2-yr-ft^3/s with a standard deviation of 0.7 tons/mi^2-yr-ft^3/s for all phases (Table 4.2 and Figure 4.1). During the pre-notching time period, the downstream normalized sediment load was 3.7 tons/mi^2-yr-ft^3/s. As expected, the downstream normalized sediment yield increased during the notching and the post-notching 1 phase to 14.6 and 14.0 tons/mi^2-yr-ft^3/s, respectively. The downstream normalized sediment yield (6.5 tons/mi^2-yr-ft^3/s) in the post-notching 2 time period is within 17 percent of the upstream normalized sediment yield (5.4 tons/mi^2-yr-ft^3/s) for the same time period. This result is an indication that the stream channel evolving upstream of the old dam is becoming more stable.

The sediment volume was also calculated utilizing sediment surveys of the channel throughout the study. Summaries of these surveys are presented in Appendix C and Table 4.4. The volume of sediment deposited in the lake before the removal was

estimated to be 14.47 acre-ft from an October 2002 survey. The total sediment eroded (1.92 acre-ft) computed from the October 2006 survey indicates that approximately 13.3 percent of the lake sediment was eroded after the dam was removed.

Table 4.4. Total sediment deposited in October 2002 and sediment volumes eroded from the lake by channel evolution determined from survey data upstream of the dam.

Date	Sediment Volume (acre-ft)		Sediment Load[1] (tons)	
	Time Period	Cumulative	Time Period	Cumulative
October 2002 (total sediment deposited)	---	14.47	---	---
June 15, 2003 Notching Begins	---	---	---	---
September 15, 2003	0.090	0.090	69	69
April 4, 2004	0.681	0.771	519	588
November 2, 2004	0.955	1.726	728	1,316
October 8, 2006	0.194	1.920	148	1,464

[1]Assuming a dry specific weight of 35 lbs/ft^3
--- = not applicable

The shape of the impoundment is considered important to the expected total amount of sediment eroded (MacBroom, 2005). Dams can create an upstream pool approximately the same width as the downstream river reach or the pool can be several times the width of the downstream channel width. In the Brewster Creek study, the pool width was approximately 10 times the width of the channel that evolved after dam removal. If the pool width and the evolved channel width were more similar, a higher percentage of the deposited sediment would be eroded.

The lake-surface area before removal was approximately 3.96 acres giving an average sediment thickness of 3.7 ft (14.47 acre-ft / 3.96 acres). In this case, as a rough prediction of sediment load resulting from dam removal, the average sediment thickness (3.7 ft) times the distance between the abutments of the dam structure (24 ft) could be used, and an expected meandering reach length (938-ft thalweg reach length through the

old lake bed in October 2006 (Appendix C)) through the old lake bed yields a volume of 1.91 acre-ft. This volume is within 0.5 percent of the 1.92 acre-ft of sediment eroded as determined from the survey in October 2006 (Table 4.4).

A comparison of the sediment erosion determined by the stations and the surveys were completed to check the methods (Tables 4.3 and 4.4). The sediment volumes from the surveys need to be converted to tons of sediment for comparison with the station data. Utilizing dry specific weights of bank samples collected after the removal of the dam (approximately 35 lbs/ft^3) (data presented in Section 4.3.2, *Streambank*), the volumes are converted to tons.

The sediment load calculated from the September 15, 2003, survey (69 tons) (Table 4.4) is within 15 percent of the 60 tons for the notching 1 - 3 period (Table 4.3). The cumulative sediment load calculated from the November 2, 2004, survey (1,316 tons) (Table 4.4) is within 4 percent of the 1,276 tons estimated for the notching and the post-notching 1 time periods (Table 4.3). The cumulative sediment load calculated from the October 8, 2006, survey (1,464 tons) (Table 4.4) is within 2 percent of the 1,490 tons estimated in Table 4.3 for the notching and both post-notching time periods. This comparison shows that either method can be effective in determining the sediment load, but it would be difficult to refine the survey data to temporal storm events. Also, the survey data does not address the amount of sediment entering the stream system from other sources. It may also be difficult and dangerous to survey the lake sediments immediately after notching or storm events. A dual method of gaging and surveying allows for multiple options and checks in the calculation of sediment yield. Given the close match in sediment loads from the dual method, the data are defensible and can be

used in combination with stream-channel evolution and stability data to better understand erosion dynamics from stepwise small dam removal.

4.2 Stream-channel Evolution

Upstream channel evolution progressed throughout and after the stepwise removal of the dam. The process and timing of the channel evolution will be discussed in this section.

The magnitude of streamflows during the study was important to the stream-channel evolution and stability. A variety of flows resulted in the stream channel during the study period (Figure 4.2 and Table 4.5), with peak streamflows within 10 percent of the 1.5-yr recurrence interval streamflow (139 ft^3/s) on June 12, 2004. The 1.5-yr recurrence interval streamflow and various other recurrence interval streamflows are presented in Table 4.6. These estimates of flood frequency, determined from a combination of annual peak streamflows for the current study and historic values from a crest-stage gage at Illinois Route 25 (Figure 1.2), are presented in Table 4.7. A flood-frequency analysis was completed on the peak streamflows with methods outlined in Thomas *et al*. (1998).

Because of the stepwise dam removal, Brewster Creek cut through the former lake-bed sediment in stages to establish a meandering channel (Figures 1.3, 4.3, 4.4, and 4.5). As expected, the channel evolution was most active during and after storm events (Table 4.5). The channel emerged after the first notching and gradually developed. Similar to the sediment-erosion results, a substantial evolution did not occur until after the fourth and fifth notch, when the channel widened and meanders emerged.

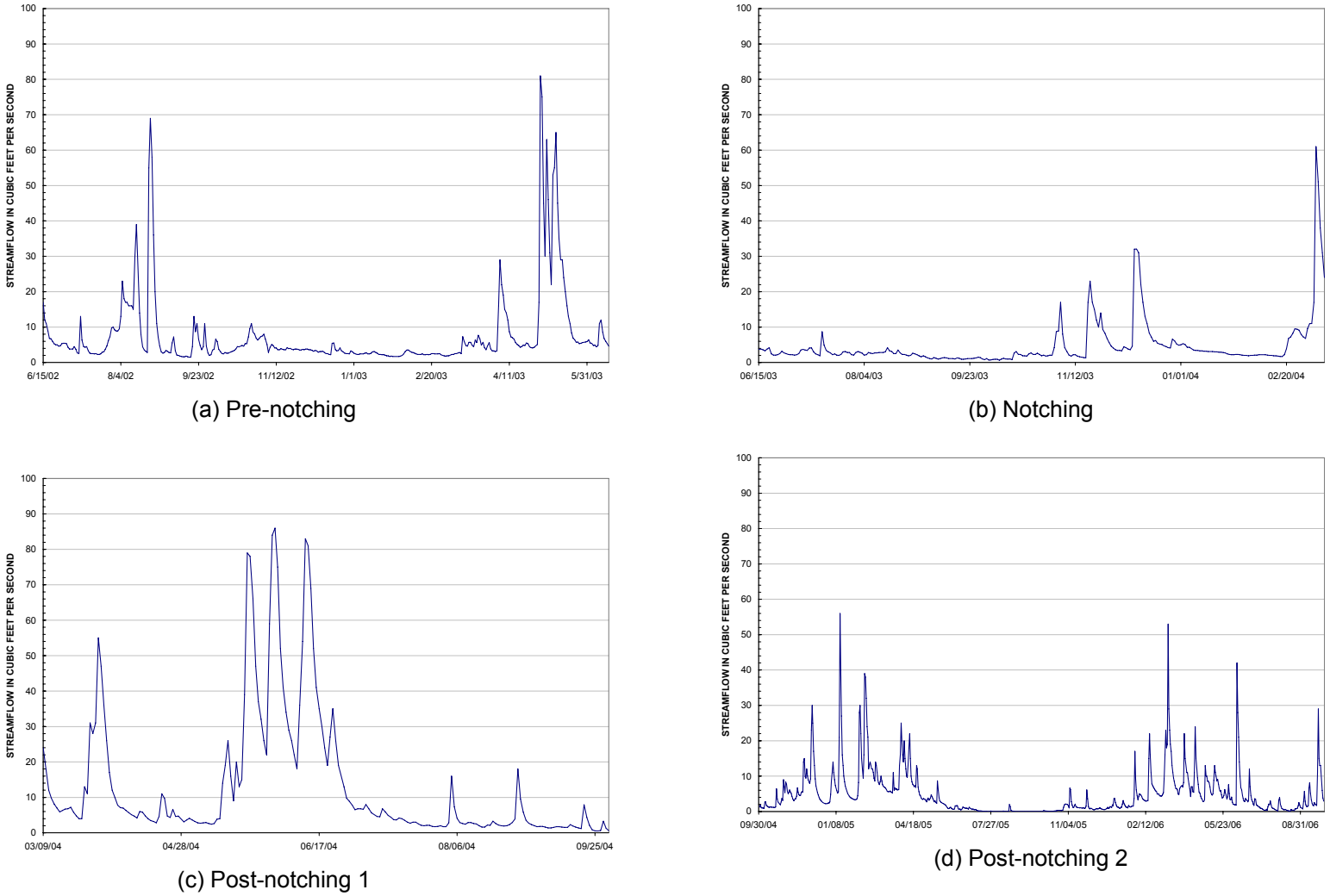

Figure 4.2. Mean-daily flows for the four time periods during the study.

Table 4.5. Highest seven mean daily and peak flows for each of the four time periods during the study.

Time Period	Date	Mean Daily (ft^3/s)	Peak Flow (ft^3/s)
Pre-notching	8/5/2002	23	27
	8/14/2002	39	42
	8/23/2002	69	74
	4/5/2003	29	36
	5/1/2003	81	95
	5/5/2003	63	87
	5/11/2003	65	89
Notching	7/15/2003	8.7	19
	11/5/2003	17	22
	11/19/2003	23	32
	11/24/2003	14	18
	12/11/2003	32	42
	2/24/2004	9.5	12
	3/5/2004	61	91
Post-notching 1	3/29/2004	55	60
	5/15/2004	26	28
	5/22/2004	79	97
	6/1/2004	86	96
	6/12/2004	83	111
	6/22/2004	35	41
	8/28/2004	18	29
Post-notching 2	12/8/2004	30	34
	1/13/2005	56	61
	2/8/2005	30	36
	2/14/2005	39	44
	3/13/2006	53	77
	6/10/2006	42	57
	9/23/2006	29	35

Table 4.6. Recurrence interval and corresponding streamflow values for Brewster Creek.

Recurrence Interval	Streamflow (ft^3/s)
1.5	139
2.0	193
2.33	221
5	354
10	477
25	646
50	780
100	920
500	1268

Table 4.7. Annual peak streamflows for the current study time period and station location, and historical values from a crest gage at Illinois Route 25 (Figure 1.3).

Water Year	Date	Peak Streamflow (ft^3/s)
1962	03/19/62	125
1963	04/30/63	73
1964	04/06/64	56
1965	02/07/65	105
1966	02/10/66	201
1967	06/10/67	687
1968	08/17/68	226
1969	06/08/69	158
1970	06/02/70	292
1971	02/19/71	408
1972	09/17/72	671
1973	04/22/73	221
1974	05/16/74	408
1975	03/18/75	325
1976	03/05/76	275
1978	07/02/78	156
1979	08/10/79	352
2003	05/02/03	100
2004	06/12/04	111
2005	01/12/05	62
2006	03/13/06	77

(a) Willow Lake pre-dam removal

(b) After Notch 1 – June 20, 2003

(c) After Notch 2 – July 16, 2003

(d) 1 month after Notch 3 – September 15, 2003

Credit: Figures 4.3(a) and (d) photographs were taken by Karen Kosky, KCDEM

Figure 4.3. Repeated photographs taken from the footbridge 15 ft downstream of the old dam looking upstream.

(a) Stream-channel evolution as of November 4, 2003

(b) After Notch 4 – November 20, 2003

(c) Stream-channel evolution as of December 29, 2003

(d) 2 weeks after Notch 5 – March 5, 2004

(e) Stream-channel evolution as of March 8, 2004

(f) Stream-channel evolution as of March 30, 2004

Credit: Photographs were taken by Karen Kosky, KCDEM

Figure 4.4. Repeated photographs taken from the footbridge 15 ft downstream the old dam looking upstream.

(a) Stream-channel evolution and vegetative response throughout the summer of 2004 – June 23, 2004

(b) Stream-channel evolution and vegetative response throughout the summer of 2004 – July 26, 2004

(c) Stream-channel evolution and vegetative response throughout the summer of 2004 – August 25, 2004

(d) Photograph on August 23, 2006

Credit: Figures 4.5(a)-(c) photographs were taken by Karen Kosky, KCDEM

Figure 4.5. Repeated photographs taken from the footbridge 15 ft downstream the old dam looking upstream.

The end result was similar to channel evolution models (CEMs) discussed in previous studies (Schumm *et al*., 1984; Simon and Hupp, 1986; Doyle *et al*., 2003a; MacBroom, 2005). In this study, the erosion dynamics of stepwise dam removal on channel evolution were analyzed and the CEM studies are used to provide a conceptual framework for analysis. The pre-dam impoundment could be classified in the conceptual

CEMUD (MacBroom, 2005) as a dam with fine sediment present and uniform sediment distribution (Figure 2.3). The channel-evolution process was similar to the 1-yr study on Koshkonong River (Doyle *et al*., 2003a). The deposited sediments at Brewster Creek were primarily silts and clays, and the old streambed was composed of primarily sand, gravel, cobble, and resistive cohesive material. Once the incision from the base lowering of the dam encountered the more resistant old streambed material, the channel began the widening process.

After the first notching, a knickpoint was established and developed over time with further notchings and storms (Figures 4.6, 4.7, 4.8, 4.9, and 4.10, and Table 4.8). A knickpoint is an oversteepened reach of a stream or old lake bed where erosion can occur if the eroding forces of the flow are greater than the resisting forces of bed material (Schumm *et al*., 1984). The base-level lowering of the dam determines the size of the knickpoint. A more stepwise drop in base level will allow a staged progression and size of knickpoint. Most of the sediment will erode as the knickpoint progresses through the old stream channel. If a large flood occurs immediately after lowering the dam, floodplain sediments could be eroded. As in the case of Brewster Creek, if the floodplain sediments are allowed to dewater and vegetate, the stability of these sediments will increase and be less likely to erode. Given these stabilizing effects of the stepwise lowering, sediment yield would be less during and after lowering than if the entire dam were removed at one time.

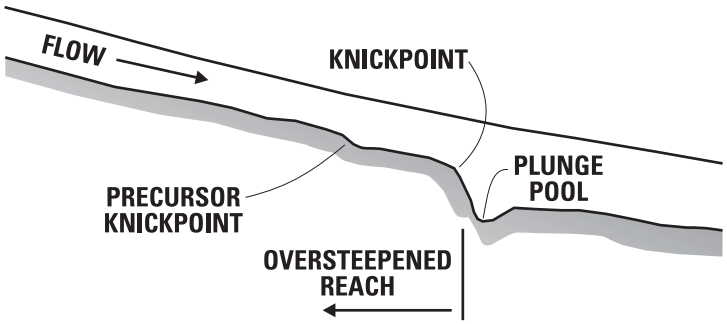

Figure 4.6. Diagram of a knickpoint (modified from Schumm *et al*. (1984)).

(a) Knickpoint progression on April 4, 2004 (views looking upstream)

(b) Knickpoint progression on the morning of May 17, 2004 (view looking downstream)

(c) Knickpoint progression on May 25, 2004 (view looking upstream)

Credit: Figure 4.7(a) photographs taken by Don Roseboom, Figure 4.7(b) photograph taken by Gary Johnson, and Figure 4.7(c) photograph taken by David Soong all of the USGS

Figure 4.7. Knickpoint progression after stepwise dam removal of Brewster Creek dam near St. Charles, Illinois.

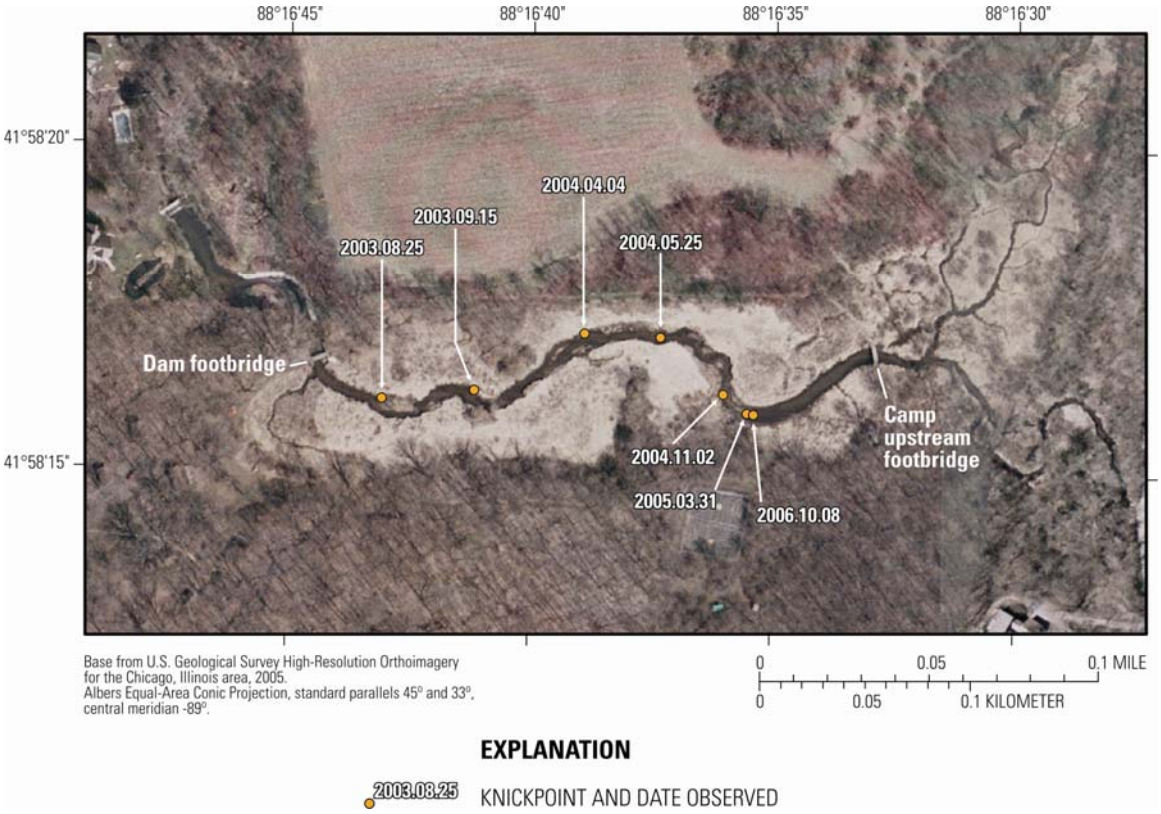

Figure 4.8. Primary knickpoint location throughout the study and selected cross-section locations.

Credit: Photograph taken by Don Roseboom, USGS

Figure 4.9. Knickpoint on October 18, 2006 after stepwise dam removal of Brewster Creek dam near St. Charles, Illinois (view looking upstream).

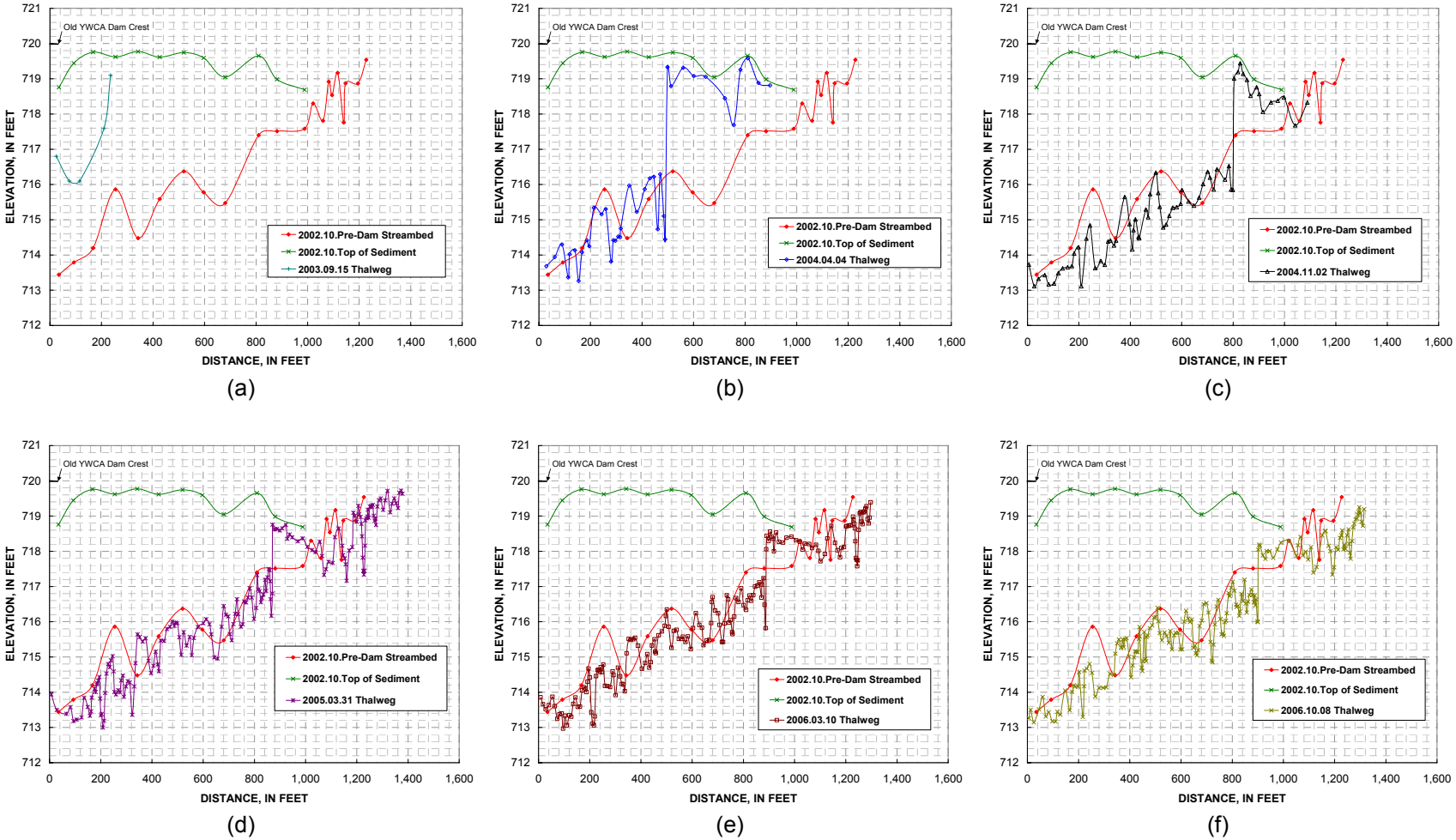

Figure 4.10. Surveyed top of deposited sediment and assumed pre-dam streambed in 2002, and thalweg and knickpoint locations surveyed at various times throughout the study.

Table 4.8. Knickpoint height and migration lengths between observations or surveys.

Knickpoint Observation or Stream-channel Survey		End Date Knickpoint Height (ft)	Time Period Duration (days)	Migration Length		Migration Rate (ft/day)
Start Date	End Date			Time Period (ft)	Cumulative (ft)	
06/22/2003	08/25/2003	1.5	64	115	115	1.80
08/25/2003	09/15/2003	1.5	21	110	225	5.24
09/15/2003	04/04/2004	4.3	202	274	499	1.36
04/04/2004	05/25/2004	4.3	51	122	621	2.39
05/25/2004	11/02/2004	2.8	161	206	827	1.28
11/02/2004	03/31/2005	1.6	149	43	870	0.29
03/31/2005	03/10/2006	1.4	344	20	890	0.06
03/10/2006	10/08/2006	1.3	212	38	908	0.18

4.2.1 Knickpoint Shear Calculations

Seven surveys of the channel were completed at different times during the study. A one-dimensional flow model (using Hydrologic Engineering Center, River Analysis System (HEC-RAS) (U. S. Army Corps of Engineers (USACE), 2001)) was developed for each set of survey data to analyze the knickpoint and stream-channel stability. Utilizing the HEC-RAS model built for each survey, the shear stress acting upon the knickpoint and streambed were analyzed at various streamflows, locations, and times throughout the study. The knickpoint height and downstream backwater effect influence shear stress exerted to move the knickpoint. The shear stress across the knickpoint was calculated using the following equation with the parameters shown in Figure 4.11:

$$\tau_{kn} = \gamma \; HDC \; Sf_{ac} \qquad \textbf{Equation (4.1)}$$

where

τ_{kn} = shear stress across the knickpoint;

γ = specific weight of water;

HDC = main-channel hydraulic depth upstream of the knickpoint; and

Sf_{ac} = friction slope across the knickpoint = ($EGE\text{-}US - EGE\text{-}DS$) / D_{ac}.

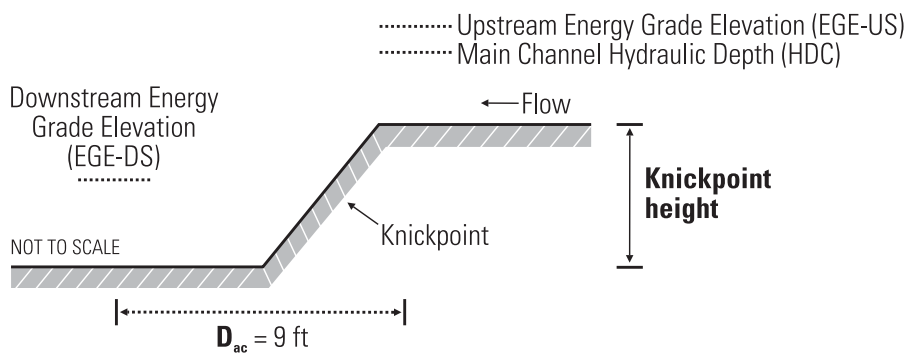

Figure 4.11. Knickpoint shear-stress parameter diagram.

The results of the model simulations for the knickpoints are presented in Table 4.9, and Figures 4.12 and 4.13 show how the flow causing the highest shear-stress changes for the different knickpoint locations and heights. Note that the abutments and embankments for the old dam were left in place after the removal leaving a 24-ft wide opening to convey the various flows. The 100-yr streamflow does not overtop the embankments. The results indicate that the remnant abutments and embankments create a sediment and stormwater detention area for the 10- and 100-yr streamflows for all the dates and locations. The backwater effects from the downstream remnant abutments and embankments limited the shear stresses acting on knickpoints for the 10- and 100-yr streamflows. With the dam only partially removed at September 15, 2003, the backwater from the remaining structure (essentially a lateral constriction weir) has a reduced shear

stress on the knickpoint for streamflows greater than or equal to 100 ft^3/s. The results for the October 8, 2006, location also show that backwater from channel control can have a reduced shear stress on the knickpoint for flows greater than or equal to 100 ft^3/s. The streamflows occurring during the study were some of the most critical for knickpoint migration (Figure 4.2, and Tables 4.5 and 4.7). The results from this section are used in relating knickpoint shear stress and measured sediment load.

Table 4.9. Shear stress for various flows across the surveyed knickpoints.

Date and Location (Figure 4.10)	Shear Stress (in Pa) for Various Flows Across the Knickpoint (Calculations in Appendix D)						
	5 CFS	13 CFS	50 CFS	100 CFS	Q1.5 (139 CFS)	Q10 (477 CFS)	Q100 (920 CFS)
09/15/2003 Station 225	37.4	53.2	101.6	3.2	3.9	8.1	11.7
04/04/2004 Station 487	56.7	60.4	192.8	168.7	136.1	9.0	14.0
11/02/2004 Station 802	62.1	73.3	108.4	136.2	143.5	25.4	16.0
03/31/2005 Station 829	49.0	47.3	46.0	96.4	141.3	32.1	13.5
10/08/2006 Station 900	59.8	69.3	74.2	27.5	20.7	6.5	8.9

CFS = cubic feet per second

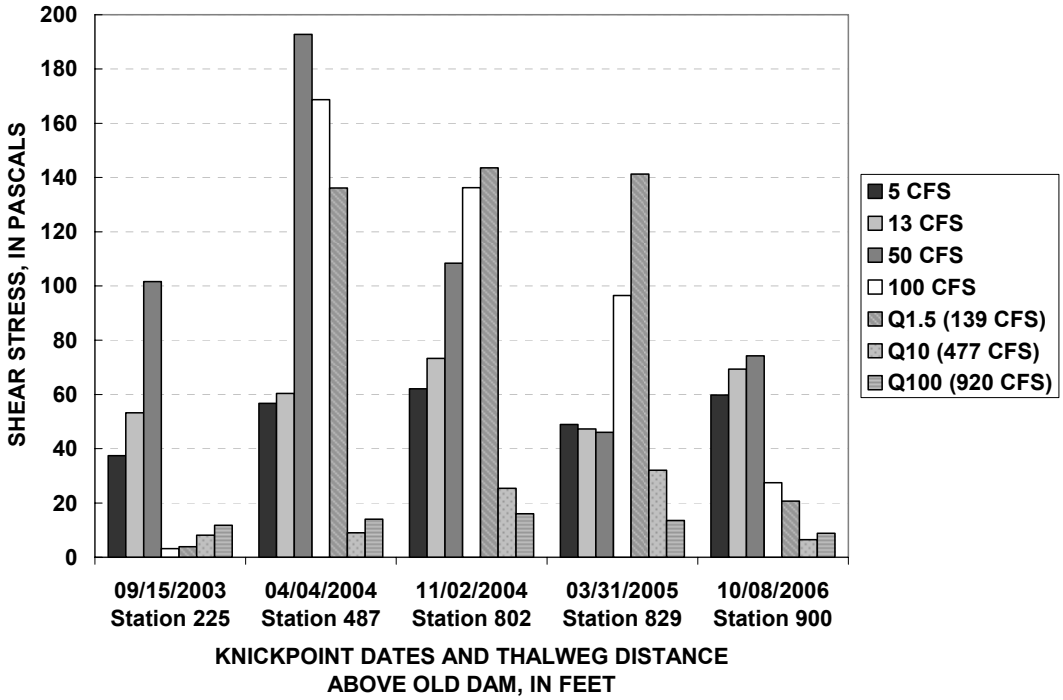

Figure 4.12. Variation in shear stress, flow, and knickpoint location and survey date.

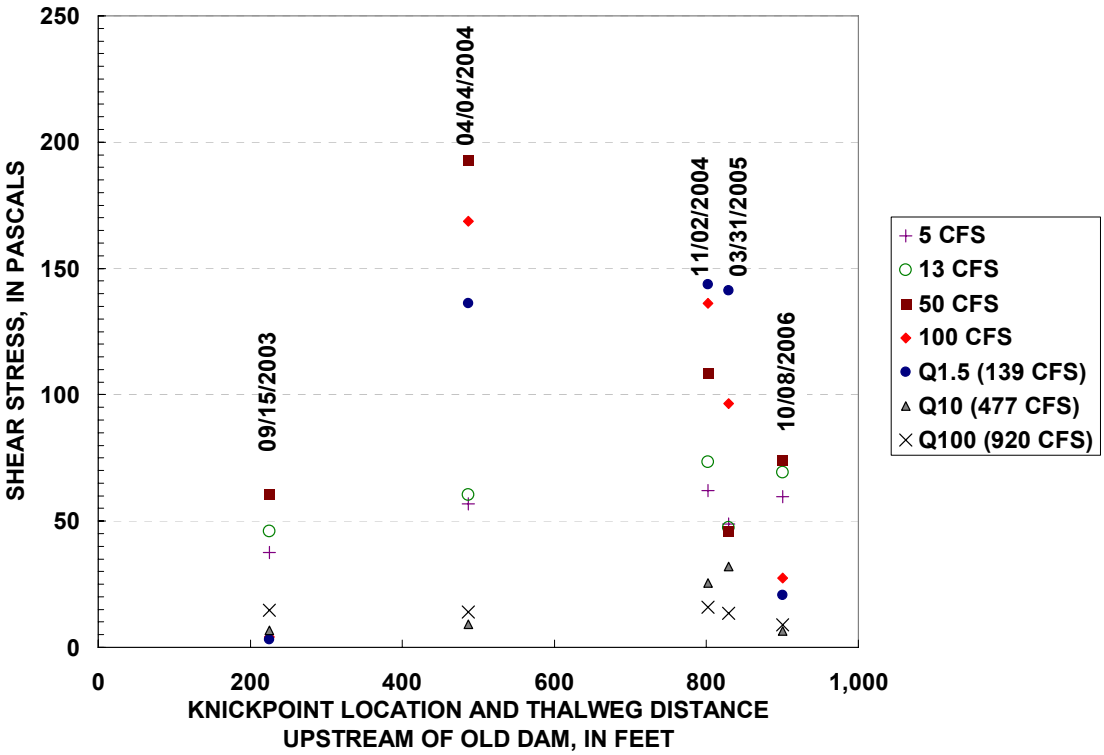

Figure 4.13. Knickpoint shear stress and knickpoint location and thalweg distance upstream of old dam.

4.2.2 Knickpoint Shear Stress and Sediment Erosion Relation

An equation to predict the erosion amounts during channel evolution was determined by relating the measured sediment loads to knickpoint shear stress for storm events throughout the study. The largest storms with a storm event maximum mean-daily flow over 10 ft^3/s during and post-notching through February 2005 were selected for this analysis (Table 4.10). The eroded sediment for sixteen storms (1,297 tons) from November 2003 through February 2005 (Table 4.10) accounts for approximately 87 percent of the total sediment eroded (1,490 tons) during channel evolution (Tables 4.3 and 4.10).

Table 4.10. Sediment load, streamflow, and knickpoint characteristics for each of the largest storms during and after notching.

Storm Time Period	Sediment Load		Sediment Eroded (*SE = SD - SU*) (tons)	Maximum Mean-daily Flow for Storm (*MMDF*) (ft^3/s)	Knickpoint Shear Stress for *MMDF* (Pa)	Erosion Index *EI = SE/MMDF* (tons/(ft^3/s))	Percent of Total Erosion (1,490 tons as of 09/30/2006)	Survey for Knickpoint Shear Stress	Knickpoint Height (ft)
	Downstream (*SD*) (tons)	Upstream (*SU*) (tons)							
11/01/2003 - 11/08/2003	41.4	10.8	30.6	17.0	58.47	1.8	2	09/15/2003	1.5
11/17/2003 - 11/28/2003	56.4	20.3	36.1	23.0	66.31	1.6	4	09/15/2003	1.5
12/08/2003 - 12/19/2003	158.6	54.7	103.9	32.0	128.39	3.2	11	04/04/2004	4.3
02/18/2004 - 03/09/2004	303.4	91.9	211.5	38.0	149.86	5.6	26	04/04/2004	4.3
03/23/2004 - 04/01/2004	388.4	153.7	234.7	55.0	190.40	4.3	41	04/04/2004	4.3
04/16/2004 - 04/27/2004	26.8	10.9	15.9	11.0	59.46	1.4	42	04/04/2004	4.3
05/04/2004 - 05/25/2004	386.3	111.0	275.3	79.0	178.83	3.5	61	04/04/2004	4.3
05/29/2004 - 06/07/2004	260.7	95.8	164.9	86.0	175.45	1.9	72	04/04/2004	4.3
06/09/2004 - 06/15/2004	233.1	74.6	158.5	83.0	176.90	1.9	83	04/04/2004	4.3
06/20/2004 - 06/23/2004	40.8	27.9	12.9	35.0	94.18	0.4	84	11/02/2004	2.8
07/31/2004 - 08/05/2004	13.7	11.0	2.7	16.0	76.15	0.2	84	11/02/2004	2.8
08/27/2004 - 08/29/2004	10.0	6.2	3.8	18.0	78.04	0.2	84	11/02/2004	2.8
12/05/2004 - 12/13/2004	40.8	29.8	11.0	30.0	89.44	0.4	85	11/02/2004	2.8
01/10/2005 - 01/23/2005	77.4	51.9	25.5	56.0	111.76	0.5	86	11/02/2004	2.8
02/02/2005 - 02/11/2005	24.7	27.3	-2.6	30.0	46.73	-0.1	86	03/31/2005	1.6
02/12/2005 - 02/19/2005	57.0	45.1	11.9	39.0	46.41	0.3	87	03/31/2005	1.6
Total 11/01/2003 - 02/19/2005			**1297**						
Total 11/01/2003 - 06/15/2004			**1231**						

The knickpoint shear stress was calculated for the maximum mean-daily streamflows during each storm (Table 4.10). The knickpoint shear-stress relation (Table 4.9) used for each storm time period was determined by the proximity of the storm to the survey. The eroded sediment was calculated for each storm by subtracting the downstream sediment load by the upstream sediment load (Table 4.10).

The knickpoint shear stress was then plotted with eroded sediment for each storm (Figure 4.14). For the storms that occurred before 84 percent of the sediment was eroded from the lake sediments, the relation between sediment eroded and knickpoint shear stress is given by the equation:

$$SE = 0.0081\tau_{kn}^{1.965}$$ **Equation (4.2)**

where

SE = sediment eroded during channel evolution for the storm event in tons; and

τ_{kn} = knickpoint shear stress for the flow conditions at the maximum of the mean-daily flows for the storm event.

For the storms that occurred after 84 percent of the sediment was eroded from the lake sediments, the relation between sediment eroded and knickpoint shear stress is given by the equation:

$$SE = 0.1312\tau_{kn}$$ **Equation (4.3)**

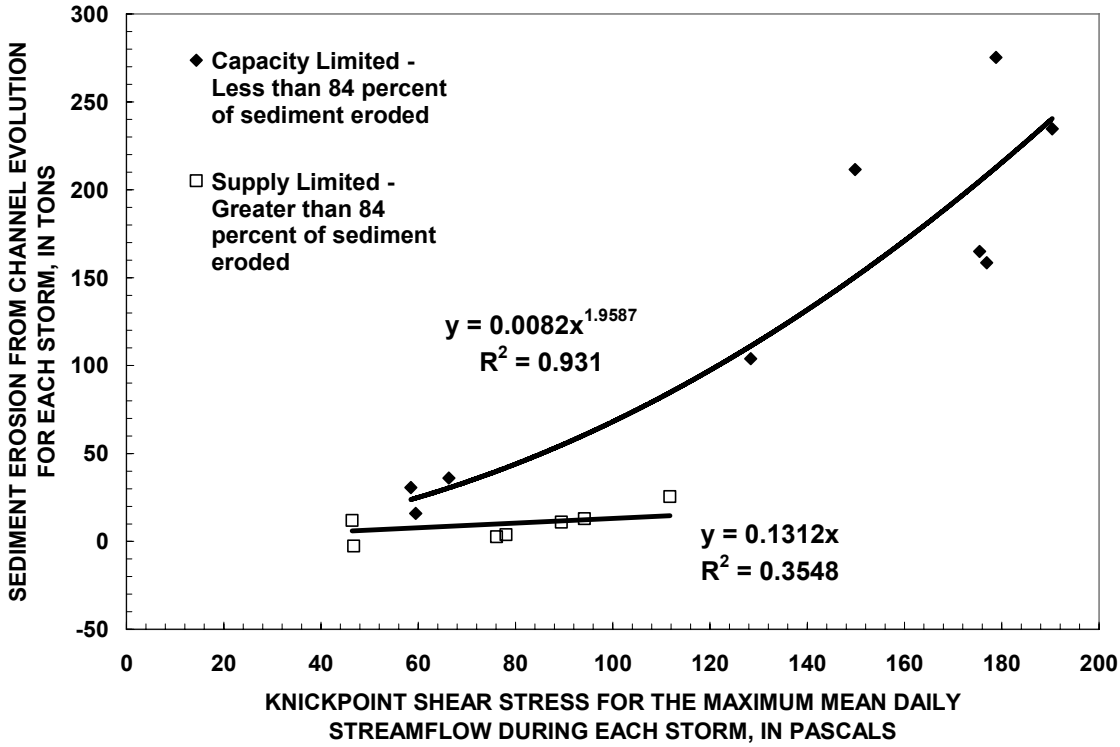

Figure 4.14. Sediment erosion from channel evolution and knickpoint shear stress.

The storms used to develop Equation (4.2) are considered to be capacity limited and the storms used to develop Equation (4.3) are considered to be supply limited. The capacity-limited relation shows that sediment eroded increased with higher values of knickpoint shear stress. The supply-limited relation shows that the sediment available for erosion limits the amount of erosion for a given knickpoint shear stress. To further validate the capacity- and supply-limited concept, an erosion index was established by dividing the sediment eroded by the maximum of the mean-daily flows during the storm (Figure 4.10). The erosion index does support the capacity- and supply-limited concept, with storms included in the capacity-limited equation having an erosion index greater than 1.3 and the storms included in the supply-limited equation having an erosion index less than 0.6.

The empirical equations (4.2 and 4.3) provide a way to estimate sediment load for any hydraulically modeled knickpoint shear stress. These empirical equations are applicable to lake impoundments with similar cohesive sediments.

4.2.3 Cohesive-erosion Testing Results

Laboratory tests on undisturbed cohesive-sediment samples were completed to test erosive response to increasing velocity, shear stress, and specific stream power. The results from the cohesive-erosion testing are used in the knickpoint-migration method and the assessment of streambed stability. Cohesive-sediment samples were obtained from four locations upstream of the dam-removal site (Figure 4.15). One Shelby tube sample was tested from B1, B2B, and B3. Two flume samples were tested from B2 and B3, and one sample at B1. The samples at B2B and B2 represent the consolidated lake bottom that was the streambed after the dam removal. Location B1 represents the historical cohesive-streambed channel that emerged as the lake bed sediments were eroded. It is uncertain whether samples at B3 represent the lake bed or historical streambed.

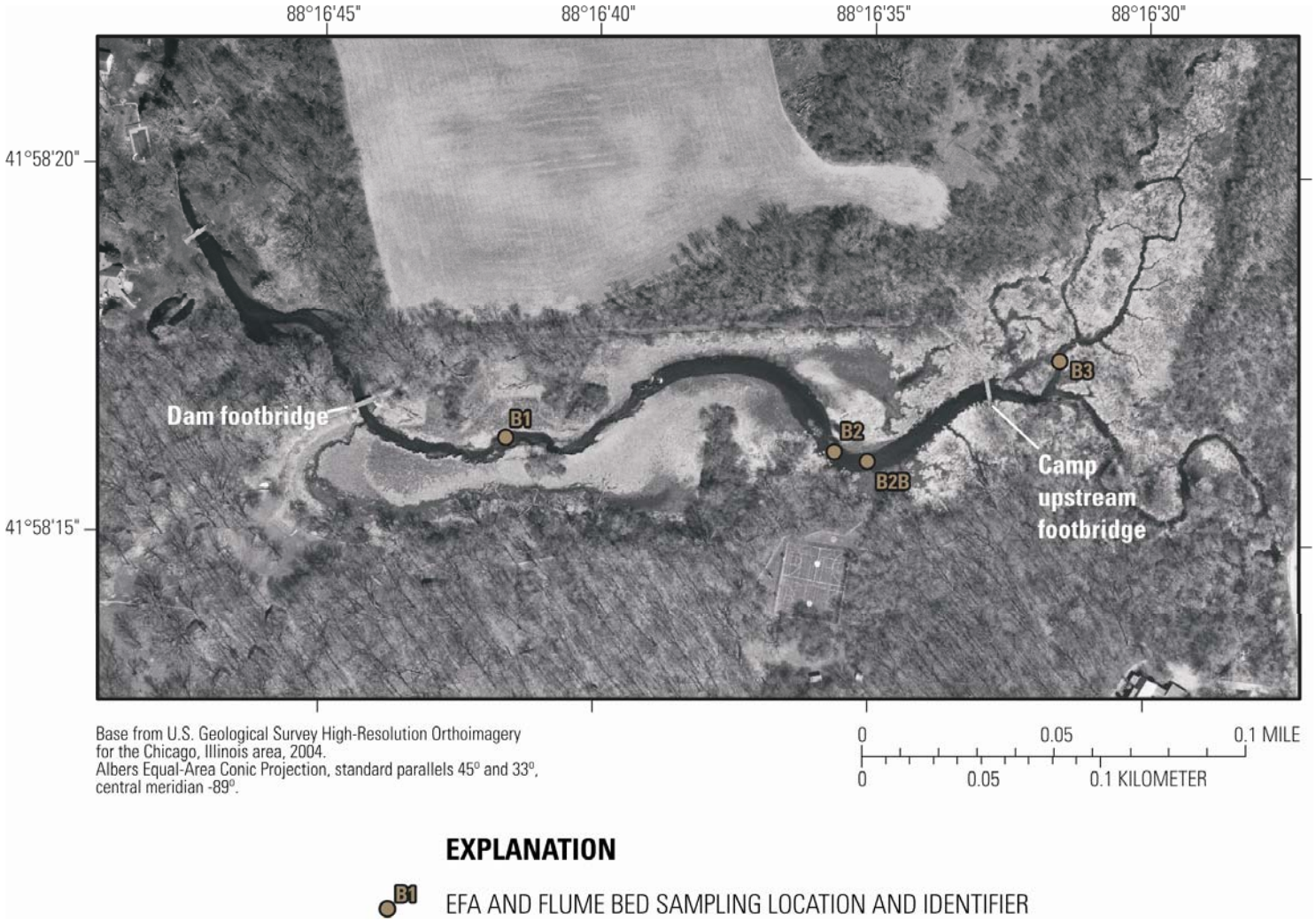

Figure 4.15. Locations along Brewster Creek where cohesive-sediment samples were obtained for EFA and flume testing.

Various soil properties were tested on the samples and used in the development of an empirical equation to relate soil properties, flow conditions, and erosion rates. The empirical equation will be useful for future dam-removal projects in that, ideally, a minimal amount of soil-property testing would be needed to predict erosion rate of cohesive material. Results from particle-size (Table 4.11, Figure 4.16, and Appendix E), Atterberg Limits (Figure 4.17, Table 4.12, Appendix F), specific weight (Table 4.12), moisture content (Table 4.12), and torvane tests (Table 4.13) were among the properties considered in the empirical equation.

Table 4.11. Summary of particle-size analysis on cohesive-streambed samples assuming the sand-silt break is at 0.063 mm.

Sample	D_{50} (mm)	Percent Sand	Percent Silt	Percent Clay
B1-1-FL	0.0054	9.2	46.4	44.4
B1-EFA (0 - 177.8 mm)	0.0048	19.5	33.8	46.7
B2-1-FL	0.018	20.9	54.6	24.5
B2-2-FL	0.011	9.6	63.6	26.8
B2B-EFA (0 - 76.2 mm)	0.0097	7.8	61.0	31.1
B2B-EFA (76.3 - 279.4 mm)	0.027	33.3	48.2	18.5
B3-1-FL	0.201	68.6	16.6	14.8
B3-2-FL	0.099	53.9	24.5	21.6
B3-EFA (0 - 101.6 mm)	0.10	55.7	26.6	17.7
B3-EFA (0 - 101.6 mm) Fines Only	0.016	22.2	47.1	30.7

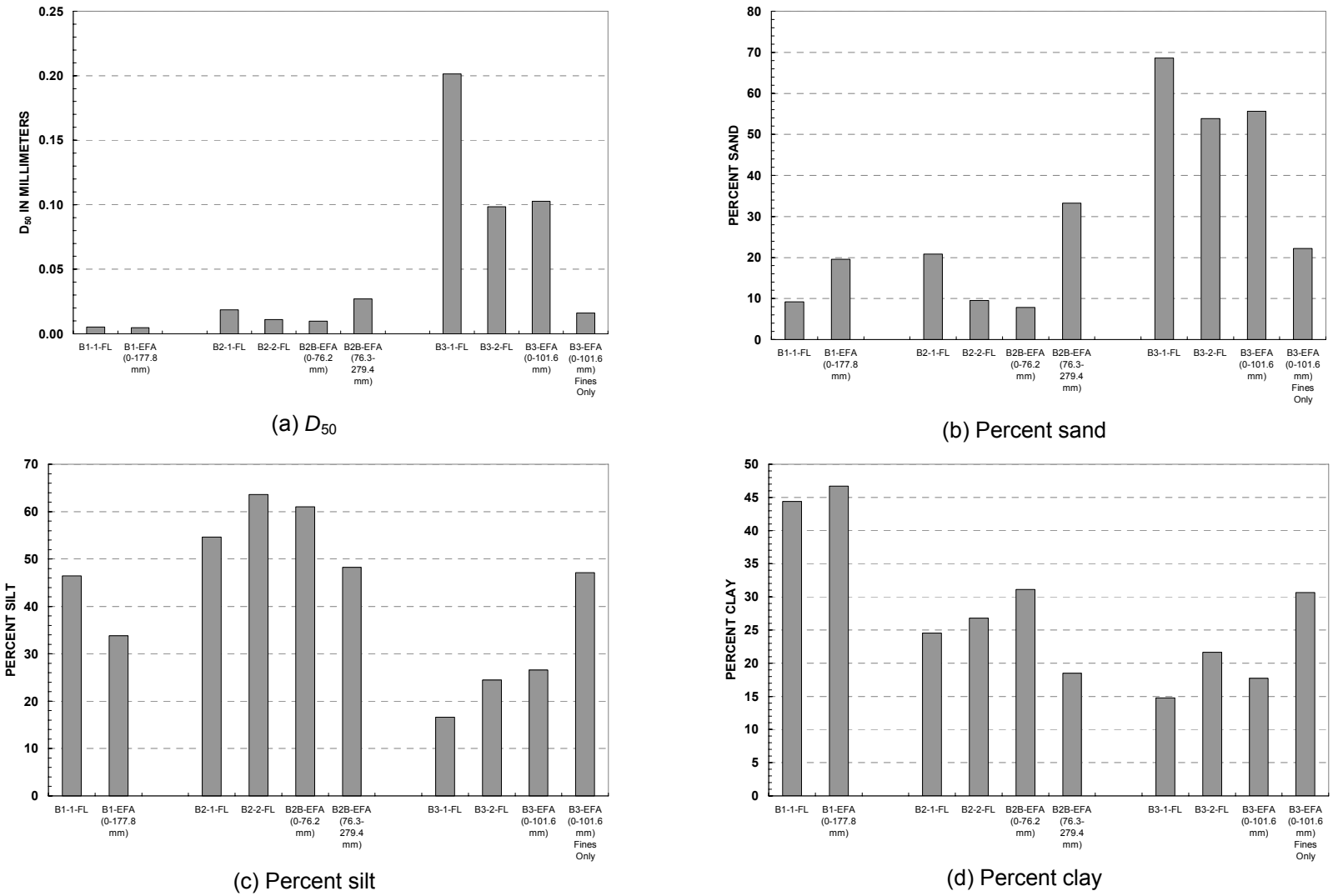

(a) D_{50}

(b) Percent sand

(c) Percent silt

(d) Percent clay

Figure 4.16. Summary of particle-size analysis on cohesive-streambed samples.

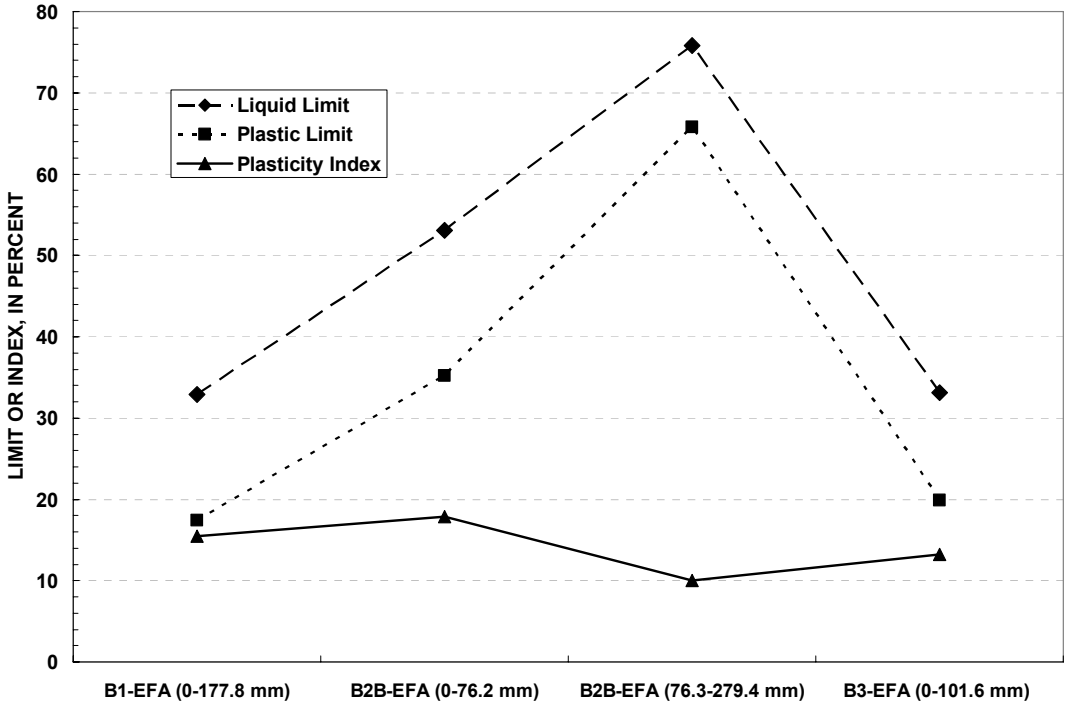

Figure 4.17. Summary of Atterberg Limits on cohesive-streambed samples.

Table 4.12. Summary of Atterberg Limits on cohesive-streambed samples.

Sample	Liquid Limit	Plastic Limit	Plasticity Index	Visual Description by the Illinois Department of Transportation (IDOT)
B1-EFA (0 - 177.8 mm)	32.9	17.4	15.5	Gray silty clay and clay with isolated gravel.
B1-EFA (177.8 - 254.0 mm)	16.2	14.1	2.1	Gray silt loam and sand.
B2B-EFA (0 - 76.2 mm)	53.1	35.2	17.9	Gray organic clayey silt, spongy.
B2B-EFA (76.3 - 279.4 mm)	75.8	65.8	10.0	Black peat and muck with wood debris.
B3-EFA (0 - 101.6 mm)	33.1	19.9	13.2	Gray silty clay loam and silty clay with sand pockets and lenses.

Table 4.13. Summary of specific weight and moisture content on cohesive-streambed samples.

Sample	Wet Specific Weight (lb/ft^3)	Dry Specific Weight (lb/ft^3)	Moisture Content (percent)
B1-1-FL	122.9	98.0	20
B1-EFA (0 - 177.8 mm)	138.6	---	15
B2-1-FL	64.4	41.0	36
B2-2-FL	60.4	36.5	40
B2B-EFA (0 - 76.2 mm)	59.1	---	52
B3-2-FL	124.5	98.4	21
B3-EFA (0 - 101.6 mm)	120.3	---	31

--- = not measured

Erosion rates and critical shear determined from the EFA samples are presented in Figure 4.18, Tables 4.14 and 4.15, and Appendix G. The critical shear is determined by the shear value before 1 mm/hr of erosion occurs (i.e., the break in slope from 0.5 mm/hr to 1 mm/hr of erosion (Figure 4.18)). Although the determination of critical shear is important, of more importance with cohesive materials is how the erosion rate changes with increasing shear values. Given the results from the EFA, an empirical equation was developed using the various soil properties and flow conditions. The soil sample B2B-EFA (76.3 - 279.4 mm) (Table 4.12) is described as composed of peat and muck with wood debris. The composition made it not suitable for the empirical-equation analysis, although it is included in Figure 4.18 to show that the lake-bed sediments are highly variable and include a wide range of erosion potential.

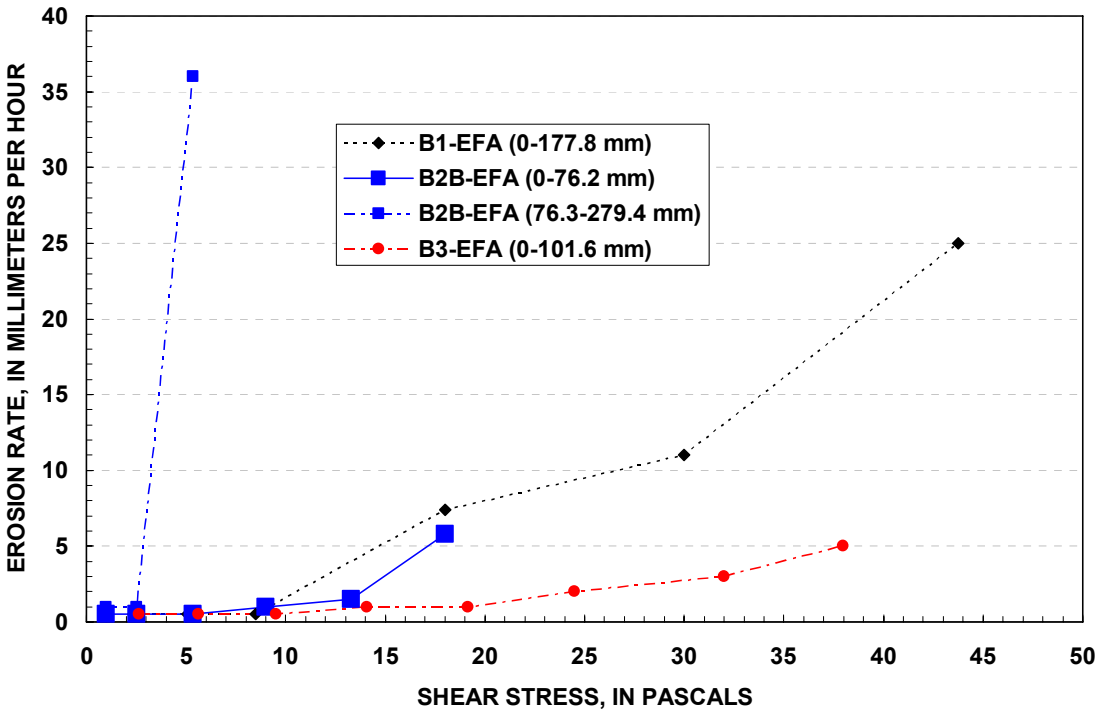

Figure 4.18. EFA results showing shear stress and erosion rate.

Table 4.14. Critical shear values for EFA samples.

Sample	Critical Shear (Pa)
B1-EFA (0 - 177.8 mm)	8.5
B2B-EFA (0 - 76.2 mm)	5.3
B2B-EFA (76.3 - 279.4 mm)	1.0
B3-EFA (0 - 101.6 mm)	9.5

Table 4.15. Soil properties, flow conditions, and erosion rates for the EFA samples.

Sample	Shear Stress (Pa)	Stream Power (W/m^2)	Plasticity Index	Percent Finer than 0.063 mm	Erosion Rate (mm/hr)	
					EFA Measured	Equation (4.4) Computed
B1 (0 - 177.8 mm)	8.5	17.0	15.5	80.5	0.5	1.0
	18.0	54.0	15.5	80.5	7.4	4.1
	30.0	120.0	15.5	80.5	11.0	11.1
	43.8	218.8	15.5	80.5	25.0	23.1
B2B (0 - 76.2 mm)	5.3	8.0	17.9	92.2	0.5	0.4
	9.0	18.0	17.9	92.2	1.0	1.1
	13.3	33.2	17.9	92.2	1.5	2.3
	18.0	54.0	17.9	92.2	5.8	4.2
B3 (0 - 101.6 mm)	9.5	19.0	13.2	77.8	0.5	0.4
	14.1	35.2	13.2	77.8	1.0	0.7
	19.1	57.4	13.2	77.8	1.0	1.4
	24.5	85.8	13.2	77.8	2.0	2.2
	32.0	128.0	13.2	77.8	3.0	3.7
	38.0	170.9	13.2	77.8	5.0	5.1

Several combinations of soil properties, flow conditions, and erosion rates were used to attempt to determine a suitable empirical equation (Table 4.15). The final method utilized multiple-linear regression analysis to relate the logarithm of the EFA erosion rate (*ER*) results to the logarithms of the shear stress, plasticity index (*PI*), and percent finer than 0.063 mm (*PF*). The equation for the erosion-rate estimation (in mm/hr) that yielded the highest R^2 value is:

$$ER = 1.012 \times 10^6 \tau^{1.940} PI^{9.802} PF^{-10.228}$$ **Equation (4.4)**

where

ER = erosion rate in mm/hr;

τ = shear stress (for values greater than or equal to critical shear for a given material in Pa);

PI = plasticity index; and

PF = percentage of sediment sample that is finer than 0.063 mm.

The coefficient of determination (R^2) and standard error for the logarithmic data resulting from multiple combinations of shear stress and soil properties are listed in Table 4.16. Using stream power alone ($R^2 = 0.70$) yields an R^2 of 0.01 greater than shear stress alone ($R^2 = 0.69$) (Table 4.16), but shear stress was still used for Equation (4.4) given the broader use of shear stress in erosion estimation. Equation (4.4) explains 90 percent of the variance in the logarithms or erosion rate. The erosion rates estimated using Equation (4.4) and the measured values from the EFA results are presented in Table 4.15 and Figure 4.19. Equation (4.4) will be used in the knickpoint-migration method in this study.

Table 4.16. Coefficient of determination and standard error for logarithmic data in the equations for estimating erosion rate for the three sample locations at Brewster Creek.

Parameter	R^2	Standard Error
Shear Stress	0.69	0.73
Stream Power	0.70	0.71
Shear Stress and *PI*	0.87	0.46
Shear Stress and *PF*	0.77	0.61
Shear Stress, *PI*, and *PF*	0.90	0.39

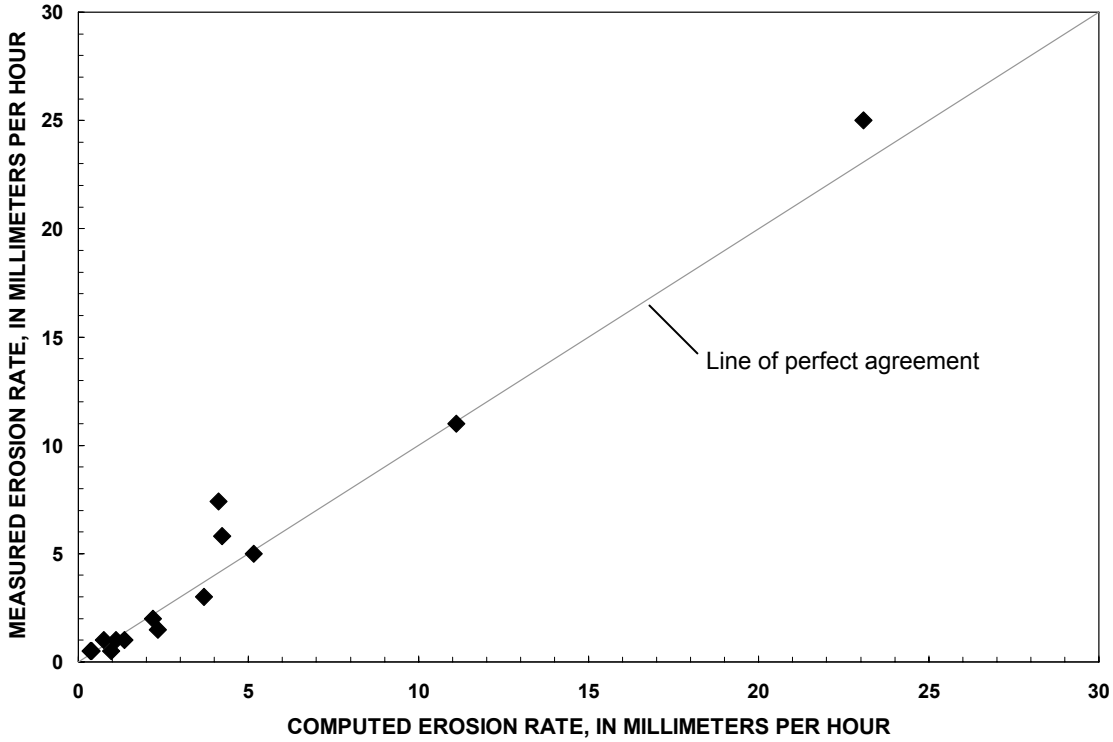

Figure 4.19. Erosion rate at three sample locations for EFA-measured results and computed values as a function of shear stress, plasticity index, and percent finer that 0.063.

To validate the EFA results, the erosion rates for both the EFA and flume samples are plotted in Figure 4.20. For an approximate range of 2 to 30 W/m^2, the flume-test erosion rates were up to 4 mm/hr greater than the EFA tests. Variations in soil properties of the larger flume sample and extensive bed readings in the flume testing could account for the higher erosion rates. Also, the differences in methods to measure velocity and shear between the EFA and the flume could account for the difference in erosion rates. Given the trends in both data sets (Figure 4.20), if the flume were capable of higher stream-power flows, the erosion rates could be more similar. In both the flume and EFA tests, moments of significant transport, generally associated with increases in flow, were

followed by periods of minimal transport. Also, the sediment was primarily moved in chunks and not by individual entrainment of the fine soil particles.

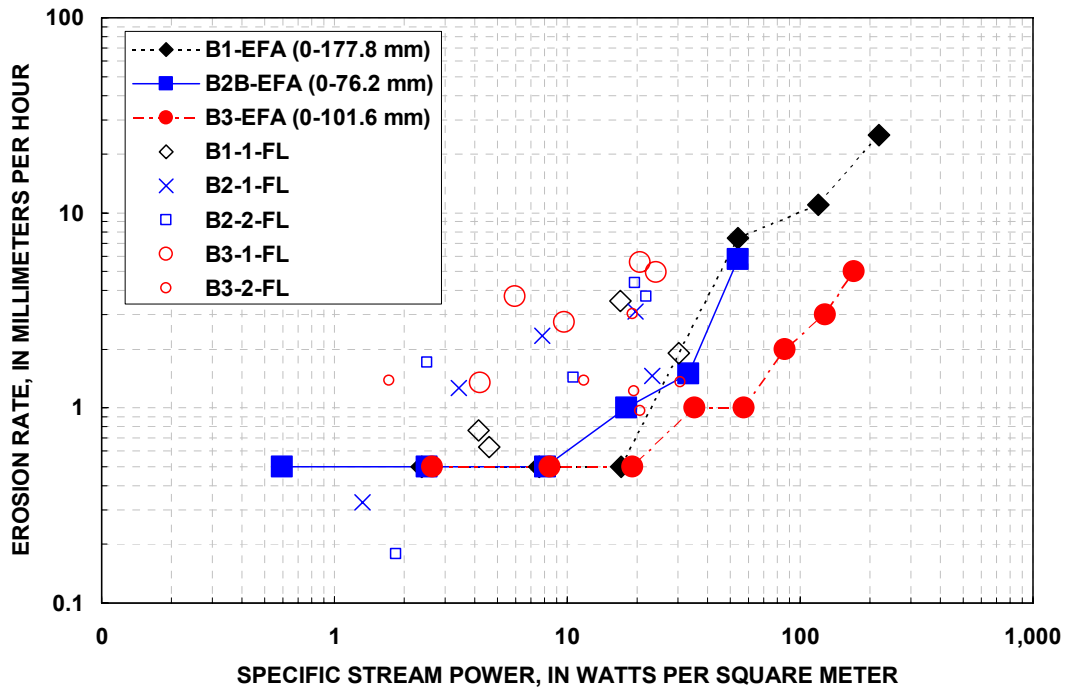

Figure 4.20. Erosion Function Apparatus (EFA) and flume (FL) erosion rate and specific stream power results for similar sites and materials at Brewster Creek.

To possibly better predict erosion potential, torvane measurements were recorded six times for each flume sample after the hydraulic testing. The statistical results of the torvane measurement (Table 4.17) reveal a range in the means of the mechanical shear strength of the cohesive sediments from 14.5 to 21.4 kPa. The coefficient of variation ranged from 16.7 to 31.0 percent indicating a reasonably tight clustering of the measurements about the mean and reproducible torvane measurements for the samples. The mean values are similar to those found by Zimbone *et al*. (1996), for clay, silty-loam, and sandy-loam soils.

Table 4.17. Mechanical shear strength of flume samples measured with a torvane.

Sample	Mean Shear Strength (kPa)	Standard Deviation (kPa)	Coefficient of Variation (Percent)
B1-FL	21.1	6.5	31.0
B2-1-FL	14.5	4.1	28.4
B2-2-FL	15.5	3.5	22.4
B3-1-FL	17.3	2.9	16.7
B3-2-FL	21.4	4.6	21.6

It is useful to stratify the data set on the basis of the torvane measurements that give an indication of the erosion potential of the cohesive sediments. Sample B3-2-FL had the highest torvane measurement (shear strength) of 21.4 kPa and samples in the B2 location had the lowest vane shear (14.5 and 15.5 kPa). When these two data sets are plotted (Figure 4.21), the effect of the cohesive-sediment shear strength is evident. There is no discernable pattern between stream power and the erosion rate for the stiffer B3-2-FL sample. Based on these observations, the case of the stiff B3-2-FL sample may have simply been that a threshold flow condition was not exceeded where pieces of sediment could be removed rather than individual entrainment.

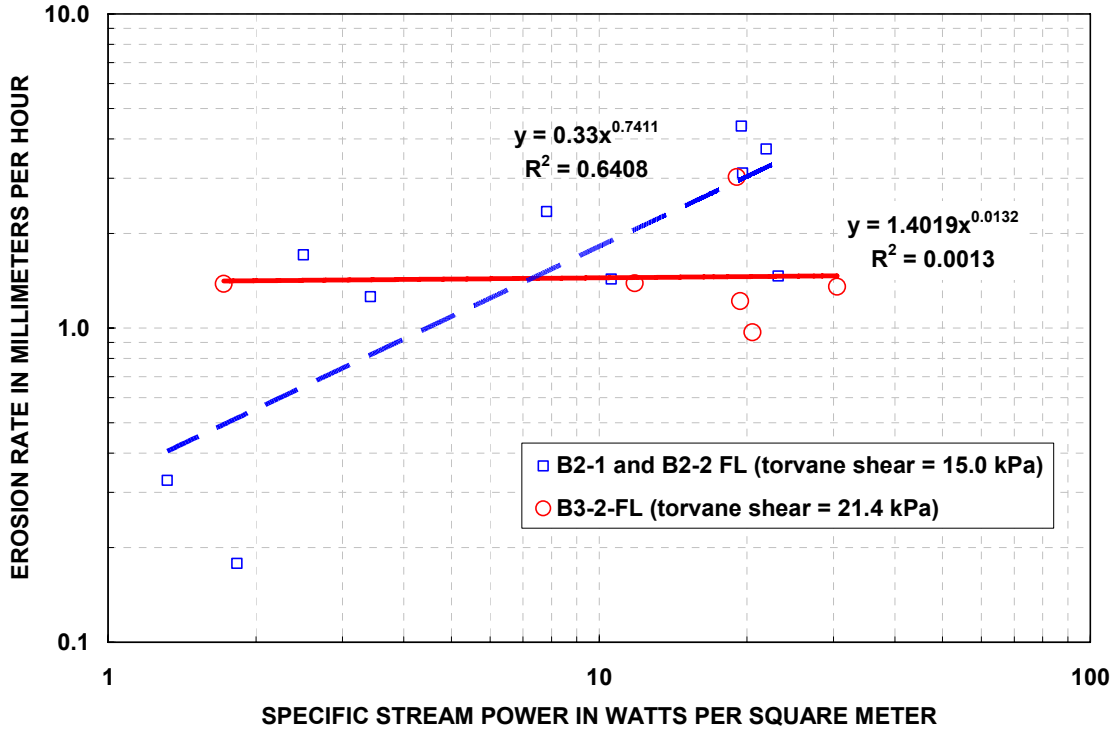

Figure 4.21. Highest and lowest torvane-measured samples presented by erosion rate and specific stream power flume (FL) sample tests.

In the jet-test apparatus, higher shear values have been recorded (Hanson and Cook, 2003) than can be achieved with either the EFA or flume tests. Note that the EFA, flume, and jet-test apparatus all measure shear differently and this should be considered when performing comparisons. Also, the jet-test apparatus is an in-situ device, whereas the EFA and flume require extraction of a sample for laboratory testing. The average erosion rates and shear values for areas of the midwestern United States as measured with the jet-test apparatus (Hanson and Simon, 2001) are plotted with the EFA results in Figure 4.22. It appears that it would be valid to extend the EFA erosion-rate relations for higher values of shear, if needed. The results from the cohesive-erosion testing are used in the knickpoint-migration method and the assessment of streambed stability.

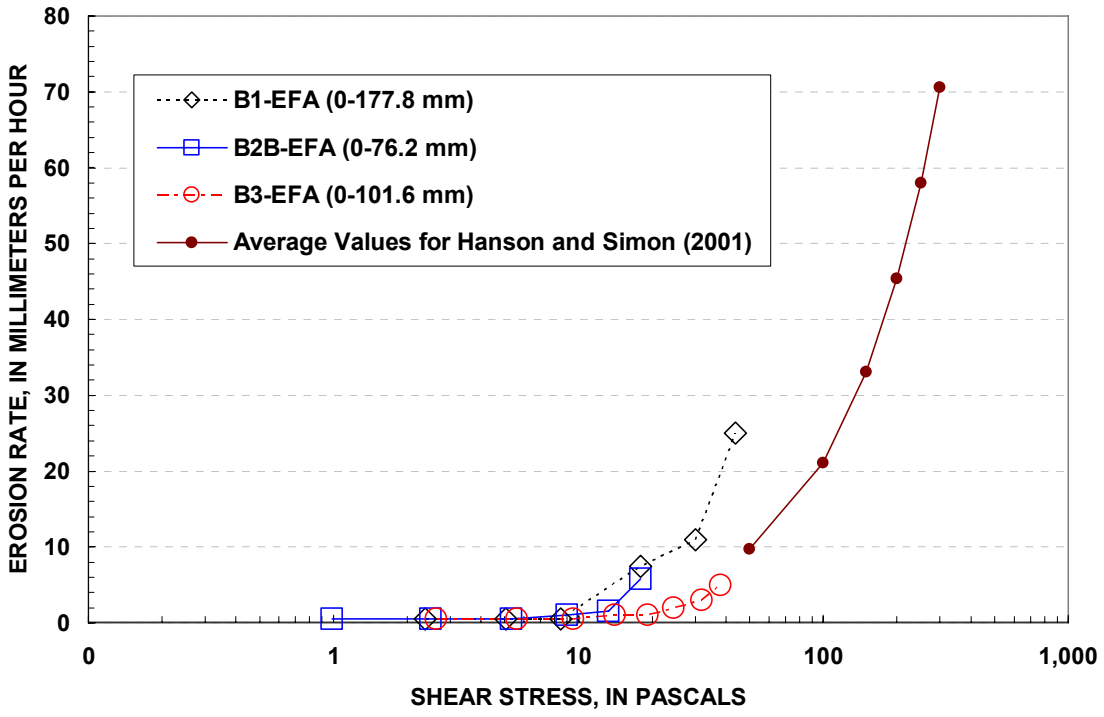

Figure 4.22. The average erosion rates and shear values for jet-test apparatus (Hanson and Simon, 2001) and the EFA erosion rate and shear values.

4.2.4 Knickpoint Migration Method

The Cohesive Knickpoint Parallel Retreat (CKPR) method was developed utilizing the cohesive-erosion laboratory testing results. The method predicts the knickpoint migration and volume of cohesive sediment eroded. Many streambed adjustment models are available (Exner, 1925; Fredsoe, 1974, 1978; Schumm *et al*., 1984; Simon and Hupp, 1986; Watson *et al*., 1986; Bennett, 1999a,b; Bennett *et al*., 2000a,b; Langendoen, 2000; Langendoen *et al*., 2000; Casalí and Bennett, 2001; Goodell and Bradley, 2005; Thomas, 2005; Gibson and Little, 2006; Watson and Biedenharn, 2006). The conceptual model of parallel retreat (Gardner, 1983) (Figure 2.7) is expanded on in the CKPR method. Most methods simulate streambed erosion in a horizontal

direction, but the majority of the erosion at Brewster Creek resulted from a vertical parallel retreat as shown in the first three surveys (Figure 4.10). Also for each survey (Figure 4.10) and maximum knickpoint shear condition (Table 4.9), the relations in Stein and Julien (1993) for homogeneous cohesive soil predict that the knickpoint will migrate in a stepped (parallel) mode for knickpoint heights greater than 2 ft. Heights near or greater than 2 ft are predominant in the storms used for model input (Table 4.10).

A conceptual diagram of the method is shown in Figure 4.23. The CKPR method only simulates upstream erosion and does not simulate where or how the sediment is deposited downstream. It is assumed that sediment being transported into the stream system is transported out of the system without being deposited.

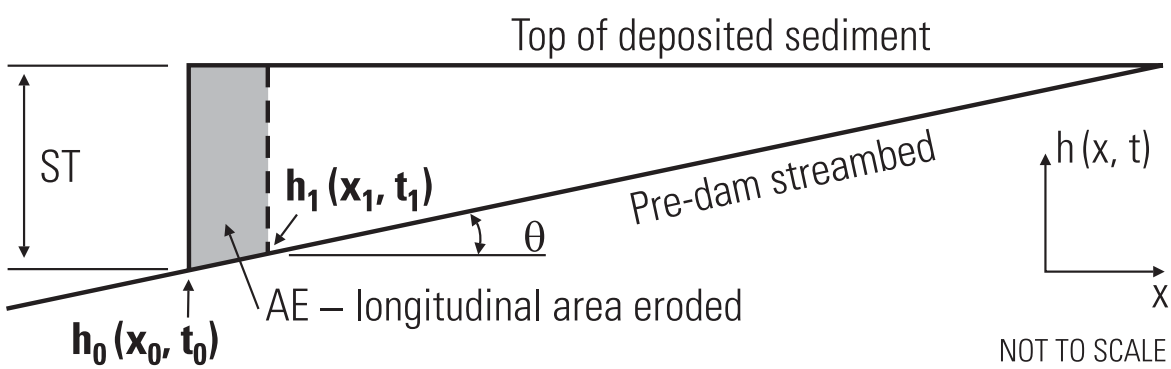

Figure 4.23. Conceptual diagram of the CKPR method.

The longitudinal area (*AE*) is eroded on the downstream vertical face of the sediment. Assuming that the bottom slope (θ) of the longitudinal area eroded is the same as the pre-dam streambed, the migration along the pre-dam streambed slope is calculated with the equation:

$$h_{n+1} = h_n + S_b \cdot (x_{n+1} - x_n)$$ **Equation (4.5)**

where

h = elevation of the pre-dam streambed (m);

S_b = slope of the pre-dam streambed (m/m) ($S_b = \tan\theta$); and

x = streamwise distance (m).

Assuming the erosion is only on the downstream vertical face of the deposited sediment, the migration in the x direction can be calculated with the equation:

$$x_{n+1} = x_n + ER \cdot t \qquad \textbf{Equation (4.6)}$$

where

ER = erosion rate (m/hr); and

t = time (hrs).

The erosion rate is calculated by transforming Equation (4.4) to predict erosion in meters per hour instead of millimeters per hour and replacing the shear-stress variable with the knickpoint shear stress and is given as:

$$ER = 1.012 \times 10^3 \tau_{kn}^{1.940} PI^{9.802} PF^{-10.228} \qquad \textbf{Equation (4.7)}$$

where

ER = erosion rate (m/hr);

τ_{kn} = knickpoint shear stress (for values greater than or equal to critical shear) (Pa);

PI = plasticity index; and

PF = percentage of sediment sample finer than 0.063 mm.

The longitudinal area eroded and corresponding volume are calculated with the following equations:

$$AE = \frac{1}{2}\left(ST_{n+1} + ST_n\right) \cdot \left(x_{n+1} - x_n\right) \qquad \textbf{Equation (4.8)}$$

where

AE = longitudinal area eroded (m^2); and

ST = sediment thickness (m) and can be calculated with the following equation:

$$ST_{n+1} = ST_n - (h_{n+1} - h_n) \qquad \textbf{Equation (4.9)}$$

The volume of sediment eroded can then be calculated by the following equation:

$$Vol = AE \cdot W \qquad \textbf{Equation (4.10)}$$

where

Vol = volume eroded (m^3); and

W = representative channel width (m).

The CKPR method was applied to results from the Brewster Creek dam removal. Because the erosion from each notch was not maximized before the next notch was removed, the method testing was simplified by assuming the dam was completely removed in November 2003. This is considered a reasonable assumption, given the limited erosion as of November 2003 (Figure 4.4) and because 87 percent of the sediment eroded during sixteen storms from November 2003 through February 2005 (Table 4.10). The storms and knickpoint shear stresses in Table 4.10 were used as input events to test

the method. The approximate duration of the storm hydrograph rising limb and peak was input for each storm (Table 4.18). The highest sediment concentrations occur during the rising limb and peak as discussed in the *Methods of Investigation* chapter. A streambed slope (S_b) of 0.0043 m/m and sediment depth at the dam of 1.8 m were determined from Figure 4.10 and used in the method. The estimated stream width was determined by the distance between the old dam abutments, 7.3 m. The soil properties for the EFA sample B2B (0 - 76.2 mm) (PF = 92.2 percent and PI = 17.9) were chosen as input into the erosion-rate Equation (4.7).

Table 4.18. Approximate duration of the storm hydrograph rising limb and peak for each storm modeled. Note that some storm time periods have multiple peaks (Figure 4.2).

Storm Number	Storm Time Period	Approximate Duration of the Storm Hydrograph Rising Limb and Peak (days)
1	11/01/2003 -11/08/2003	3
2	11/17/2003 - 11/28/2003	4
3	12/08/2003 - 12/19/2003	3
4	02/18/2004 - 03/09/2004	8
5	03/23/2004 - 04/01/2004	5
6	04/16/2004 - 04/27/2004	2
7	05/04/2004 - 05/25/2004	8
8	05/29/2004 - 06/07/2004	4
9	06/09/2004 - 06/15/2004	3
10	06/20/2004 - 06/23/2004	2
11	07/31/2004 - 08/05/2004	1
12	08/27/2004 - 08/29/2004	1
13	12/05/2004 - 12/13/2004	3
14	01/10/2005 - 01/23/2005	3
15	02/02/2005 - 02/11/2005	2
16	02/12/2005 - 02/19/2005	2

The method predicted the eroded volume, knickpoint height, and migration length within 17, 20, and 6 percent, respectively, of measured values (Table 4.19). Given the difference in shape of the conceptual diagram and measured top of sediment (Figures 4.10 and 4.23, respectively), the differences between the results and measured values are acceptable.

Table 4.19. CKPR method results and measured values for erosion dynamics at Brewster Creek.

Parameter	Measured	Modeled	Percent Difference
Eroded Volume (m^3) (Sixteen Storms from Table 4.10)	2,089	2,448	17
Knickpoint Height (m) (03/31/2005 survey)	0.49	0.59	20
Knickpoint Migration Length (m) (03/31/2005 Survey)	265	280	6

4.2.5 Notching Assessment

The CKPR method developed in this study may be applicable to assess future stepwise small dam removals, with similar dams, sediments, lakes, and watersheds, by minimizing the number of notches and sediment yield per notch. The assessment technique was utilized to focus on two sediment erosion results from the study:

1. The sediment load during the first three notches (60 tons) was 14 percent of the load that occurred during the final two notches (382 tons) (Table 4.3).
2. The sediment load during the 7 months after the fifth notch (834 tons) was approximately 56 percent of the total sediment load eroded (1,490 tons) (Table 4.3).

The first three notches could have been combined to help minimize cost without risking the release of large amounts of sediment. Combining these three notches would

still allow for dewatering of the lake, channel initiation, and development of vegetation (Figure 4.24). Note that if the first notch is removed during the dormant season for vegetation, then the dewatered surface will remain exposed longer, increasing erosion risks (Graber *et al*., 2001).

Combining the first three notches also starts to address the issue with the second result by allowing more time between the final two notches. Allowing more time between the notches would reduce the sediment loads that occur as a result of any one notch. The impacts of the final two notches would then be a more gradual channel degradation and widening (Figure 4.24). The channel evolution continues after the final notch with aggradation, widening, and finally reaches a quasi-equilibrium or stable state similar to Schumm *et al*. (1984), Simon and Hupp (1986), and Doyle *et al*. (2003a).

The impact of the alternative stepwise notches can be quantified utilizing the CKPR method for the Brewster Creek study. Parameters and results for three stepwise notches utilizing the CKPR method are presented in Table 4.20. The first thirteen storm knickpoint shear stresses and durations (approximately 1 yr) in Table 4.10 and Table 4.18, respectively, would be needed for the sediment to erode from each notch (Table 4.20). The results were compared to the observed conditions on March 31, 2005, with a surveyed migration length equal to 265 m (Table 4.8). The results show that if all the sediment is eroded after each notch, the sediment load resulting from a given notch will be minimized. The sediment yield for the material being eroded from the lake would range from 18 to 51 tons/mi^2-yr. Adding the maximum sediment yield coming into the stream system (77 tons/mi^2-yr, Table 4.2), makes the maximum total sediment load equal 128 tons/mi^2-yr, which is 16 percent less than the lowest regional estimate

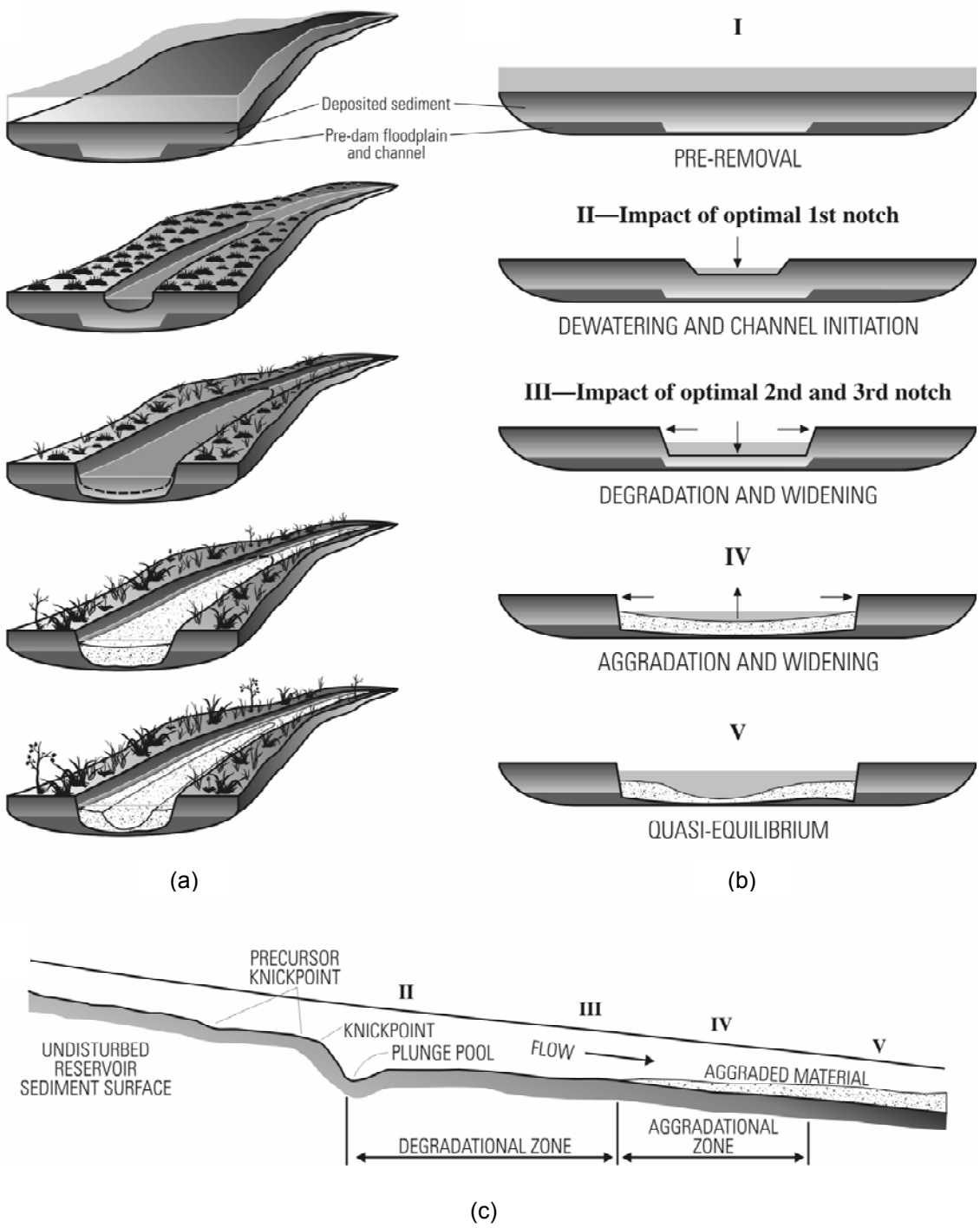

Figure 4.24. Impact of optimized notching on the conceptual CEM upstream of the dam-removal site (modified from Doyle *et al*. (2003a); Schumm *et al*. (1984); Simon and Hupp (1986)).

Table 4.20. Parameters and results for alternative three stepwise notches modeled with the CKPR method for approximately 1 yr (using the first thirteen storm knickpoint shear stresses and durations in Tables 4.10 and 4.18, respectively).

Parameter	Notch 1	Notch 2	Notch 3
Sediment Thickness Exposed near Dam (m)	0.914	0.457	0.457
Channel Width Formed (m)	3.00	5.50	7.32
Eroded Slope Formed (m/m)	0.0030	0.0037	0.0043
Volume Eroded (m^3)	411	873	1,158
Eroded Sediment Load (tons)	254	540	716

(153 tons/mi^2-yr) for sediment yield and 30 percent less than the sediment yield during the 7 months after the last notch (183 tons/mi^2-yr, Table 4.2) in the Brewster Creek dam removal.

The CKPR method developed in this study can be applied to future stepwise small dam-removal projects with similar dams, sediments, lakes, and watersheds. The backwater effects from the channel and the downstream abutments and embankments need to be remodeled for each dam and notching plan to obtain a reasonable range of knickpoint shear stresses. The knickpoint height and downstream backwater effect influence shear stress exerted to move the knickpoint. The plasticity index and percent fines of the deposited material need to be determined for the CKPR method to predict the erosion rate varying with cohesive-sediment material. Also, a final stable channel slope and width are needed and can be determined from the stream-channel stability assessment.

4.3 Stream-channel Stability

During and after stream-channel evolution, it is important to assess the stability of the channel. This assessment can be done by looking at the channel geometry and reach slope. The following four streambed-stability indicators were used:

1. width-to-depth ratio (1.5-yr streamflow);
2. top width ratio (100- and 1.5-yr streamflow);
3. slope ratio (friction slope and valley slope); and
4. shear stress (1.5-yr streamflow) and bed material comparison.

Values from the first two indicators will be compared to a cross section in a stable reach with a width-to-depth ratio of 18.6 and top-width ratio of 6.1 (surveyed in October 2002). The Bank Stability and Toe Erosion Model – Static Version 4.1 was used to assess the stability of the banks (Simon, 1989; Langendoen *et al*., 1999). The cross-section locations shown in Figure 4.25 were selected to determine both streambed and bank stability. The cross-section shapes over time are shown in Figure 4.26.

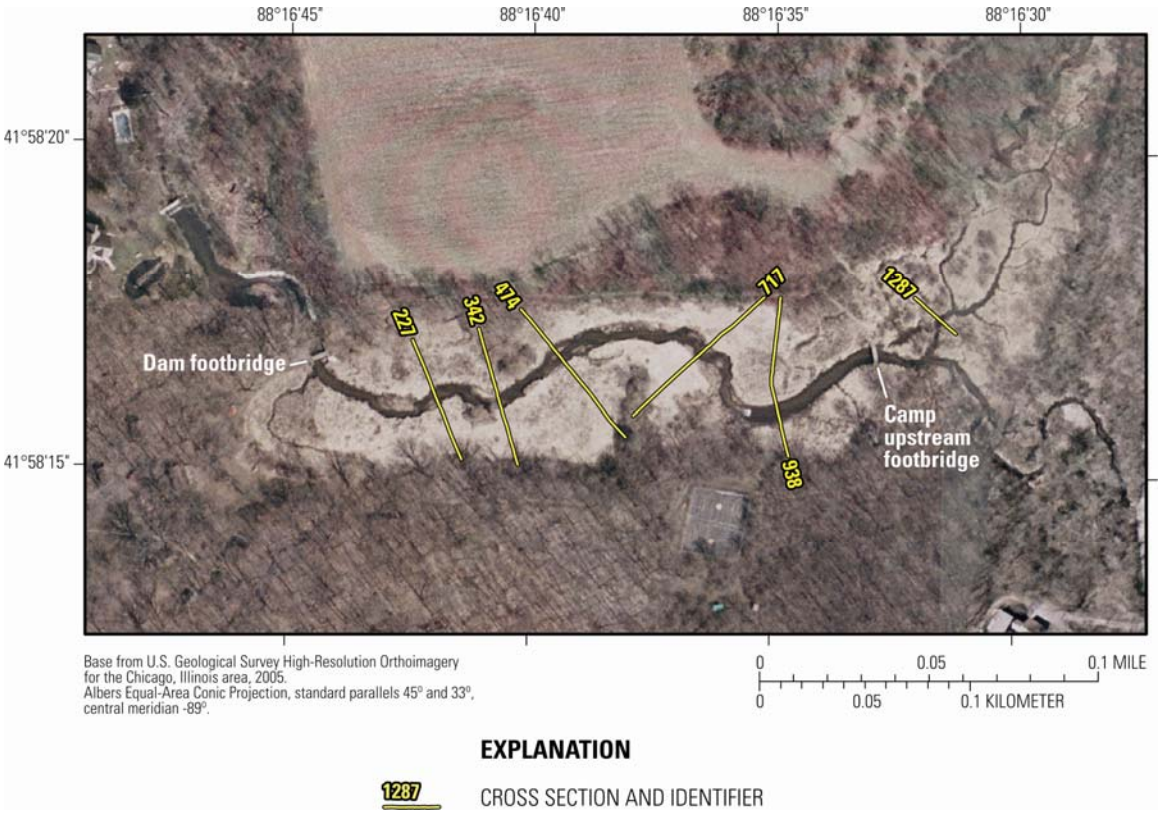

Figure 4.25. Selected cross-section locations. The cross sections are identified as the cross-section thalweg distance above the old dam for October 2006 conditions.

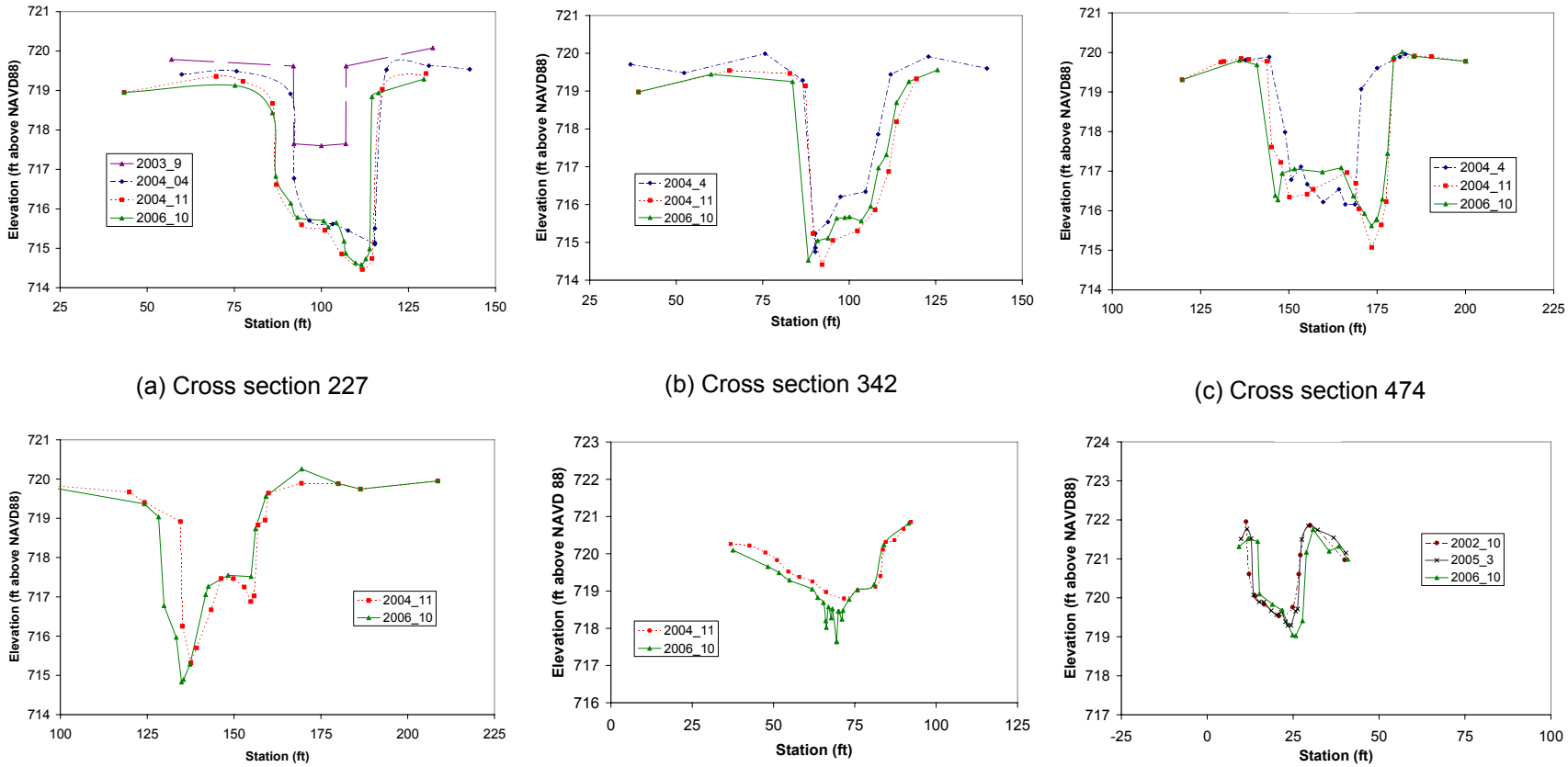

(a) Cross section 227

(b) Cross section 342

(c) Cross section 474

(d) Cross section 717

(e) Cross section 938

(f) Cross section 1287

Figure 4.26. Selected cross-sectional surveys at selected times throughout the study period. The plots are labeled as the cross section thalweg distance above the old dam for October 2006 conditions. The cross-section plots only show the main channel, not the full floodplain. The locations of the cross sections are shown in Figure 5.25.

4.3.1 Streambed

The main-channel top-width (*TW*) and main-channel hydraulic-depth (*HD*) ratio (*TW*/*HD*) were determined by using the inundated main-channel (*ch*) dimensions at the 1.5-yr streamflow (Table 4.21). The main-channel hydraulic depth is considered an approximate average depth and is calculated by dividing the main-channel flow (1.5-yr streamflow) area by the main-channel top width. In October 2006, the width-to-depth ratio of cross sections 227, 342, 474, 717, and 1287 ranged from 12.9 to 25.0 with an average value of 17.8 and a standard deviation of 5.2. The average ratio (17.8) is within 5 percent of the width-to-depth ratio (18.6) of a stable cross section approximately 1,000 ft downstream of the old dam (surveyed in October 2002). The ratio at cross section 938 (264) in October 2006 was 14 times higher than the stable cross section. The value of 264 is the same order of magnitude of the 449 value at cross section 227 on September 2003 (Table 4.21). The 2003 value at cross section 227 results from the small channel that was initiated from the first three notches. The 2006 value at cross section 938 results from the precursor knickpoint moving through the cross section. In both cases, the high values are a sign of an undersized channel and that stability has not been reached.

The top-width ratio or entrenchment ratio was determined by dividing the *TW* at the 100-yr streamflow by the main-channel *TW* at the 1.5-yr streamflow (Table 4.21). In October 2006, the top-width ratio of cross sections 227, 342, 474, 717, and 1287 ranged from 5.4 to 8.1 with an average value of 6.2 and a standard deviation of 1.1. The average ratio (6.2) is within 2 percent of the top-width ratio (6.1) of a stable cross section approximately 1,000 ft downstream of the old dam (surveyed in October 2002). Visual inspection of cross sections 227, 342, 474, and 717 in Figure 4.26

Table 4.21. Channel and reach characteristics including width-to-depth and entrenchment ratio and friction slope.

Cross-section		Top Width (*TW*) 1.5-yr Flow (ft)	Top Width 100-yr Flow (ft)	Hydraulic Depth (*HD*) 1.5-yr Flow (ft)	*TW* / *HD* 1.5-yr Flow	TW_{100} / $TW_{1.5}$	Friction Slope 1.5-yr Flow (ft/ft)	Friction Slope 100-yr Flow (ft/ft)
Location	Survey Date							
227	09/15/2003	211.2	225.1	0.47	449.4	1.1	0.0034	0.0036
	04/04/2004	25.0	184.4	1.62	15.4	7.4	0.0045	0.0036
	11/02/2004	28.8	89.4	1.29	22.3	3.1	0.0067	0.0056
	10/08/2006	27.1	150.1	1.25	21.7	5.5	0.0063	0.0049
342	04/04/2004	20.2	139.8	1.56	12.9	6.9	0.0050	0.0035
	11/02/2004	23.5	149.4	1.73	13.6	6.4	0.0044	0.0043
	10/08/2006	25.6	149.7	1.7	15.1	5.8	0.0045	0.0037
474	04/04/2004	23.6	223.2	2.08	11.3	9.5	0.0037	0.0012
	11/02/2004	33.5	220.6	1.34	25.0	6.6	0.0046	0.0015
	10/08/2006	35.1	220.9	1.4	25.0	6.3	0.0045	0.0015
717	11/02/2004	22.0	226.0	1.68	13.1	10.3	0.0045	0.0011
	10/08/2006	27.9	226.8	1.93	14.4	8.1	0.0024	0.0010
938	11/02/2004	84.5	248.4	0.89	94.9	2.9	0.0027	0.0021
	03/31/2005	49.0	248.7	0.83	59.1	5.1	0.0074	0.0021
	10/08/2006	145.2	249.4	0.55	264.0	1.7	0.0046	0.0017
1287	10/2002	17.5	102.2	1.52	11.5	5.8	0.0008	0.0008
	03/31/2005	14.5	72.6	1.52	9.5	5.0	0.0029	0.0032
	10/08/2006	15.9	85.3	1.23	12.9	5.4	0.0044	0.0024

show that these cross sections may be in quasi-equilibrium (Stage V of the CEM) (Figure 4.24). The top-width ratio at cross section 938 (1.7) is over three times lower than the stable cross-section ratio. This result shows a sign of an undersized channel and that stability has not been reached.

The comparison of friction slope at the 1.5-yr streamflow and the valley slope can be an indicator of stability in a reach (for example, if the friction slope at the 1.5-yr streamflow is steeper than the valley slope, this may be a sign of instability). Surrogates for the valley slope can be obtained from topographic maps or the friction slope at the 100-yr recurrence interval (if the flow is not contained within the main channel). Valley slopes from a topographic map were presented in Figure 4.1 for Brewster Creek with values ranging from 0.0043 to 0.0092 ft/ft immediately upstream and downstream of Willow Lake. The friction slope for the 1.5-yr streamflow ranges from 0.0044 to 0.0063 ft/ft in 2006 (at cross sections 227, 342, 474, 938, and 1287), all of which fall into the range of the valley slopes immediately upstream and downstream of Willow Lake. Because the friction slope falls within the range of upstream and downstream valley slopes, the stream is assumed to be developing a stable slope. The friction slope at cross section 717 (0.0024) is less than the range and could be an indication that this reach is in the aggradational stage from the knickpoint progressing upstream of it. Depending on the material in this reach (discussed below), this reach could still be in an adjustment phase. Although the previous two indicators showed signs of instability at cross section 938, the friction slope and valley slope indicator do not.

The friction slope at the 100-yr streamflow is less than the friction slope at the 1.5-yr flow at almost every time period and cross section, the 100-yr value is affected by

backwater effects from the old dam embankments and abutments, and does not provide a useful indicator when compared to the friction slope at the 1.5-yr streamflow.

Additionally, stability can be assessed by comparing the shear stress available to move bed material and the bed material in the channel. The average main-channel shear stress and specific stream power for each site were determined using the following equations:

$$\tau_{ch} = \gamma \, HD_{ch} \, S_f \qquad \textbf{Equation (4.11)}$$

where

τ_{ch} = main-channel shear stress;

γ = specific weight of water;

HD_{ch} = main-channel hydraulic depth; and

S_f = average reach friction slope.

$$\omega_{ch} = \tau_{ch} V_{ch} \qquad \textbf{Equation (4.12)}$$

where

ω_{ch} = main-channel specific stream power; and

V_{ch} = main-channel velocity.

Shields (1936) determined the threshold conditions for incipient motion of noncohesive material. Julien (1998) summarized the Shields work and a Highway Research Board (1970) study for relations between critical shear stress and median grain size on a flat surface. Utilizing the above information, the corresponding particle size moved at a given shear stress was determined (Table 4.22). The values of shear stress

Table 4.22. Main-channel shear stress, channel velocity, specific stream power, estimated particle size moved at the given shear stress, and size of bed material in the riffle or nearby cohesive material (summarized in Section 4.2.3, *Cohesive-erosion Testing Results*).

Cross-section									
Location	Survey Date	Shear 1.5-yr Flow (Pa)	Shear 100-yr Flow (Pa)	Velocity 1.5-yr Flow (m/s)	Velocity 100-yr Flow (m/s)	Specific Stream Power 1.5-yr Flow (W/m^2)	Specific Stream Power 100-yr Flow (W/m^2)	Approximate Particle Size Moved (mm)	Riffle Median Particle Size and/or Nearby Cohesive Material (mm)
227	09/15/2003	4.8	15.2	0.4	0.9	2.1	13.3		
	04/04/2004	21.7	15.3	1.1	1.6	22.8	24.4		
	11/02/2004	25.8	24.5	1.1	2.4	29.5	58.1		33.1 (B1)
	10/08/2006	23.4	17.0	1.3	2.1	29.4	36.4	30	37.9 (B1)
342	04/04/2004	23.2	14.1	1.3	2.1	31.1	29.9		
	11/02/2004	22.7	19.7	1.0	1.7	23.8	33.2		27.2
	10/08/2006	23.0	17.2	1.0	1.7	22.3	28.8	30	21.0
474	04/04/2004	22.9	5.8	0.9	1.1	19.8	6.5		
	11/02/2004	18.3	7.1	0.9	1.2	17.3	8.3		
	10/08/2006	18.9	7.3	0.9	1.1	16.3	8.2	22	21.0
717	11/02/2004	22.6	5.2	1.1	1.2	25.9	6.3		
	10/08/2006	13.9	5.1	0.8	1.1	10.9	5.7	16	11.1
938	11/02/2004	7.2	10.2	0.6	0.8	4.1	7.7		
	03/31/2005	18.3	9.5	1.1	1.0	19.4	9.4		B2 and B2B
	10/08/2006	7.6	8.1	0.7	0.9	5.0	7.2	8	B2 and B2B
1287	10/2002	3.8	4.1	0.8	1.0	3.1	4.1		
	03/31/2005	13.1	16.6	1.0	1.5	12.7	24.9		
	10/08/2006	16.1	12.4	1.1	1.3	17.7	16.0	19	15.8 (B3)

(5.1 to 23.4 Pa) and stream power (5.7 to 36.4 W/m^2) at 1.5- to 100-yr streamflows indicate that particles, up to approximately 30 mm, will become entrained.

To assess whether the calculated main-channel shear stresses will cause bed instability, bed-material samples were taken at various locations throughout the reach. Stability is assumed as the D_{50} of the substrate becomes greater than the particle size that can be moved by shear stress for the 1.5-yr streamflow. Pool and riffle bed-material sampling locations are shown in Figure 4.27. The particle-size distribution of the riffle substrate was completed using the pebble count technique (Bunte and Abt, 2001). The median particle size (D_{50}) of the samples is presented in Table 4.22, and Figures 4.27 and 4.28, and the particle-size distributions in Figures 4.29, 4.30, and 4.31.

At Riffles 1 and 2, the average D_{50} from the samplings in 2004 and 2006 was 29.8 mm (Figure 4.27). Riffles 1 and 2 are located near cross sections 227, 342, and 474 (Figures 4.25 and 4.27). The average shear stress for the 1.5-yr streamflow at these three cross sections (October 2006 conditions) is 21.8 Pa (Table 4.22). This shear stress indicates an average particle size moved of 27.3 mm, which is 8 percent less than the average D_{50} at Riffles 1 and 2.

At Riffle 3, the D_{50} in 2006 was 11.1 mm (Figure 4.27). Riffle 3 is located near cross section 717, which has a shear stress for the 1.5-yr streamflow (October 2006 conditions) of 13.9 Pa (Figures 4.25 and 4.27, and Table 4.22). This shear stress indicates an average particle size moved of 16.1 mm, which is 45 percent greater than the D_{50} at Riffle 3.

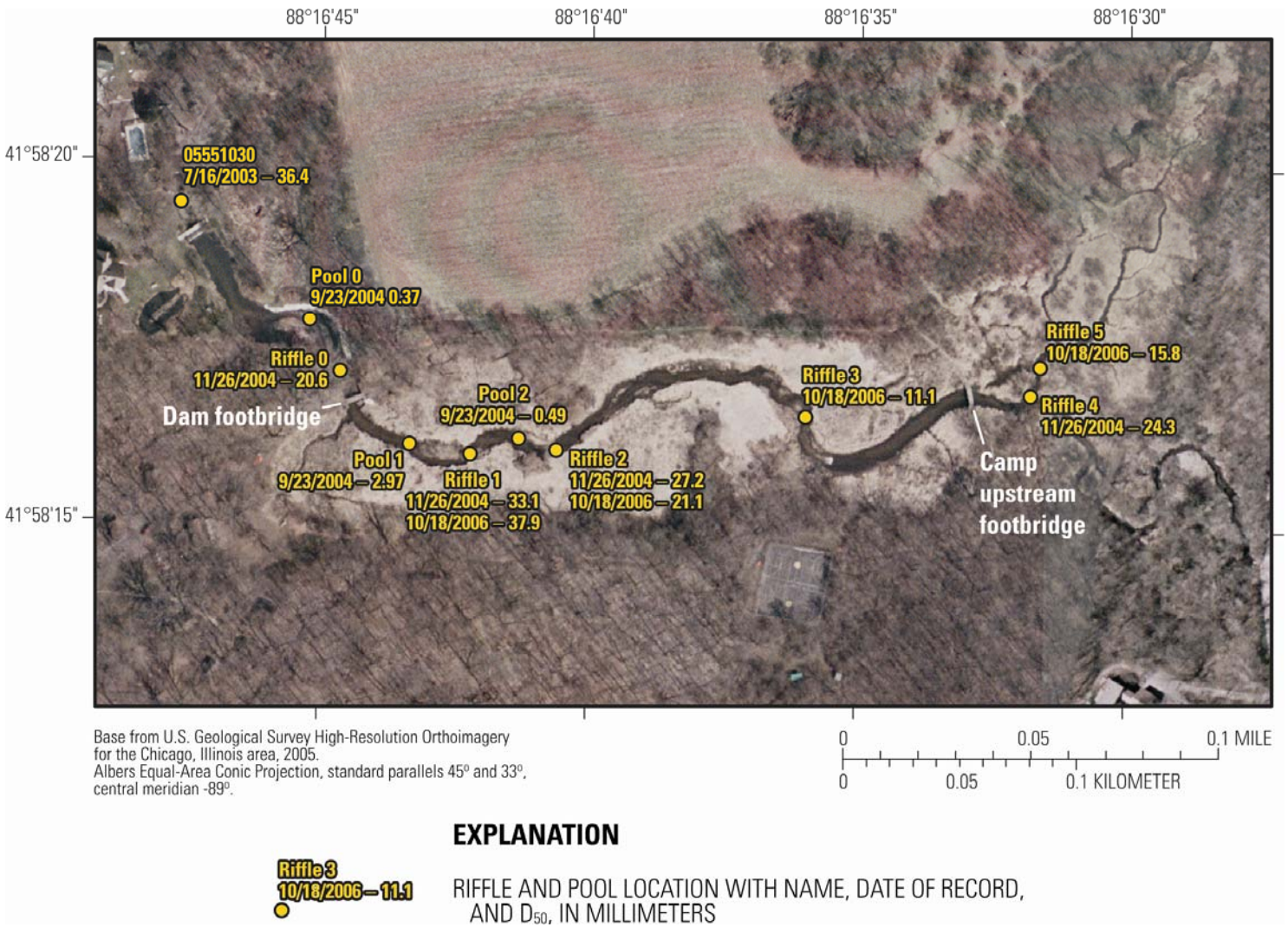

Figure 4.27. Riffle and pool locations for bed-material sampling.

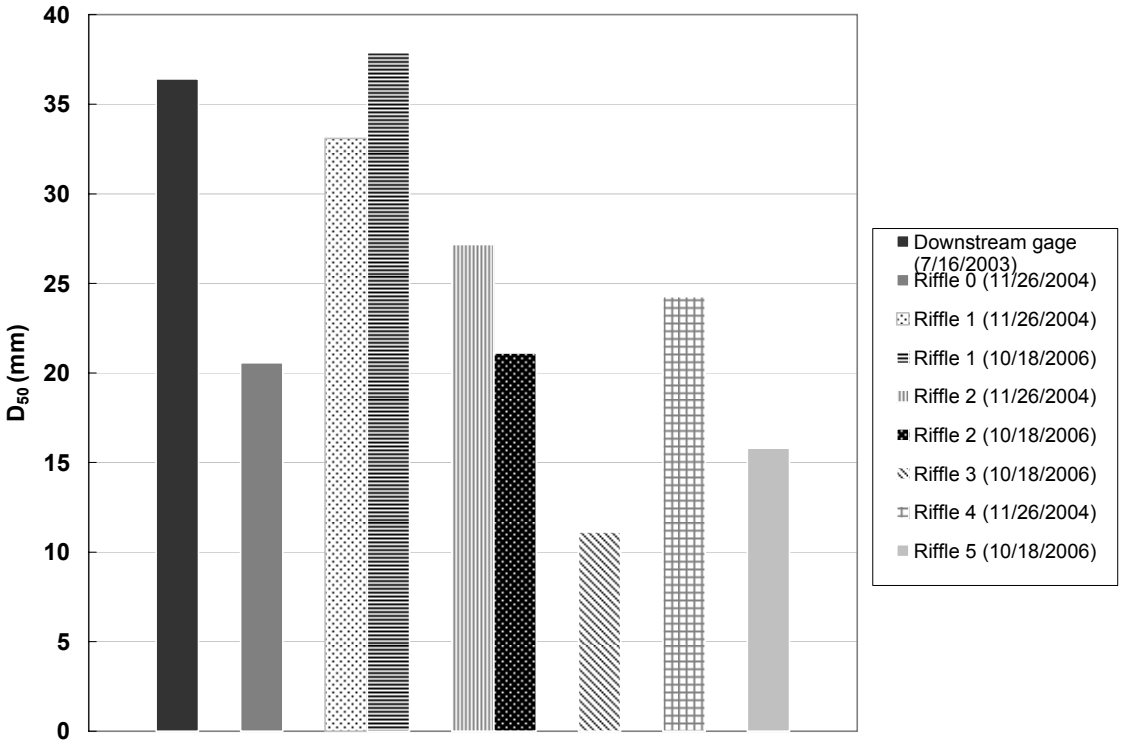

Figure 4.28. Median particle size of samples at various riffle locations in 2004 and 2006.

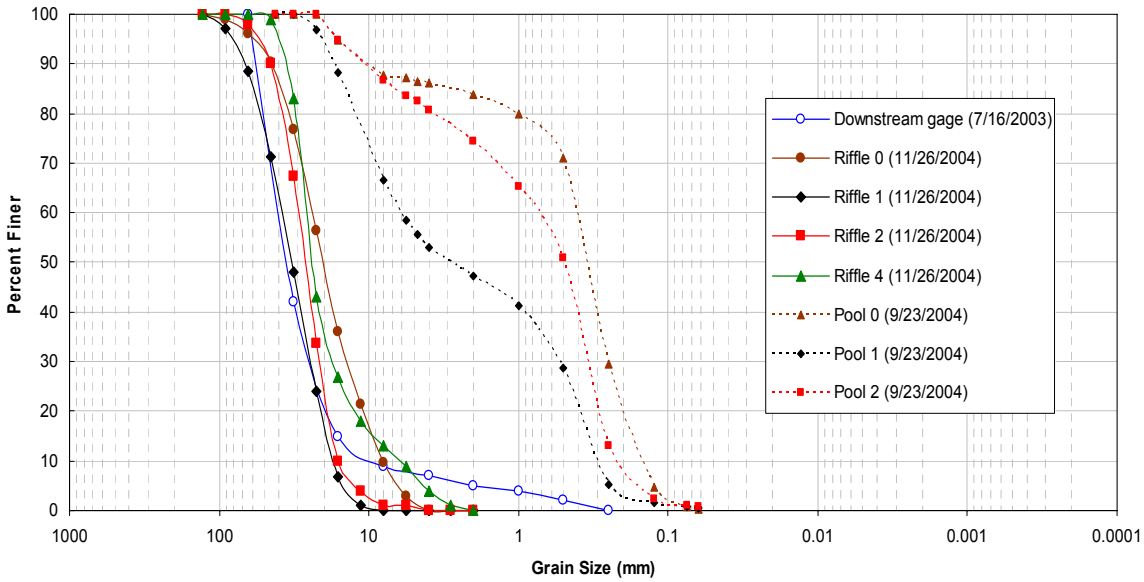

Figure 4.29. Particle-size distribution of samples at various riffle and pool locations in 2003 and 2004.

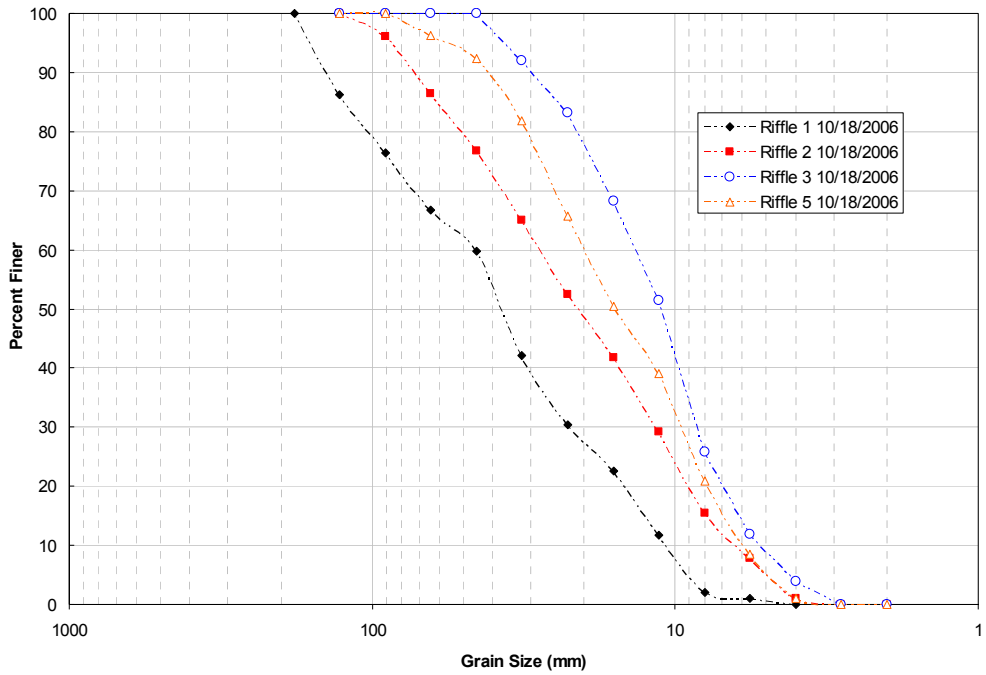

Figure 4.30. Particle-size distribution of samples at various riffle locations in 2006.

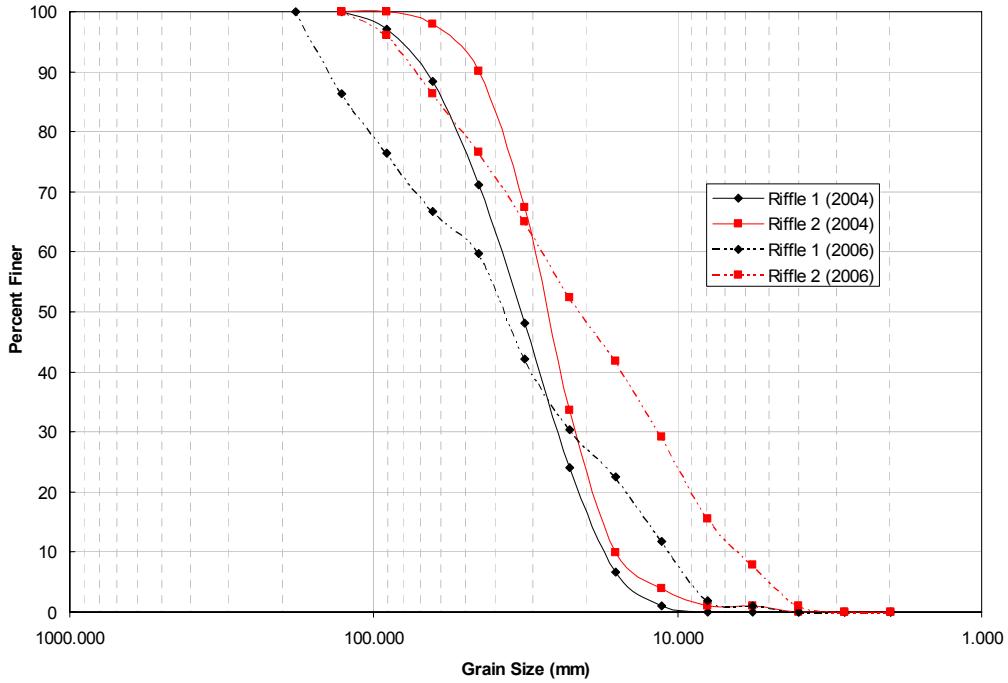

Figure 4.31. Particle-size distribution of samples at various riffle locations in 2004 and 2006.

At Riffles 4 and 5, the average D_{50} from the samplings in 2004 and 2006 was 20.5 mm (Figure 4.27). Riffles 4 and 5 are located near cross section 1287 (Figures 4.25 and 4.27). The shear stress for the 1.5-yr streamflow at this cross section (October 2006 conditions) is 16.1 Pa (Table 4.22). This shear stress indicates an average particle size moved of 19.0 mm, which is 8 percent less than the average D_{50} at Riffles 4 and 5.

The critical shear of the cohesive sample B1-EFA (8.5 Pa) (Table 4.14 and Figure 4.15) is 62 percent less than the available shear for the 1.5-yr streamflow (23.4 Pa) (Table 4.22) at cross section 227 (October 2006 conditions) (Figure 4.25). The area where the sample was taken has eroded and cobble covers much of the area.

The precursor knickpoint moved or was in the process of moving through the area near cross section 938 in the October 2006 conditions (Figure 4.26). This cross section is also near the cohesive sampling area B2B-EFA (Figures 4.15 and 4.25) with critical shears ranging from 1.0 to 5.3 Pa. The shear stress at cross section 938 for the 1.5-yr streamflow (October 2006 conditions) was 7.6 Pa (Table 4.22).

The critical shear of the cohesive sample B3-EFA (9.5 Pa) (Table 4.14 and Figure 4.15) is 41 percent less than the available shear for the 1.5-yr streamflow (16.1 Pa) (Table 4.22) at cross section 1287 (October 2006 conditions) (Figure 4.25). Erosion was seen in the field in this area with cobble filling in the eroded areas similar to the area near cross section 227.

Overall, the streambed appears to be stabilizing with the cobble and gravel from the old stream channel. Areas where the knickpoint has more recently moved through or is in the process of moving through are still transitioning to a stable state.

4.3.2 Streambank

Additional sampling of the streambanks and bed were taken with Shelby tube cores (Figure 4.32). The 3-in. Shelby tube cores allowed for geotechnical testing including the particle size, Atterberg Limits, and unconsolidated-undrained triaxial compression tests (UU) (Table 4.23 and Figure 4.33). The Bank Stability and Toe Erosion Model – Static Version 4.1 was used to assess the stability of the banks (Simon, 1989; Langendoen *et al*., 1999). To model the banks that formed downstream of the knickpoint at cross sections 227, 342, 474, and 717, a bank height of 4.5 ft, bank angle of 85 degrees (Figure 4.26), and bank composition of silt (Table 4.23) was chosen as input. The model was run with the water table at full, half, and zero bank height. All model runs were done with the water depth equal to 0.5 ft. The model was also run without tension cracks and with a 1.5-ft deep tension crack. The results of the modeling are shown in Table 4.24. Given a modeled factor of safety (*FS*) value for a bank, the following are criteria for determining stability (Simon, 1989; Langendoen *et al*., 1999):

- *FS* greater than 1.3 are considered stable;
- *FS* between 1.0 and 1.3 are considered conditionally stable (stable but with little safety margin); and
- *FS* less than 1.0 are unstable.

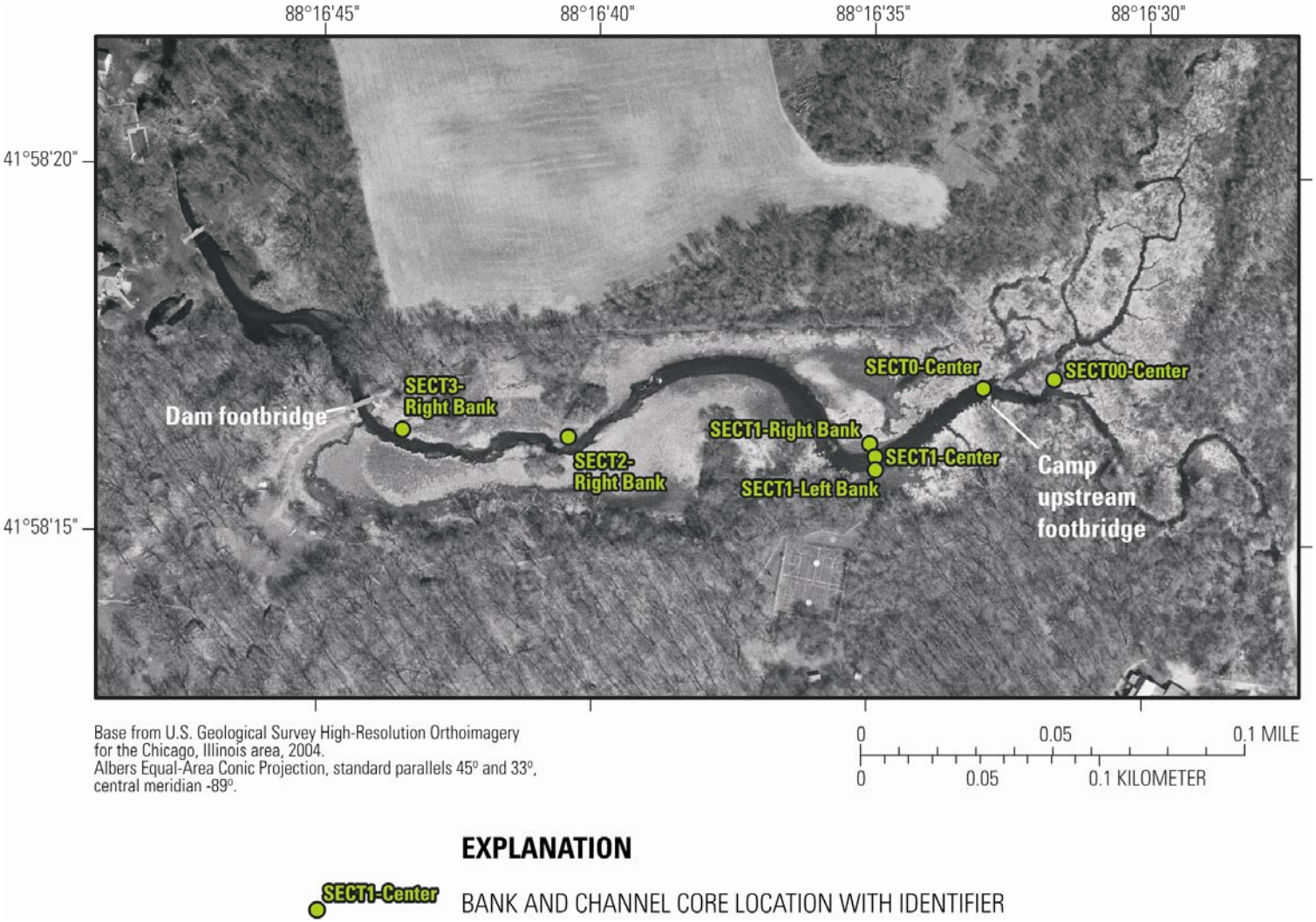

Figure 4.32. Location of Shelby tube samples taken to determine stability of banks.

Table 4.23. Summary of water content, specific weight Atterberg Limits, particle size, and type of geotechnical tests completed on streambank and streambed samples.

Sample Location	Depth (in.)	Water Content (percent)	Specific Weight		D_{50} (mm)	Percent Finer than 0.063 mm	Liquid Limit (percent)	Plastic Limit (percent)	Plasticity Index (percent)	Soil Type	UU Triaxial		Cohesion (psf)	Friction Angle (degrees)
			Wet (lb/ft^3)	Dry (lb/ft^3)							σ_3 (psf)	σ_1 (psf)		
Sect 00 Streambed	0-12 (0-4)	33.5	115.8	86.8	0.216	35.5	40.2	21.1	19.0	CL				
Sect 0 Streambed	3'6" - 6'				3.171	28.3	27.7	17.9	9.8	CL				
Sect 0 A	3'6" - 6'	39.5	109.2	78.3							750	2078	590	15
Sect 0 B	3'6" - 6'	33.1	115.5	86.8							500	2391	590	15
Sect 0 C	3'6" - 6'	31.7	121.9	92.6							288	2032	590	15
Sect 1 Left Bank	6-21 (17-21)	154.9	50.1	19.6	0.005	98.2								
Sect 1	6-21						NP	NP	NP					
Sect 2 Right Bank	20-35				0.014	98.7	63.3	34.0	29.3	MH				
Sect 2 A	30-35	73.0	61.4	35.5							750	1685	265	21
Sect 2 B	25-30	60.3	62.5	39.0							500	1812	265	21
Sect 2 C	20-25	91.1	57.9	30.2							288	1372	265	21
Sect 3 Right Bank	30-60				0.007	98.5	56.4	29.9	26.5	MH				
Sect 3 A	30-60	18.1	86.7	73.4							750	2089	210	19
Sect 3 B	30-60	83.8	60.0	32.6							500	1379	210	19
Sect 3 C	30-60	91.9	57.7	21.6							288	1169	210	19

CL = Inorganic clays of low to medium plasticity, gravelly clays, sandy clays, silty clays, lean clays
MH = Inorganic silts, micaceous or diatomaceous fine sands or silts, elastic silts
NP = non-plastic
UU = unconsolidated-undrained triaxial compression test
σ_1 = major principal stress
σ_3 = confining or chamber pressure

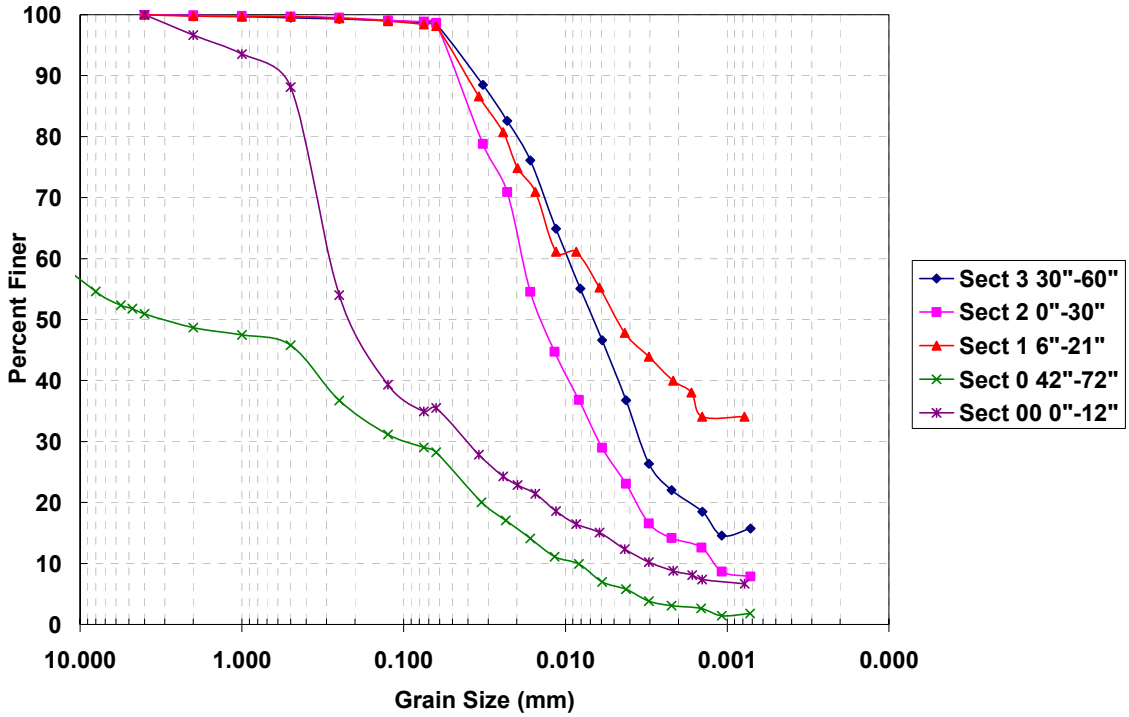

Figure 4.33. Particle-size distribution for streambank and streambed samples.

Table 4.24. Bank-stability model results.

	Factor of Safety	
Water-table Level	**No Tension Crack**	**Tension Crack (1.5-ft deep)**
Full-bank Height	1.0	0.8
Half-bank Height	1.3	1.2
Zero-bank Height	1.7	1.3

The banks with no tension cracks are considered stable (*FS* = 1.7) with a water table at zero-bank height. During storms, it is assumed that the stream will recede before the banks are fully drained. With a water table at half (*FS* = 1.3) or full-bank height (*FS* = 1.0), the streambanks were determined to be conditionally stable without tension cracks. In similar analysis after a dam removal in Wisconsin, model-simulation results showed strong control of bank stability by water-table levels (Doyle *et al*., 2003b).

Tension cracks were observed in the field and the banks were determined to be unstable (*FS* = 0.8) with the water table at full-bank height. With a water table at half (*FS* = 1.2) or zero-bank height (*FS* = 1.3), the streambanks were determined to be conditionally stable with tension cracks.

CHAPTER 5

SUMMARY, CONCLUSIONS, AND RECOMMENDATIONS

The objectives of this research were to evaluate erosion dynamics of a stepwise small dam removal on Brewster Creek near St. Charles, Illinois and develop analytical techniques for future application on small dams similar to the Brewster Creek dam. A stepwise dam-removal project, consisting of cutting five 12- to 18-in. notches in the dam, was completed from June 2003 through February 2004. The study area included Willow Lake with an 8-ft high and 30-ft wide dam.

5.1 Summary and Conclusions

In 2002, the lake had a surface area of 3.96 acres and had filled with sediment with an average water depth of less than 1 ft, sediment volume equaling 14.47 acre-ft, and average sediment thickness of 3.7 ft. The deposited sediments consisted of 67 to 99 percent silts and clays. The stream channel downstream of the dam consisted primarily of sand, gravel, and cobble.

The total sediment eroded during and after dam removal was approximately 13 percent of the lake sediment. The downstream normalized sediment yield (sediment yield divided by the mean-daily flow) during the notchings and the first 7 months after the notchings (June 15, 2003, through September 30, 2004) was 14 tons/mi^2-yr-ft^3/s.

From October 1, 2004, through September 30, 2006, the downstream normalized sediment yield (6.5 tons/mi^2-yr-ft^3/s) was within 17 percent of the upstream normalized sediment yield (5.4 tons/mi^2-yr-ft^3/s). This result is an indication that the stream channel evolving upstream of the old dam is becoming more stable.

After the first notching, a knickpoint established upstream of the dam and developed over time with further notchings and storms. A HEC-RAS flow model was applied to determine the shear stress acting upon the knickpoint for five surveyed conditions. The maximum knickpoint shear stress for each condition was always a result of flow between 50 ft^3/s and the 1.5-yr streamflow (139 ft^3/s). The backwater effects caused by the remnant abutments and embankments limited the shear stresses acting on the knickpoints for the two higher streamflows modeled (10- and 100-yr streamflows, 477 ft^3/s and 920 ft^3/s, respectively).

Empirical equations were determined to relate the knickpoint shear stress with eroded sediment for sixteen storms from November 2003 through February 2005. The eroded sediment for the sixteen storms (1,297 tons) accounts for approximately 87 percent of the total sediment eroded (1,490 tons) during stream-channel evolution. The empirical equations provide a way to estimate eroded sediment for any hydraulically modeled knickpoint shear stress for similar cohesive sediments.

Laboratory tests on undisturbed cohesive-sediment samples were completed to relate soil properties, flow conditions, and erosion rates. Several combinations of soil properties, flow conditions, and erosion rates were used to determine a suitable empirical equation. The final method utilized regression analysis to relate the erosion rate to the

shear stress of the flow, plasticity index of the soil, and percentage of the sample material finer than 0.063 mm.

A Cohesive Knickpoint Parallel Retreat method was developed utilizing the erosion-rate equation determined in this research from the cohesive-erosion laboratory testing results. The method was applied to the Brewster Creek study and predicted the eroded volume, knickpoint height, and migration length within 17, 20, and 6 percent, respectively, of measured values.

5.2 Recommended Analytical Techniques for Dam-removal Assessment

The following four steps are recommended for the analytical assessment of dam removal:

1. Determine the amount of deposited sediment and estimate potential amount to be eroded after dam removal.
2. Establish physical properties of the deposited sediment and pre-dam stream substrate.
3. Develop a model to simulate erosion rates, channel evolution, and final channel stability after dam removal.
4. Conduct a sediment balance of sediment passing upstream of the pool, in the pool, and downstream of the dam before and after dam removal.

General details of each step are discussed in the following sections.

5.2.1 Step 1 – Determine the amount of deposited sediment and estimate potential amount to be eroded after dam removal

The sediment thickness can be determined using a simple probing method or by using geophysical methods. The sediment thickness can be converted to volume of deposited sediment by multiplying each thickness measurement by a representative area. To estimate the potential amount to be eroded after dam removal, the average sediment thickness can be multiplied by an estimated channel width and reach length. The channel width can be obtained from looking at downstream reaches and/or measuring the abutment widths of the existing dam structure. The reach length can be obtained from the thalweg distance of the bottom of the deposited sediment. The estimate of eroded sediment calculated by this method was within 0.5 percent of the measured eroded sediment after dam removal in the Brewster Creek study. The estimates from this method can be used as a check of the proposed modeling in Step 3.

5.2.2 Step 2 – Establish physical properties of the deposited sediment and pre-dam stream substrate

Generally, the deposited sediment needs to be tested for contaminants. The material for the cores obtained for the sediment-quality testing can also be used to run tests on the physical properties like particle-size distribution, Atterberg Limits, specific weight, and shear strength. Also, the pre-dam substrate properties need to be determined and can be estimated from substrate in the channel upstream of the impoundment and/or downstream of the dam, if the material cannot be obtained from coring. Laboratory and field tests should continue to be run on undisturbed cohesive-sediment samples to better relate soil properties, flow conditions, and erosion rates. The properties from both the

deposited sediments and pre-dam substrate are important parameters in modeling the erosion rates, channel evolution, and final channel stability after dam removal.

5.2.3 Step 3 – Develop a model to simulate erosion rates, channel evolution, and final channel stability after dam removal

Depending on the properties of the deposited sediment and pre-dam stream substrate, an appropriate model should be chosen to simulate erosion rates, channel evolution, and final channel stability after dam removal. Due to the cohesive sediment deposited upstream of the Brewster Creek dam, a Cohesive Knickpoint Parallel Retreat method was developed to assess sediment erosion. After the method was applied using observed data, the impact of alternative stepwise notches was quantified utilizing the method. The assessment showed that the first three notches (with an eroded sediment equal to 60 tons) could have been combined to help minimize cost of dam removal without risking the release of large amounts of sediment. It was also shown that the maximum sediment yield for the alternative stepwise notches equaled 128 tons/mi^2-yr, which was 30 percent less than the maximum sediment yield that occurred during the 7 months after notching (183 tons/mi^2-yr) in the Brewster Creek dam removal.

The CKPR method may be applicable to future stepwise small dam-removal projects with similar dams, sediments, lakes, and watersheds. The backwater effects from the channel and the downstream abutments and embankments need to be remodeled for each dam and notching plan to obtain a reasonable range of knickpoint shear stresses for model input. Also, the plasticity index and percent fines of the deposited material need to be determined for the CKPR method to predict the erosion rate varying with cohesive-sediment material.

5.2.4 Step 4 – Conduct a sediment balance of sediment passing upstream of the pool, in the pool, and downstream of the dam before and after dam removal

Conducting a sediment balance before and after dam removal can help in understanding the processes of erosion, channel evolution, and channel stability as a result of dam removal. With more case studies and data like the Brewster Creek study, analytical techniques can continue to be improved to better assess future stepwise dam removals by minimizing the number of notches and sediment yield per notch.

CHAPTER 6

REFERENCES

Aberle, J., Nikora, V., and Walters, R., 2004, Effects of bed material properties on cohesive sediment erosion: *Marine Geology*, v. 207, pp. 83-93.

American Rivers, 2005, Dams slated for removal in 2005 and dams removed from 1999-2004, http://www.americanrivers.org/site/DocServer/Dam_Removal_Summary_2005.pdf?docID=2381.

American Society of Civil Engineers, 1997, Guidelines for retirement of dams and hydroelectric facilities, pp. 109-154.

American Society of Civil Engineers, 2005, Environmental and water resources institute dam removal workshops, http://www.ewrinstitute.org/damremoval04/ (accessed November 3, 2005).

American Society for Testing and Materials Standards, 2007, Thin-walled tube geotechnical sampling of soils, Standard D1587, http://www.astm.org/.

Ariathurai, R., and Arulanandan, K., 1978, Erosion rates of cohesive soils: *Journal of the Hydraulics Division*, v. 104, no. HY2, pp. 279-283.

Arulanandan, K., 1975, Fundamental aspects of erosion in cohesive soils: *Journal of the Hydraulics Division*, v. 101, no. HY5, Proceedings of the ASCE, New York, New York, pp. 635-639.

Arulanandan, K., Loganathan, P., and Krone, R.B., 1975, Pore and eroding fluid influence on surface erosion of soil: *Journal of the Geotechnical Engineering Division*, ASCE, New York, NY, v. 101, no. GT1, pp. 51-66.

Begin, Z.B., Meyer, D.F., and Schumm, S.A., 1980, Sediment production of alluvial channels in response to base level lowering: *Transactions of the American Society of Agricultural Engineers*, v. 23, no. 5, pp. 1183-1188.

Bennett, S.J., 1999a, Effect of slope on the growth and migration of headcuts in rills: *Geomorphology*, v. 30, no. 3, pp. 273-290.

Bennett, S.J., 1999b, An experimental study of headcut growth and development in upland concentrated flows, Channel & Watershed Processes Research Unit National Sedimentation Laboratory 13, pp. 1-190.

Bennett, S.J., Alonso, C.V., Prasad, S.N., and Romkens, M.J.M., 2000a, Experiments on headcut growth and migration in concentrated flows typical of upland areas: *Water Resources Research*, v. 36, no. 7, pp. 1911-1922.

Bennett, S.J., Robinson, K.M., Simon, A., and Hanson, G.J., 2000b, Stable knickpoints formed in cohesive sediment, In: Proceedings of the 2000 Joint Conference on Water Resources Engineering and Water Resources Planning and Management, Minneapolis, MN.

Bhowmik, N.G., Adams, J.R., Bonini, A.P., Klock, A.M., and Demissie, M., 1986, Sediment loads of Illinois streams and rivers, Report of Investigation 106, 167 p.

Bonini, A.P., Bhowmik, N.G., Allgire, R.L., and Davie, D.K., 1983, Statewide Instream Sediment Monitoring Program for Illinois, Annual Report – Water Year 1981, SWS Contract Report 318A, pp. 1-45.

Born, S.M., Genskow, K.D., Filbert, T.L., Hernandez-Mora, N., Keefer, M.L., and White, K.A., 1998, Socioeconomic and institutional dimensions of dam removals: The Wisconsin experience: *Environmental Management*, v. 22, no. 3, pp. 359-370.

Briaud, J., Ting, F., Chen, H.C., Gudavilli, R., Kwak, K., Philogene, B., Han, S., Perugu, S., Wei, G., Nurtjahyo, P., Cao, Y., and Li, Y., 1999, SRICOS: Prediction of scour rate at bridge piers, The Texas A&M University System TX-00/2937-1, pp. 1-126.

Briaud, J.-L., Ting, F.C.K., Chen, H.C., Gudavalli, S.R., and Kwak, K., 2002, Maximum scour depth around a bridge pier in sand and in clay: Are they equal? In: Proceedings of the International Deep Foundations Congress, Orlando, FL, pp. 385-395.

Briaud, J.L., Chen, H.C., Nurtjahyo, P., and Wang, J., 2003, Complex pier scour and contraction scour in cohesive soils, National Cooperative Highway Research Program Report 24-15.

Bunte, K., and Abt, S.R., 2001, Sampling surface and subsurface particle-size distributions in wadable gravel- and cobble-bed streams for analysis in sediment transport, hydraulics, and streambed monitoring, U. S. Department of Agriculture, Forest Service General Technical Report RMRS-GTR-74.

Bushaw-Newton, K.L., Hart, D.D., Pizzuto, J.E., Thomson, J.R., Egan, J., Ashley, J.T., Johnson, T.E., Horwitz, R.J., Keeley, M., Lawrence, J., Charles, D., Gatenby, C.,

Kreeger, D.A., Nightengale, T., Thomas, R.L., and Velinsky, D.J., 2002, An integrative approach towards understanding ecological responses to dam removal: The Manatawny Creek study: *Journal of the American Water Resources Association*, v. 38, no. 6, pp. 1581-1599.

Cantelli, A., Paola, C., and Parker, G., 2004, Experiments on upstream-migrating erosional narrowing and widering of an incisional chanel casued by dam removal: *Water Resources Research*, v. 40, no. 3, W03304.03301-W03304.03312.

Cantelli, A., Wong, M., and Parker, G., 2006, Numerical study of the response of a reservoir deposit to sudden dam removal, In: Proceedings of the Eighth Federal Interagency Sedimentation Conference, Reno, NV.

Casagrande, A., 1948, Classification and identification of soils: *Transactions of the American Society of Civil Engineers*, 113, pp. 901-991.

Casalí, J., and Bennett, S.J., 2001, Effect of initial step height on headcut development in upland concentrated flows, Channel & Watershed Processes Research Unit National Sedimentation Laboratory 19, pp. 1-169.

Cutshaw, S.R., Mills, P.C., Hogan, J.L., and Fazio, D.J., 2004, Water resources data – Illinois, Water Year 2004, U. S. Geological Survey Water-Data Report IL-04, 841 p.

Das, B.M., 2002, Principles of Geotechnical Engineering, Brooks/Cole, 589 p.

Doyle, M.W., and Harbor, J.M., 2003, Forum: Toward policies and decision-making for dam removal: *Environmental Management*, v. 31, no. 4, pp. 453-465.

Doyle, M.W., and Stanley, E.H., 2005, Stream ecosystem response to experimental dam removals, In: Proceedings of the 2005 Watershed Management Conference:

Managing Watersheds for Human and Natural Impacts, Williamsburg, VA, Environmental and Water Resources Institute, American Society of Civil Engineers.

Doyle, M.W., Stanley, E.H., and Harbor, J.M., 2003a, Channel adjustments following two dam removals in Wisconsin: *Water Resources Research*, v. 39, no. 1, 1011, pp. 1-15.

Doyle, M.W., Stanley, E.H., Selle, A.R., Stofleth, J.M., and Harbor, J.M., 2003b, Predicting the depth of erosion in reserviors following dam removal using bank stability analysis: *International Journal of Sediment Research*, v. 18, no. 2, pp. 115-121.

Dunn, I.S., 1959, Tractive resistance of cohesive channels: *Journal of Soil Mechanics and Foundations Division*, v. 85, no. SM3, Proceedings Paper No. 2062, ASCE, New York, NY, pp. 1-24.

Edwards, T.K., and Glysson, G.D., 1999, Field methods for measurement of fluvial sediment, U. S. Geological Survey Techniques of Water-Resources Investigations Report, book 3, chapter C2, 89 p.

Enger, P.F., Smerdon, E.T., and Masck, F.D., 1968, Task Committee on Erosion of Cohesive Soils, July 1968, Erosion of Cohesive Soils: *Journal of the Hydraulics Division*, v. 94, no. HY4, Proceedings of the ASCE, pp. 1017-1049.

Exner, F.M., 1925, Uber die wechselwirkung zwischen wasser und geschiebe in flussen, Sitzenberichte der Academie der Wissenschaften, Wien, Austria, Sec. IIA, pp. 133:199.

Fredsoe, J., 1974, On the development of dunes in erodible channels: *Journal of Fluid Mechanics*, v. 64, no. 1, pp. 1-16.

Fredsoe, J., 1978, Sedimentation of river navigation channels: *Journal of Hydraulics Division*, v. 104, no. 2, pp. 223-236.

Gardner, T.W., 1983, Experimental study of knickpoint and longitudinal profile evolution in cohesive, homogeneous material: *Geological Society of America Bulletin*, v. 94, no. 5, pp. 664-672.

Gibson, S.A., and Little, Jr., C.D., 2006, Implementation of the sediment impact assessment model (SIAM) in HEC-RAS, In: Proceedings of the Eighth Federal Interagency Sedimentation Conference, Reno, NV.

Goodell, C.R., and Bradley, J.B., 2005, Sediment management for dam removal: An HEC-6 approach, In: Proceedings of the 2005 Watershed Management Conference: Managing Watersheds for Human and Natural Impacts, Williamsburg, VA, Environmental and Water Resources Institute, American Society of Civil Engineers.

Graber, B.E., Carney, R.S., Fisher, M., Bowman, M., Doyle, M.W., Mackey, S.D., and Wildman, L., 2001, Technical issues in small dam removal engineering, In: The Future of Dams and Their Reservoirs, 21st Annual USSD Lecture Series, Denver, CO.

Graf, W.L. (Ed.), 2002, Dam removal research: Status and prospects, In: The Heinz Center's Dam Removal Research Workshop, Washington, DC, The H. John Heinz III Center for Science, Economics and the Environment, pp. 1-151.

Guy, H.P., 1970, Fluvial sediment concepts, U. S. Geological Survey Techniques of Water-Resources Investigations Report, book 3, Applications of Hydraulics, chapter C1, 55 p., accessed at http://water.usgs.gov/pubs/twri/.

Hanson, G.J., and Simon, A., 2001, Erodibility of cohesive streambeds in the loess area of the midwestern USA: *Hydrological Processes*, v. 15, pp. 23-38.

Hanson, G.J., and Cook, K.R., 2003, Apparatus, test procedures, and analytical methods to measure soil erodibility in situ: *Applied Engineering in Agriculture*, v. 20, pp. 455-462.

Hanson, G.J., Robinson, K.M., Cook, K.R., and Temple, D.M., 2004, Modeling of erosion from headcut development in channelized flow, In: Proceedings of the Sixth International Conference on Hydro-Science & Engineering, Brisbane, Australia.

Heinz Center, 2002, Dam removal: Science and decision making, The H. John Heinz III Center for Science, Economics and the Environment, pp. 1-221.

Highway Research Board, 1970, Tentative design procedure for riprap-lined channels. Report no. 108 Washington, DC, National Academy of Sciences, National Cooperative Highway Research Program.

Hotchkiss, R.H., and McClenathan, J.T., 1997, Physical processes of cohesive stream bed erosion in Eastern Nebraska, In: Proceedings of the Conference on Management of Landscapes Distributed by Channel Incision.

Julien, P.Y., 1998, Erosion and Sedimentation, Cambridge University Press, New York, NY, 280 p.

Julien, P.Y., 2002, River Mechanics, Cambridge University Press, New York, NY, 434 p.

Kane County Environmental Management, 2006, Brewster Creek: Dam removal and stream restoration, http://www.co.kane.il.us/kcstorm/brewster/ywca.asp.

Kelly, E.K., and Gularte, R.C., 1981, Erosion resistance of cohesive soils: *Journal of the Hrdraulics Division*, v. 107, no. HY10, Proceedings of the ASCE, New York, NY, pp. 1211-1224.

Kwak, K., Briaud, J.-L., and Chen, H.C., 2001, SRICOS: Computer program for bridge pier scour, In: Proceedings of the Fifteenth International Conference on Soil Mechanics and Geotechnical Engineering, Istanbul, Turkey, A. A. Balkema Publishers.

Langendoen, E.J., Simon, A., Curini, A., and Alonso, C.V., 1999, Field validation of an improved process-based model for streambank stability analysis, In: Proceedings 1999 International Water Resources Engineering Conference, Seattle, WA, http://www.ars.usda.gov/Business/docs.htm?docid=5457&pf=1&cg_id=0.

Langendoen, E.J., 2000, CONCEPTS – Conservational channel evolution and pollutant transport system, Research Report No. 16, 180 p.

Langendoen, E.J., Simon, A., and Alonso, C.V., 2000, Modeling channel instabilities and mitigation strategies in eastern Nebraska, In: Proceedings 2000 Joint Conference on Water Resources Engineering and Water Resources Planning & Management, Minneapolis, MN, http://www.ars.usda.gov/Business/docs.htm?docid=5457&pf=1&cg_id=0.

Langendoen, E.J., Simon, A., and Thomas, R.E., 2001, CONCEPTS – A process-based modeling tool to evaluate stream-corridor restoration designs, In: Proceeding 2001 Wetland Engineering & River Restoration Conference, Reno, NV, U. S.

Department of Agriculture, Agricultural Research Service, http://www.ars.usda.gov/Business/docs.htm?docid=5457&pf=1&cg_id=0.

Langendoen, E.J., Thomas, R.E., and Binger, R.L., 2002, Numerical simulation of the morphology of the Upper Yalobusha River, Mississippi between 1968 and 1997, In: River Flow 2002, Proceedings of the International Conference on Fluvial Hydraulics, Louvain-la-Neuve, Belgium, U. S. Department of Agriculture, Agricultural Research Service, http://www.ars.usda.gov/Business/docs.htm?docid=5457&pf=1&cg_id=0.

Langendoen, E.J., Wells, R.R., and Simon, A., 2005, Numerical simulation of post dam removal sediment dynamics along the Kalamazoo river between Otsego and Plainwell, Michigan, In: Proceedings of the 2005 Watershed Management Conference: Managing Watersheds for Human and Natural Impacts, Williamsburg, VA, Environmental and Water Resources Institute, American Society of Civil Engineers.

Langendoen, E.J., and Wells, R.R., 2006, Numerical simulation of channel adjustment of the Kalamazoo River following the removal of two low-head dams between Otsego and Plainwell, Michigan, In: Proceedings of the Eighth Federal Interagency Sedimentation Conference, Reno, NV.

Leighton, M.M., Ekblaw, G.E., and Horberg, L., 1948, Physiographic divisions of Illinois, Illinois State Geological Survery, Department of Registration and Education: Reprinted from the *Journal of Geology*, v. 56, no. 1, p. 33.

Lyle, W.M., and Smerdon, E.T., 1965, Relation of compaction and other soil properties to erosion and resistance of soils: *Transaction of the American Society of Agricultural Engineers*, v. 8, no. 3.

MacBroom, J.G., 2005, Evolutions of channels upstream of dam removal sites, In: Proceedings of the 2005 Watershed Management Conference: Managing Watersheds for Human and Natural Impacts, Williamsburg, VA, Environmental and Water Resources Institute, American Society of Civil Engineers.

Mehta, A.J., Hayter, E.J., Parker, W.R., Krone, R.B., and Teeter, A.M., 1989, Cohesive sediment transport, Part I: Process description: *Journal of Hydraulic Engineering*, v. 115, no. 8, pp. 1076-1093.

Moody, L.F., 1944, Friction factors for pipe flow: *Transaction of the American Society of Mechanical Engineers*, v. 66, pp. 671-684.

Orr, C.H., and Stanley, E.H., 2006, Vegetation development and restoration potential of drained reserviors following dam removal in Wisconsin: *River Research and Applications*, v. 22, no. 3, pp. 281-295.

Papanicolaou, A.N., 2001, Erosion of cohesive streambeds and banks, State of Washington Water Research Center Report WRR-08, 20 p.

Parchure, T.M., and Mehta, A.J., 1985, Erosion of soft cohesive sediment deposits: *Journal of Hydraulic Engineering*, v. 111, no. 10, pp. 1309-1326.

Pizzuto, J., 2002, Effects of dam removal on river form and process: *BioScience*, v. 52, no. 8, pp. 683-691.

Porterfield, G., 1972, Computation of fluvial-sediment discharge, U. S. Geological Survey Techniques of Water-Resources Investigations Report, book 3, chapter C3, 66 p., accessed at http://water.usgs.gov/pubs/twri/.

Rantz, S.E. and others, 1982, Measurement and computation of streamflow, U. S. Geological Survey Water-Supply Paper 2175, v. 1 and 2, 631 p.

Raudkivi, A.J., 1976, Loose Boundary Hydraulics, Pergamon Press, New York, NY, 276 p.

Ritter, D.F., Kochel, R.C., and Miller, J.R., 1999, The disruption of Grassy Creek: Implications concerning catastrophic events and threholds: *Geomorphology*, v. 29, no. 3-4, pp. 323-338.

Schumm, S.A., Harvey, M.D., and Watson, C.C., 1984, Incised Channels: Morphology, Dynamics and Control, Water Resources Publications, LLC, Littleton, CO, 200 p.

Sethi, S.A., Selle, A.R., Doyle, M.W., Stanley, E.H., and Kitchel, H.E., 2004, Response of unionid mussels to dam removal in Koshkonong Creek, Wisconsin: *Hydrobiologia*, v. 525, pp. 157-165.

Shields, A., 1936, Application of similarity principles and turbulence research to bedload movement, *translated from* Anwendung der Aehnlichkeitsmechanik und der Turbulenzforschung auf die Geschiebewegung: Mitteilung Preussischen Versuchanstalt für Wasserbau und Schiffbau, Berlin, no. 26, by W.P. Ott and J.C. van Uchelen, California Institute of Technology Hydro-dynamics, Pasadena, CA, Report No. 167, 43 p.

Simon, A., and Hupp, C.R., 1986, Channel evolution in modified Tennessee channels, In: Proceedings of the Federal Interagency Sedimentation Conferences, Las Vegas, NV, pp. 71-82.

Simon, A., 1989, A model of channel response in disturbed alluvial channels: *Earth Surface Processes and Landforms*, v. 14, no. 1, pp. 11-26.

Simon, A., and Thomas, R.E., 2002, Processes and forms of an unstable alluvial system with resistant, cohesive streambeds: *Earth Surface Processes and Landforms*, v. 27, pp. 699-718.

Skalak, K., and Pizzuto, J., 2005, The geomorphic effects of existing dams and historic dam removals in the mid-Atlantic region, USA, In: Proceedings of the 2005 Watershed Management Conference: Managing Watersheds for Human and Natural Impacts, Williamsburg, VA, Environmental and Water Resources Institute, American Society of Civil Engineers.

Smerdon, E.T., and Beasley, R.P., 1959, Tractive force theory applied to stability of open channels in cohesive soils, Agricultural Experiment Station, University of Missouri, Columbia, MO, Research Bulletin No. 715.

Stein, O.R., and Julien, J.P., 1993, Criterion delineating the mode of headcut migration: *Journal of Hydraulic Engineering*, v. 119, no. 1.

Stewart, G., and Grant, G., 2005, What can we learn from the removal of little dinky dams, In: Proceedings of the 2005 Watershed Management Conference: Managing Watersheds for Human and Natural Impacts, Williamsburg, VA, Environmental and Water Resources Institute, American Society of Civil Engineers.

Straub, T.D., Johnson, G.P., Roseboom, D.P., and Sierra, C.R., 2006, Suspended-sediment yields and stream-channel processes on Judy's Branch watershed in the St. Louis Metro East region in Illinois, Scientific Investigations Report 2006-5016.

Terzaghi, K., Peck, R.B., and Mesri, G., 1996, Soil Mechanics in Engineering Practice, John Wiley and Sons, Inc., New York, NY, 3rd edition, 549 p.

Thomas, W.A., 2005, Sedimentation studies for dam removal using HEC-6T, In: Proceedings of the 2005 Watershed Management Conference: Managing Watersheds for Human and Natural Impacts, Williamsburg, VA, Environmental and Water Resources Institute, American Society of Civil Engineers.

Thomas, Jr., W.O., Lumb, A.M., Flynn, K.M., and Kirby, W.H., 1998, Users manual for program PEAKFQ, annual flood-frequency analysis using Bulletin 17B guidelines, 89 p., http://water.usgs.gov/software/peakfq.html (accessed March 13, 2001).

U. S. Army Corps of Engineers, 2001, HEC-RAS river analysis system, hydraulic reference manual - version 3.0.1, various chapters plus appendices.

U. S. Department of Agriculture, Natural Resources Conservation Service, 1994, State soil geographic (STATSGO) data base – data use information, miscellaneous publication number 1492 (rev. ed.), variously paginated.

U. S. Department of Agriculture, Soil Conservation Service, 1986, Urban hydrology for small watersheds, Technical Release 55.

U. S. Department of Commerce, National Oceanic Atmospheric Administration, 2006, NOAA home page, http://www.noaa.gov/ (accessed November 21, 2006).

Watson, C.C., and Biedenharn, D.S., 2006, Judy's Branch, Illinois rehabilitation plan, In: Proceedings of the Eighth Federal Interagency Sedimentation Conference, Reno, NV.

Watson, C.C., Harvey, M.D., and Garbrecht, J., 1986, Geomorphic-hydraulic simulation of channel evolution, In: Proceedings of the Federal Interagency Sedimentation Conference, Las Vegas, NV, pp. 21-30.

Zimbone, S.M., Vickers, A., Morgan, R.P.C., and Vella, P., 1996, Field investigations of different techniques for measuring surface soil shear strength: *Soil Technology*, v. 9, pp. 101-111.

APPENDIX A

NOTCHING DISSOLVED OXYGEN DATA

Results indicate that the notchings did not drop the dissolved-oxygen concentrations below 7 mg/L in Brewster Creek (Figure A.1). Before removal of the dam, the upstream lake was almost full of sediment, with maximum water depths of approximately 2 ft. The lack of a decline in dissolved-oxygen concentration during at least the first notching could indicate a well-mixed lake with no areas of low dissolved-oxygen concentrations given the low-water depths in the lake.

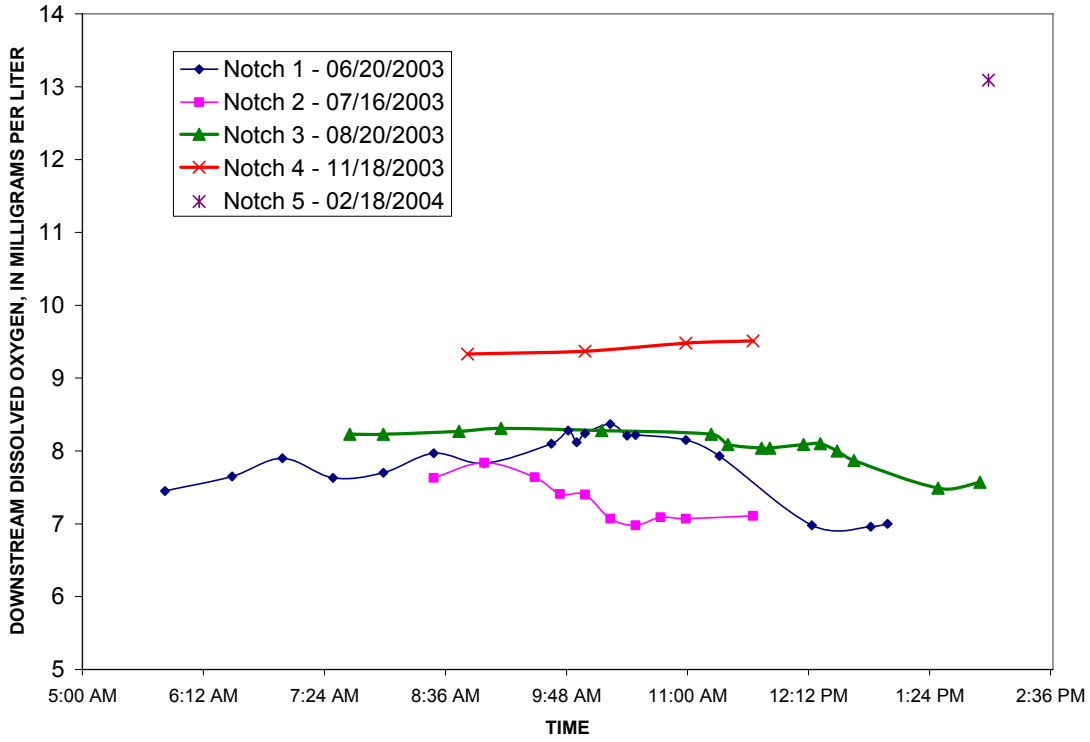

Figure A.1. Dissolved-oxygen concentrations during notching events at the downstream station on Brewster Creek near St. Charles, Illinois.

APPENDIX B

BIOTIC RESPONSE

B.1 Response of stream fisheries to sediment movement from stream-channel evolution by Steve Pescitelli, Illinois Department of Natural Resources Stream Fisheries Biologist

The YWCA Dam on Brewster Creek was removed as a part of a multi-agency effort to eliminate safety hazards and restore biological integrity in the watershed. An important goal of the project was to evaluate effects of the dam removal on physical, chemical, and biological features of the stream, particularly in the downstream areas. Pre- and post-project monitoring will also provide information on project success regarding restoration of upstream biological communities. This appendix summarizes the interim results of fish-community evaluation following completion of dam removal in February 2004 (Figure B.1 and Table B.1).

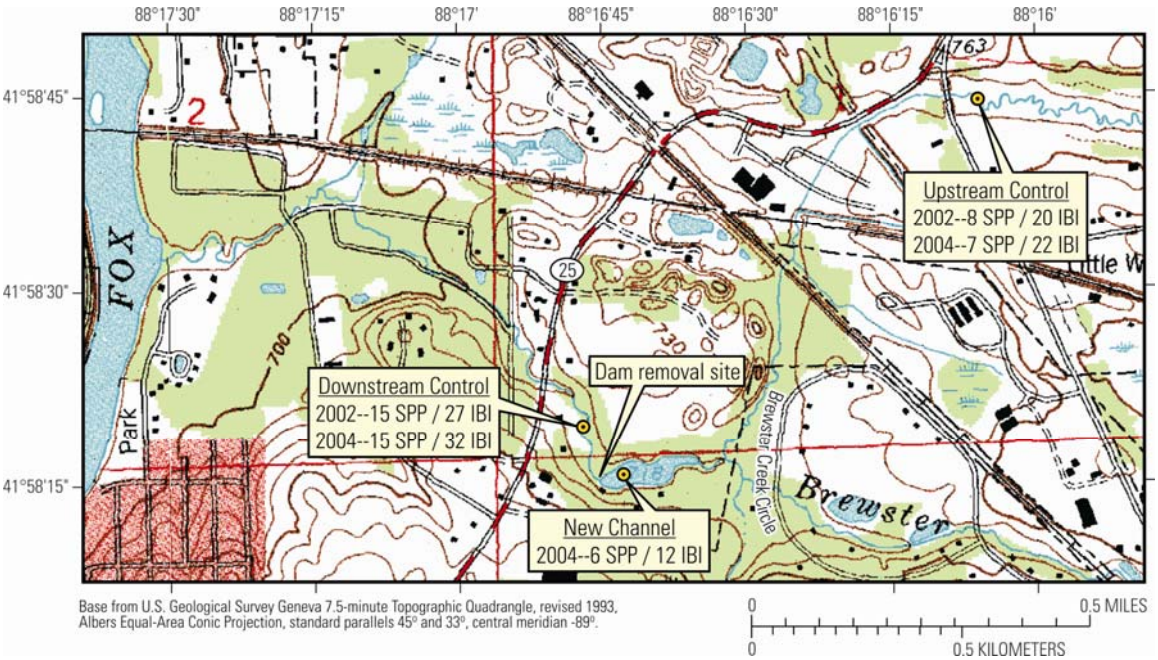

Figure B.1. Stream fish-survey locations and corresponding species (SPP) and IBI.

Table B.1. Surveyed stream fishes and corresponding IBI for each control section and the new channel.

Common Name	Downstream Control		Upstream Control		New Channel
	2002	2004	2002	2004	2004
Central mudminnow	0	0	0	1	0
Grass pickerel	1	1	0	4	1
Carp	2	0	0	0	10
Golden shiner	0	9	0	0	0
Creek chub	2	7	11	6	0
Hornyhead chub	55	34	0	0	0
Striped shiner	0	3	0	0	0
Spotfin shiner	43	68	0	0	0
Bluntnose minnow	73	64	28	0	0
White sucker	2	0	3	0	0
Channel catfish	1	0	0	0	0
Yellow bullhead	3	8	3	7	2
Stonecat	17	29	0	0	0
Largemouth bass	2	3	2	1	6
Smallmouth bass	4	4	0	0	0
Green sunfish	92	57	23	19	9
Sunfish hybrid	3	9	0	0	2
Bluegill	122	36	6	0	1
Pumpkinseed	2	5	0	0	0
Johnny darter	0	3	0	0	0
Fantail darter	0	0	5	10	0
Total fish	424	340	81	48	31
Total species	15	15	8	7	6
IBI	27	32	20	22	12

Fish-community samples were taken at three sites on August 25, 2004, using a backpack electrofishing unit. The downstream control site was located upstream of Illinois Route 25 and the upstream control site was upstream of Dunham Road; the third site was located in the new channel formed within the former lake bed, upstream of the YWCA dam-removal site. The two control stations were also sampled prior to dam removal in 2002. Each station was approximately 450 ft in length.

Results at the control stations were similar in 2002 and 2004. These results indicate no adverse effects from the dam removal. Habitat was essentially unchanged at the downstream control in 2004. Number of species, total abundance, and Index of Biotic

Integrity (IBI) were also very similar for pre- and post-construction samples, suggesting little impact resulting from sediment movement even though the survey occurred immediately after the period of greatest channel erosion and sediment transport.

Low streamflow conditions in late 2005 and early 2006 resulted in long segments of a dry stream channel. Fish monitoring was postponed until normal streamflows resulted. Monitoring of fish communities in Brewster Creek will continue over the next few years in order to evaluate effects of the YWCA Dam removal.

B.2 Response of vegetation to dam removal by Jeff Mengler, U. S. Fish and Wildlife Service Botanist, and Don Roseboom, U. S. Geological Survey Hydrologist

Revegation of the lake bed occurred within weeks after the first notch in June 2003 (Figure 4.3). A burn was conducted on the exposed overbanks in April 2004. The burn was intended to control reed canary grass and purple loosestrife. Prairie and annual rye seeds were broadcast in May 2004. By seeding, the hope was to encourage a healthy plant community as best as possible. Selective herbiciding was conducted in June 2004 to control reed canary grass and purple loosestrife. By the summer of 2004, Jeff Mengler's (U. S. Fish and Wildlife Botanist) survey of wetland vegetation of the former lake bed reported that native plants were 82 percent of the species found and dominated the landscape (Table B.2).

Low flows allowed dense revegetation of lower banks and point bars in August 2005 (Figure B.2). Continued low-flow conditions in late 2005 and early 2006 resulted in the introduction of less desirable plant species, which have not been quantified by a following plant survey. An operations and management plan intends to encourage the

natural establishment of a stable, native ecosystem with as little intervention (and cost) as possible. To achieve this goal, regular maintenance activities (burns, herbiciding, and seeding) are planned each year.

Table B.2. Plant survey on June 24, 2004 in the old lakebed by Jeff Mengler, U. S. Fish and Wildlife Service Botanist (italic green text indicates native species).

C	SCIENTIFIC NAME	W	WETNESS	PHYSIOGNOMY	COMMON NAME
0	*Acer negundo*	-2	FACW-	Nt Tree	BOX ELDER
0	*Acnida altissima*	-5	OBL	Nt A-Forb	WATER HEMP
4	*Alisma subcordatum*	-5	OBL	Nt P-Forb	COMMON WATER PLANTAIN
7	*Angelica atropurpurea*	-5	OBL	Nt P-Forb	GREAT ANGELICA
0	ARCTIUM MINUS	5	UPL	Ad B-Forb	COMMON BURDOCK
0	BARBAREA VULGARIS	0	FAC	Ad B-Forb	YELLOW ROCKET
5	*Bidens cernua*	-5	OBL	Nt A-Forb	NODDING BUR MARIGOLD
1	*Bidens frondosa*	-3	FACW	Nt A-Forb	COMMON BEGGAR'S TICKS
3	*Carex stipata*	-5	OBL	Nt P-Sedge	COMMON FOX SEDGE
0	CIRSIUM ARVENSE	5	UPL	Ad P-Forb	FIELD THISTLE
1	*Cornus racemosa*	-2	FACW-	Nt Shrub	GRAY DOGWOOD
9	*Houstonia caerulea*	0	FAC	Nt P-Forb	BLUETS
3	*Impatiens capensis*	-3	FACW	Nt A-Forb	ORANGE JEWELWEED
5	*Iris virginica shrevei*	-5	OBL	Nt P-Forb	BLUE FLAG
4	*Juncus dudleyi*	0	[FAC]	Nt P-Forb	DUDLEY'S RUSH
4	*Leersia oryzoides*	-5	OBL	Nt P-Grass	RICE CUT GRASS
5	*Lycopus americanus*	-5	OBL	Nt P-Forb	COMMON WATER HOREHOUND
0	LYTHRUM SALICARIA	-5	OBL	Ad P-Forb	PURPLE LOOSESTRIFE
5	*Mentha arvensis villosa*	-5	[OBL]	Nt P-Forb	WILD MINT
5	*Penthorum sedoides*	-5	OBL	Nt P-Forb	DITCH STONECROP
0	PHALARIS ARUNDINACEA	-4	FACW+	Ad P-Grass	REED CANARY GRASS
0	*Plantago rugelii*	0	FAC	Nt A-Forb	RED-STALKED PLANTAIN
0	POLYGONUM PERSICARIA	1	[FAC-]	Ad A-Forb	LADY'S THUMB
2	*Populus deltoides*	-1	FAC+	Nt Tree	EASTERN COTTONWOOD
4	*Potentilla simplex*	4	FACU-	Nt P-Forb	COMMON CINQUEFOIL
6	*Ranunculus sceleratus*	-5	OBL	Nt A-Forb	CURSED BUTTERCUP
7	*Ribes americanum*	-3	FACW	Nt Shrub	WILD BLACK CURRANT
4	*Rorippa palustris fernaldiana*	-5	OBL	Nt A-Forb	MARSH CRESS
0	RUMEX CRISPUS	-1	FAC+	Ad P-Forb	CURLY DOCK
8	*Rumex orbiculatus*	-5	OBL	Nt P-Forb	GREAT WATER DOCK
4	*Sagittaria latifolia*	-5	OBL	Nt P-Forb	COMMON ARROWHEAD
4	*Salix nigra*	-5	OBL	Nt Tree	BLACK WILLOW
1	*Sambucus canadensis*	-2	FACW-	Nt Shrub	ELDERBERRY
4	*Scirpus fluviatilis*	-5	OBL	Nt P-Sedge	RIVER BULRUSH
5	*Scirpus validus creber*	-5	OBL	Nt P-Sedge	GREAT BULRUSH
1	*Solidago altissima*	3	FACU	Nt P-Forb	TALL GOLDENROD
6	*Sparganium eurycarpum*	-5	OBL	Nt P-Forb	COMMON BUR REED
8	*Symplocarpus foetidus*	-5	OBL	Nt P-Forb	SKUNK CABBAGE
0	TARAXACUM OFFICINALE	3	FACU	Ad P-Forb	COMMON DANDELION
1	*Typha angustifolia*	-5	OBL	Nt P-Forb	NARROW-LEAVED CATTAIL
1	*Typha latifolia*	-5	OBL	Nt P-Forb	BROAD-LEAVED CATTAIL
2	*Urtica procera*	-1	FAC+	Nt P-Forb	TALL NETTLE
4	*Verbena hastata*	-4	FACW+	Nt P-Forb	BLUE VERVAIN
5	*Viburnum lentago*	-1	FAC+	Nt Shrub	NANNYBERRY

FLORISTIC QUALITY DATA	*Native*	*36*	*81.8%*	Adventive	8	18.2%
36 NATIVE SPECIES	Tree	3	6.8%	Tree	0	0.0%
44 Total Species	Shrub	4	9.1%	Shrub	0	0.0%
23.0 NATIVE FQI	P-Forb	18	40.9%	P-Forb	4	9.1%
20.8 W/Adventives	B-Forb	0	0.0%	B-Forb	2	4.5%
-3.3 NATIVE MEAN W	A-Forb	7	15.9%	A-Forb	1	2.3%
-2.6 W/Adventives	P-Grass	1	2.3%	P-Grass	1	2.3%
AVG: Fac. Wetland	P-Sedge	3	6.8%	P-Sedge	0	0.0%

(a) (b)

Credit: Photographs taken by Don Roseboom, USGS

Figure B.2. Photographs taken on August 24, 2005 show that low flows have allowed dense revegetation of lower banks and point bars throughout the channel that has evolved in the old lake bed (view looking downstream).

B.3 Brewster Creek Mussel Survey Results by Roger Klocek, Shedd Aquarium in Chicago

On July 10, 2002, a Unionid mussels survey was conducted at the base of the dam, as well as two additional sites further downstream. Site 1 and 2 surveys encompassed shoreline to shoreline, and were intended to secure every live mussel for relocation downstream. Site 3 was surveyed for mussel abundance only, and mussels found there were not relocated. The Site 1 survey incorporated the concrete apron at the base of the dam, that stretched about 20 ft below the dam, and included a further 80 ft of stream bottom. This bottom consisted of close-packed cobble with few gravel pockets. Site 2 started where Site 1 ended, and encompassed approximately 100 linear feet of creek. The substrate consisted of mostly fine sediment with some woody debris. Site 3 had a very high gradient, cobbly section of the creek on private land below the footbridge. The results of the mussel survey are listed in Table B.3.

Table B.3. Results of mussel survey.

Site 1:
Pyganodon grandis, giant floater, six live individuals
Site 2:
Pyganodon grandis, giant floater, twenty-nine live individuals
Lasmigona complanata, white heelsplitter, none live, relic shells only
Site 3:
Lampsilis cardium, plain pocketbook, nine live individuals
*Pyganodon grandi*s, giant floater, one live individual
Relic shells only
Lasmigona complanata, white heelsplitter
*Lasmigona comp*ressa, creek heelsplitter
Venustaconcha ellipsiformis, ellipse

The mussels from Site 1 and 2 were relocated to the end of Site 2. All dead shells were removed from Sites 1, 2, and 3 during the survey and saved as voucher specimens. Drought conditions in late 2005 and early 2006 resulted in the loss of the mussel populations throughout Brewster Creek so that a later mussel survey was postponed.

APPENDIX C

SEDIMENT VOLUME SUMMARIES

Full or partial surveys were performed in the study area seven times during the study (Figure 3.1, and Tables C.1 through C.7) as noted in *Methods of Investigation* (Chapter 3) of the dissertation. Five of these surveys were used to calculate sediment volumes as presented in the tables below. The surveys downstream of the dam in October 2002 and November 2004 were used to estimate the amount of sediment that was stored behind a structure (between the downstream station and the dam-removal site) that was kept in the stream as a control. A load of 285 tons was calculated as stored behind the structure between the two time periods and added to the sediment load at the downstream station. It was assumed that the 285 tons deposited behind the structure during the notching period and was proportionally added (weighted distribution given the loads measured at the stations) to the loads recorded by the downstream station. An attempt to purge the deposited sediment (by removing a small gate in the center of the structure) was made in May 2004 and April 2005. A small amount of sediment was released during these times and was closely monitored and recorded at the downstream station. Given that the release amount was recorded and the assumption that the structure re-impounded an equal amount of sediment that was released each time, there were no further adjustments to the station data. Even though only suspended sediment was recorded at the stations, given the survey data collected behind the structure, it can be assumed that the downstream station estimates are total sediment load.

Table C.1. Pre-dam removal (October 2002) lake cross section and reach summary.

Stationing	Representative Lake Reach (*LR*)		Lake Cross-section Area (*CA*)		Lake Reach Volume (*RV* = (*LR* x *CA*))	
	Downstream Distance (ft)	Upstream Distance (ft)	Bottom of Sediment (ft^2)	Top of Sediment (ft^2)	Bottom of Sediment (acre-ft)	Top of Sediment (acre-ft)
---	50.0	34.0	916.82	295.93	1.77	0.57
41	41.0	23.0	1125.81	266.44	1.65	0.39
87	23.0	34.5	1211.20	233.73	1.60	0.31
156	34.5	32.5	1008.09	159.89	1.55	0.25
221	32.5	39.5	941.95	155.91	1.56	0.26
300	39.5	33.0	623.13	107.45	1.04	0.18
366	33.0	43.0	890.13	147.85	1.55	0.26
452	43.0	41.0	1228.97	198.22	2.37	0.38
534	41.0	42.0	469.61	63.11	0.89	0.12
618	42.0	56.0	747.27	216.12	1.68	0.49
730	56.0	38.0	631.19	104.86	1.36	0.23
806	38.0	48.5	506.54	130.57	1.01	0.26
903	48.5	45.0	122.12	63.95	0.26	0.14

--- = not available

Total Lake Volume to Bottom of Sediment (*LVBS*) =	18.29	acre-ft
Total Lake Volume to Top of Sediment (*LVTS*) =	3.82	acre-ft
Total Sediment Volume (*SV* = *LVBS* - *LVTS*) =	14.47	acre-ft
Lake Surface Area (*LSA*) =	3.96	acres
Average Sediment Thickness (*SV/LSA*) =	3.7	ft

Table C.2. October 2002 – downstream main-channel cross section and reach summary.

Stationing	Total Main-channel Area (ft^2)	Representative Main-channel Reach		
		Downstream Distance (ft)	Upstream Distance (ft)	Volume (acre-ft)
-359	92.61	26.0	45.5	0.15
-268	118.52	45.5	26.0	0.19
-216	169.48	26.0	39.5	0.25
-137	63.28	39.5	45.0	0.12
-47	120.16	45.0	47.0	0.25
		Total Main-channel Reach Volume =		0.98

Table C.3. September 15, 2003 – main-channel cross section and reach summary.

Stationing	Total Main-channel Area (ft^2)	Representative Main-channel Reach		
		Downstream Distance (ft)	Upstream Distance (ft)	Volume (acre-ft)
25	14	25.0	25.0	0.02
75	23	25.0	20.0	0.02
115	18	20.0	47.5	0.03
210	16	47.5	12.5	0.02
235	6	12.5	0.0	0.00
		Total Main-channel Reach Volume =		0.090

Channel Formation Sediment Volume (Stationing 25-235) =	0.090	acre-ft
Channel Formation Sediment Volume (Stationing 25-235) =	3,937	ft^3
Channel Formation Sediment Tonnage (Stationing 25-235)[1] =	69	tons

[1]Assuming a dry specific weight of 35 lbs/ft^3

Table C.4. April 4, 2004 – main-channel cross section and reach summary.

Stationing	Total Main-channel Area (ft^2)	Representative Main-channel Reach		
		Downstream Distance (ft)	Upstream Distance (ft)	Volume (acre-ft)
29	76	29.0	45.5	0.13
120	79	45.5	49.0	0.17
218	83	49.0	51.5	0.19
321	67	51.5	46.5	0.15
414	42	46.5	19.0	0.06
452	77	19.0	17.5	0.06
487	---	---	---	---
		Total Main-channel Reach Volume =		0.771

--- = not available

Channel Formation Sediment Volume (Stationing 29-452) =	0.771	acre-ft
Channel Formation Sediment Volume (Stationing 29-452) =	33,590	ft^3
Channel Formation Sediment Tonnage (Stationing 29-452)[1] =	588	tons

[1]Assuming a dry specific weight of 35 lbs/ft^3

Table C.5. November 2, 2004 – upstream main-channel cross section and reach summary.

Stationing	Total Main-channel Area (ft^2)	Representative Main-channel Reach		
		Downstream Distance (ft)	Upstream Distance (ft)	Volume (acre-ft)
40	91	40.0	67.0	0.22
174	132	67.0	27.0	0.28
228	110	27.0	57.5	0.21
343	92	57.5	43.5	0.21
430	73	43.5	19.0	0.10
468	115	19.0	20.0	0.10
508	112	20.0	43.5	0.16
595	88	43.5	53.0	0.20
701	100	53.0	9.0	0.14
719	72	9.0	41.5	0.08
		Total Main-channel Reach Volume =		1.726

Channel Formation Sediment Volume (Stationing 40-719) =	1.726	acre-ft
Channel Formation Sediment Volume (Stationing 40-719) =	75,195	ft^3
Channel Formation Sediment Tonnage (Stationing 40-719)[1] =	1316	tons

[1]Assuming a dry specific weight of 35 lbs/ft^3

Table C.6. November 2, 2004 – downstream main-channel cross section and reach summary.

Stationing	Total Main-channel Area (ft^2)	Representative Main-channel Reach		
		Downstream Distance (ft)	Upstream Distance (ft)	Volume (acre-ft)
-368	74.72	17.0	44.5	0.11
-279	81.25	44.5	30.5	0.14
-218	99.24	30.5	47.5	0.18
-123	37.15	47.5	42.0	0.08
-39	56.06	42.0	39.0	0.10
Total Downstream Main-channel Reach Volume =				0.604
Total Main-channel Reach Volume (in October 2002) =				0.978

Channel Deposition Sediment Volume (Station -368 to -39) =	0.374	acre-ft
Channel Deposition Sediment Volume (Station -368 to -39) =	16,302	ft^3
Channel Deposition Sediment Tonnage (Station -368 to -39)[1] =	285	tons

[1]Assuming a dry specific weight of 35 lbs/ft^3

Table C.7. October 8, 2006 – main-channel cross section and reach summary.

Stationing	Total Main-channel Area (ft^2)	Representative Main-channel Reach		
		Downstream Distance (ft)	Upstream Distance (ft)	Volume (acre-ft)
39	77	39.0	65.5	0.18
170	123	65.5	28.5	0.27
227	92	28.5	57.5	0.18
342	96	57.5	45.0	0.23
432	60	45.0	21.0	0.09
474	111	21.0	19.5	0.10
513	110	19.5	8.0	0.07
529	123	8.0	33.0	0.12
595	62	33.0	53.5	0.12
702	87	53.5	7.5	0.12
717	80	7.5	58.0	0.12
833	98	58.0	16.5	0.17
866	65	16.5	12.5	0.04
891	121	12.5	4.5	0.05
900	109	4.5	19.0	0.06
938	147	19.0	40	0.20
			Total Main-channel Reach Volume =	2.12
			Main-channel Reach Volume in 2002 (Station 833-938) =	0.20

Channel Formation Sediment Volume (Stationing 39-938) =	1.920	acre-ft
Channel Formation Sediment Volume (Stationing 39-938) =	83,559	ft^3
Channel Formation Sediment Tonnage (Stationing 39-938)[1] =	1,462	tons

[1]Assuming a dry specific weight of 35 lbs/ft^3

APPENDIX D

KNICKPOINT SHEAR CALCULATIONS

Table D.1. Knickpoint shear calculations.

Streamflow Parameter	River Station									
	225	216	487	478	802	793	829	820	900	891
	09/15/2003		04/04/2004		11/02/2004		03/31/2005		10/08/2006	
5 CFS – Energy Grade Elevation (ft)	719.35	718.41	719.29	718.07	719.04	717.94	717.33	716.74	718.61	717.71
5 CFS – Channel Hydraulic Depth (ft)	0.12		0.14		0.17		0.25		0.2	
5 CFS – Energy Grade Slope (ft/ft)	0.1044		0.1356		0.1222		0.0656		0.1000	
5 CFS – Shear Stress (Pa)	37.4		56.7		62.1		49.0		59.8	
13 CFS – Energy Grade Elevation (ft)	719.49	718.72	719.41	718.34	719.23	718.31	717.61	717.15	718.85	718.13
13 CFS – Channel Hydraulic Depth (ft)	0.18		0.17		0.24		0.31		0.29	
13 CFS – Energy Grade Slope (ft/ft)	0.0856		0.1189		0.1022		0.0511		0.0800	
13 CFS – Shear Stress (Pa)	46.0		60.4		73.3		47.3		69.3	
50 CFS – Energy Grade Elevation (ft)	719.80	719.21	719.63	717.87	719.65	718.94	718.25	718.03	719.4	718.97
50 CFS – Channel Hydraulic Depth (ft)	0.31		0.33		0.46		0.63		0.52	
50 CFS – Energy Grade Slope (ft/ft)	0.0656		0.1956		0.0789		0.0244		0.0478	
50 CFS – Shear Stress (Pa)	60.7		192.8		108.4		46.0		74.2	
100 CFS – Energy Grade Elevation (ft)	720.18	720.15	719.8	718.59	720	719.43	718.97	718.62	719.81	719.69
100 CFS – Channel Hydraulic Depth (ft)	0.42		0.42		0.72		0.83		0.69	
100 CFS – Energy Grade Slope (ft/ft)	0.0033		0.1344		0.0633		0.0389		0.0133	
100 CFS – Shear Stress (Pa)	4.2		168.7		136.2		96.4		27.5	
Q1.5 – Energy Grade Elevation (ft)	720.28	720.26	719.88	719.06	720.16	719.7	719.43	719	720.07	720
Q1.5 – Channel Hydraulic Depth (ft)	0.48		0.5		0.94		0.99		0.89	
Q1.5 – Energy Grade Slope (ft/ft)	0.0022		0.0911		0.0511		0.0478		0.0078	
Q1.5 – Shear Stress (Pa)	3.2		136.1		143.5		141.3		20.7	
Q10 – Energy Grade Elevation (ft)	720.87	720.85	720.68	720.66	720.88	720.83	720.85	720.82	721.05	721.04
Q10 – Channel Hydraulic Depth (ft)	1.03		1.36		1.53		3.22		1.95	
Q10 – Energy Grade Slope (ft/ft)	0.0022		0.0022		0.0056		0.0033		0.0011	
Q10 – Shear Stress (Pa)	6.8		9.0		25.4		32.1		6.5	
Q100 – Energy Grade Elevation (ft)	721.40	721.37	721.46	721.44	721.74	721.72	721.68	721.67	721.79	721.78
Q100 – Channel Hydraulic Depth (ft)	1.47		2.11		2.41		4.08		2.67	
Q100 – Energy Grade Slope (ft/ft)	0.0033		0.0022		0.0022		0.0011		0.0011	
Q100 – Shear Stress (Pa)	14.6		14.0		16.0		13.5		8.9	

APPENDIX E

COHESIVE EROSION TESTING PARTICLE SIZE

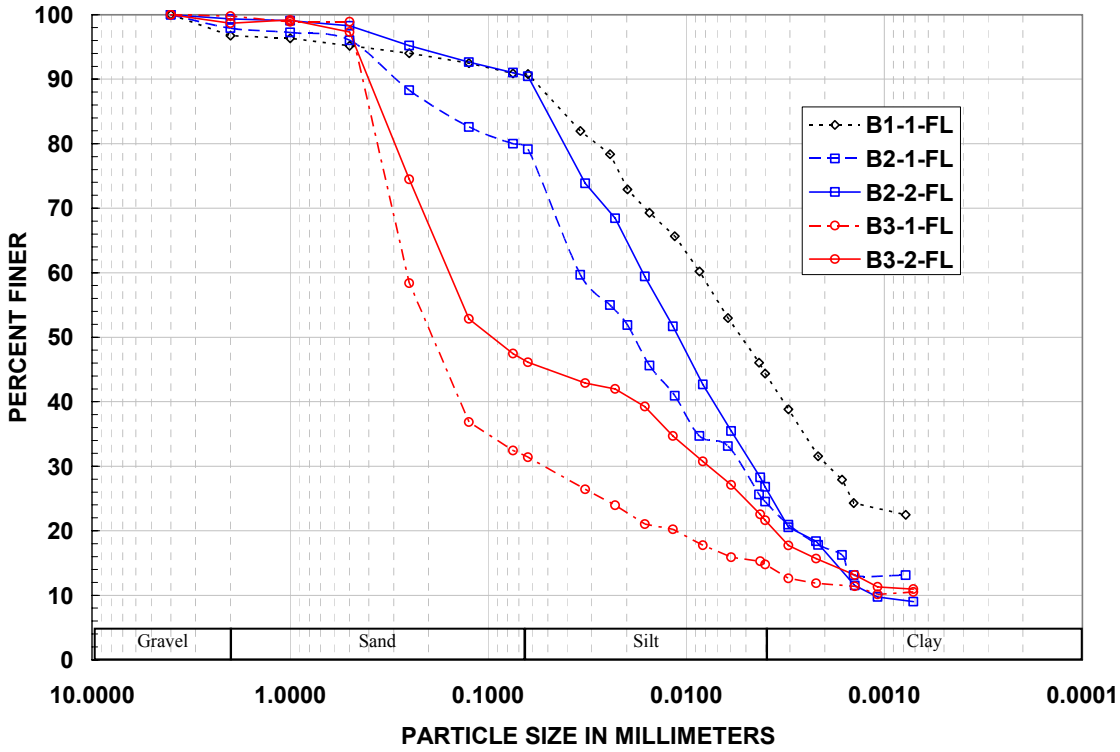

Figure E.1. Particle-size distribution for samples used in the flume.

Table E.1. Particle-size distribution for samples used in the flume.

Particle Size (mm)	B1-1-FL	B2-1-FL
	Percent Finer	
4.0	100	100
2.0	96.74	97.89
1.0	96.33	97.23
0.500	95.19	96.01
0.250	94.03	88.30
0.125	92.48	82.60
0.075	90.88	80.01
0.063	90.80	79.15
0.034	81.98	59.68
0.024	78.35	54.99
0.020	72.91	51.87
0.015	69.28	45.62
0.011	65.66	40.93
0.0086	60.21	34.68
0.0062	52.96	33.12
0.0043	46.07	25.62
0.0040	44.37	24.53
0.0031	38.81	20.93
0.0022	31.56	17.81
0.0016	27.93	16.25
0.0014	24.30	13.12
0.00078	22.49	13.12

Particle Size (mm)	B2-2-FL	B3-1-FL	B3-2-FL
	Percent Finer		
4.0	100	100	100
2.0	99.34	99.79	98.70
1.0	99.07	98.91	99.19
0.500	98.27	98.90	97.32
0.250	95.22	58.40	74.49
0.125	92.64	36.85	52.84
0.075	91.02	32.44	47.47
0.063	90.44	31.41	46.10
0.032	73.85	26.42	42.90
0.023	68.44	23.94	41.98
0.016	59.44	21.04	39.25
0.012	51.69	20.23	34.68
0.0083	42.69	17.76	30.76
0.0059	35.48	15.90	27.11
0.0042	28.28	15.28	22.54
0.0040	26.80	14.77	21.62
0.0031	20.53	12.62	17.71
0.0022	18.37	11.88	15.70
0.0014	11.53	11.38	13.14
0.0011	9.73	10.15	11.32
0.00071	9.01	10.52	10.95

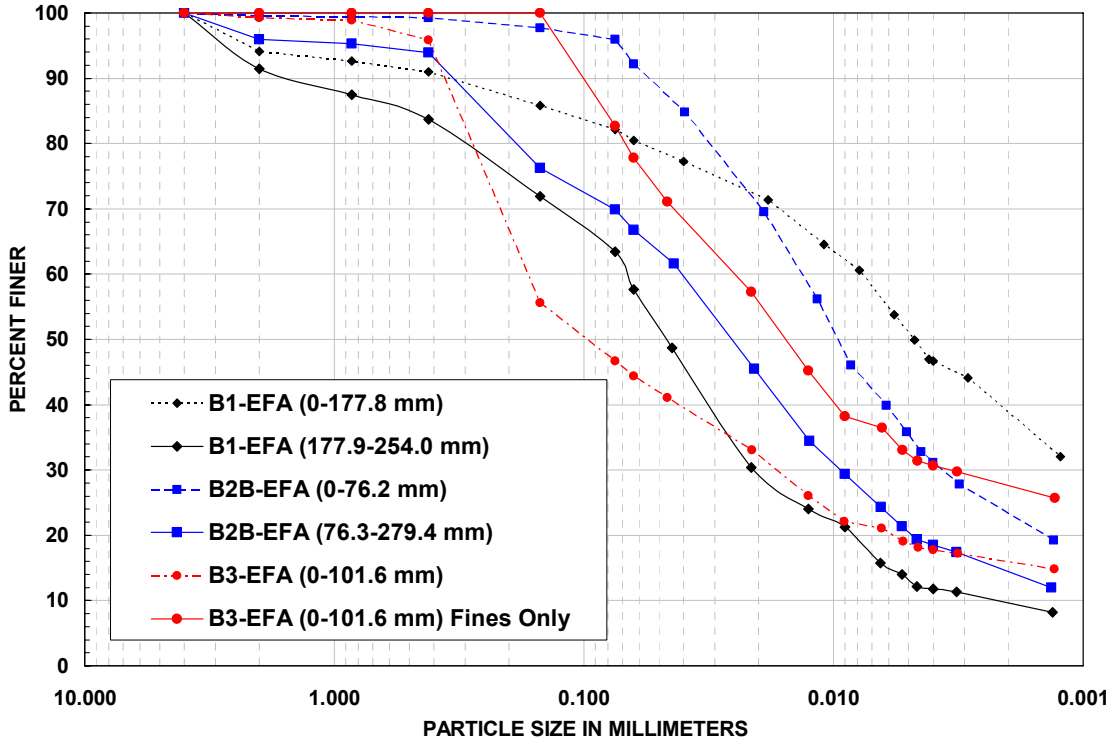

Figure E.2. Particle-size distribution for samples used in the EFA.

Table E.2. Particle-size distribution and summary characteristics for samples used in the EFA.

B1-EFA (0 - 177.8 mm)		B1-EFA (177.9 - 254.0 mm)		B2B-EFA (0 - 76.2 mm)		B2B-EFA (76.3 - 279.4 mm)		B3-EFA (0 - 101.6 mm)		B3-EFA Fines Only (0 - 101.6 mm)	
Particle Size (mm)	Percent Finer	Particle Size (mm)	Percent Finer	Particle Size (mm)	Percent Finer	Particle Size (mm)	Percent Finer	Particle Size (mm)	Percent Finer	Particle Size (mm)	Percent Finer
4.0	100	4.0	100	4.0	100	4.0	100	4.0	100	4.0	100
2.0	94.14	2.0	91.42	2.0	99.53	2.0	95.95	2.0	99.28	2.0	100
0.85	92.62	0.85	87.50	0.85	99.45	0.85	95.31	0.85	98.86	0.85	100
0.42	91.02	0.42	83.74	0.42	99.23	0.42	93.91	0.42	95.90	0.42	100
0.15	85.85	0.15	71.92	0.15	97.66	0.15	76.20	0.15	55.62	0.15	100
0.075	82.13	0.075	63.41	0.075	95.91	0.075	69.93	0.075	46.72	0.075	82.68
0.063	80.48	0.063	57.64	0.063	92.15	0.063	66.73	0.063	44.35	0.063	77.82
0.040	77.28	0.044	48.72	0.040	84.81	0.044	61.59	0.046	41.04	0.046	71.06
0.018	71.40	0.021	30.42	0.019	69.54	0.021	45.51	0.021	33.09	0.021	57.29
0.011	64.52	0.013	24.00	0.012	56.20	0.012	34.42	0.013	26.09	0.013	45.17
0.0079	60.59	0.0090	21.23	0.0085	46.00	0.0090	29.35	0.0090	22.05	0.0090	38.18
0.0057	53.78	0.0065	15.76	0.0062	39.89	0.0065	24.34	0.0064	21.04	0.0064	36.44
0.0047	49.91	0.0053	13.95	0.0051	35.85	0.0053	21.35	0.0053	19.09	0.0053	33.05
0.0041	47.01	0.0046	12.15	0.0044	32.82	0.0046	19.37	0.0046	18.12	0.0046	31.37
0.0040	46.67	0.0040	11.76	0.0040	31.13	0.0040	18.50	0.0040	17.74	0.0040	30.68
0.0029	44.15	0.0032	11.29	0.0031	27.80	0.0032	17.42	0.0032	17.19	0.0032	29.76
0.0012	32.08	0.0013	8.19	0.0013	19.27	0.0013	12.01	0.0013	14.81	0.0013	25.65

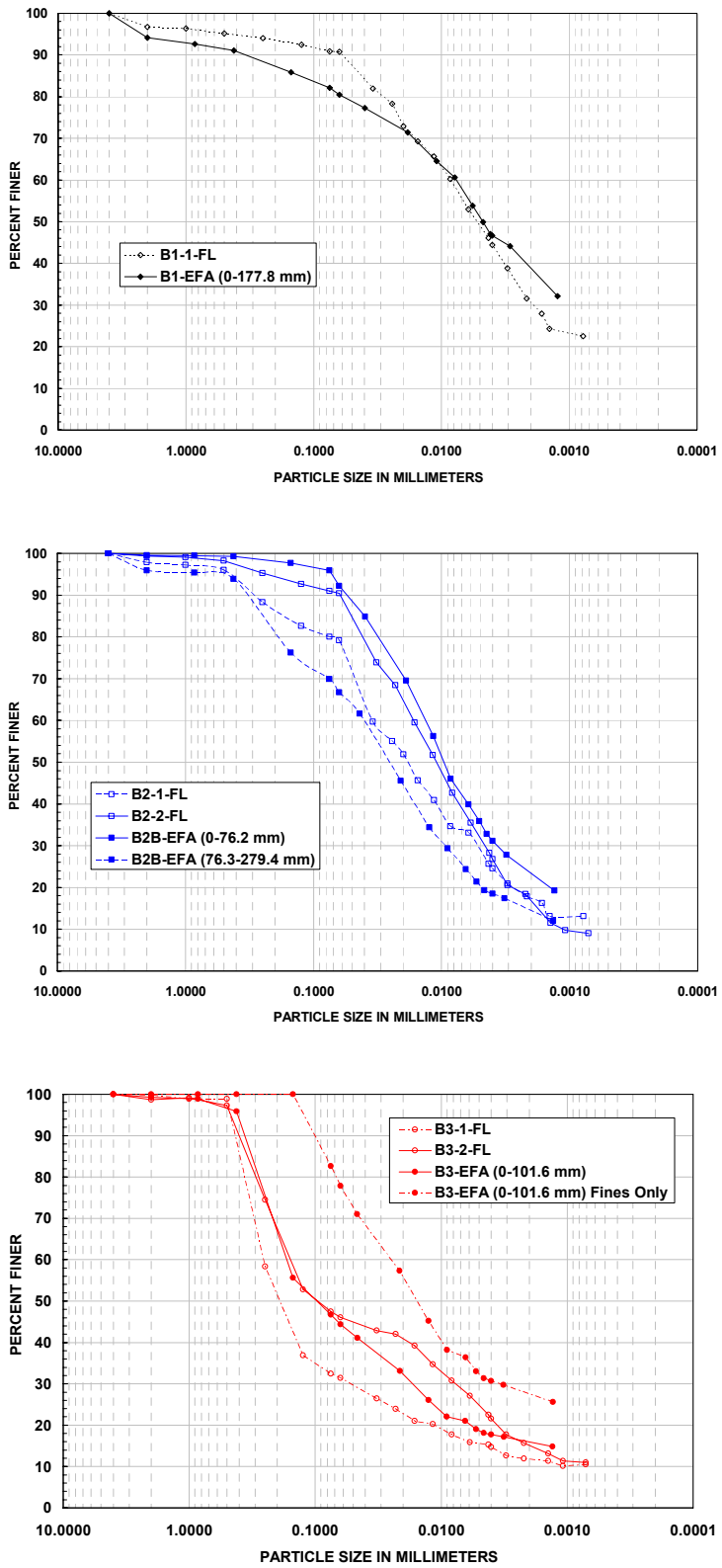

Figure E.3. Particle-size distribution for samples used in the EFA and flume.

APPENDIX F

ATTERBERG LIMITS

Atterberg limits commonly are used to classify soils and provide information on the behavior of fine-grained soils including liquid limit (LL), plastic limit (PL), and plasticity index (PI) as defined in Terzaghi *et al*. (1996). The LL is the moisture content at which the soil loses its consistency and behaves like a viscous fluid. The PL is the moisture content at which the soil may plastically deform without crumbling. The PI is a measure of how much water a soil can absorb before behaving as a fluid. The PI is obtained by subtracting the PL from the LL; thus, the PI defines the range of moisture contents where the soil exhibits plastic behavior. The PI and the LL often are correlated to cohesive strength. The soil is more compressible and has a lower saturated strength at higher values of the PI. Soil plasticity is a function of clay content and mineralogy. Higher PIs and LLs result from higher clay contents. Silt and clay soils with high PIs typically have greater proportions of clay minerals with thin, platy-shaped particles. The nomenclature for soil groups as established in the Unified Soil Classification (USC) (Casagrande, 1948) is explained in Table F.1.

Table F.1. Soil group symbols and typical names for cohesive soils as established in the USC (Casagrande, 1948) for soils found in the St. Louis Metro East region in Illinois.

Soil Class Symbol	Definition
ML	Inorganic silt and very fine sand, silty or clayey fine sand, or clayey silt with low plasticity
CL	Inorganic clay of low to medium plasticity, gravelly clay, sandy clay, silty clay, lean clay
OL	Organic silt and organic silty clay of low plasticity
MH	Inorganic silt, micaceous, or diatomaceous fine sandy
CH	Inorganic clay of high plasticity, fat clay
OH	Organic clay of medium to high plasticity

APPENDIX G

EROSION FUNCTION APPARATUS AND FLUME RESULTS

Table G.1. EFA summary: Sample B1-EFA (0 - 177.8 mm).

Mass Density (ρ)	1000	kg/m^3
Kinematic Viscosity (ν)	0.000001	m^2/s
Flume Height (a)	0.0508	m
Flume Width (b)	0.1016	m
Flume Area (A)	0.0052	m
Flume Perimeter (P)	0.3048	m
Hydraulic Diameter (D)	0.0677	m

Mean Particle Size (D_{50})	0.0048	mm
Surface Roughness (ε)	0.0000024	m
Relative Roughness (ε/D)	0.0000354	

Velocity v (m/s)	Reynold's Number Re	Friction Factor f	Shear Stress τ (N/m^2)	Specific Stream Power τv (W/m^2)	Erosion Rate (mm/hr)	
					Tube 1	Tube 2
1	67,733	0.019	2.4	2.4	0.5	
1.5	101,600	0.018	5.1	7.6	0.5	
2	135,467	0.017	8.5	17.0	0.5	0.5
3	203,200	0.016	18.0	54.0	7.4	10.3
4	270,933	0.015	30.0	120.0		11.0
5	338,667	0.014	43.8	218.8		25.0

Table G.2. EFA summary: Sample B2B-EFA (0 - 76.2 and 76.3 - 279.4 mm).

Mass Density (ρ)	1000	kg/m^3
Kinematic Viscosity (ν)	0.000001	m^2/s
Flume Height (a)	0.0508	m
Flume Width (b)	0.1016	m
Flume Area (A)	0.0052	m
Flume Perimeter (P)	0.3048	m
Hydraulic Diameter (D)	0.0677	m

Mean Particle Size (D_{50})	0.0097	mm
Surface Roughness (ε)	0.0000049	m
Relative Roughness (ε/D)	0.0000716	

Velocity v (m/s)	Reynold's Number Re	Friction Factor f	Shear Stress τ (N/m^2)	Specific Stream Power τv (W/m^2)	Erosion Rate (mm/hr)		
					Tube 1 (0 - 76.2)	Tube 1 (76.3 - 279.4)	Tube 2 (0 - 76.2)
0.6	40,640	0.022	1.0	0.6	0.5	1	
1	67,733	0.020	2.5	2.5	0.5	1	
1.5	101,600	0.019	5.3	8.0	0.5	36	
2	135,467	0.018	9.0	18.0	1	79	
2.5	169,333	0.017	13.3	33.2	1.5	290	1.5
3	203,200	0.016	18.0	54.0			5.8

Table G.3. EFA summary: Sample B3-EFA (0 - 101.6 mm).

Mass Density (ρ)	1000	kg/m^3
Kinematic Viscosity (ν)	0.000001	m^2/s
Flume Height (a)	0.0508	m
Flume Width (b)	0.1016	m
Flume Area (A)	0.0052	m
Flume Perimeter (P)	0.3048	m
Hydraulic Diameter (D)	0.0677	m

Mean Particle Size (D_{50})	0.016	mm
Surface Roughness (ε)	0.0000081	m
Relative Roughness (ε/D)	0.0001196	

Velocity v (m/s)	Reynold's Number Re	Friction Factor f	Shear Stress τ (N/m^2)	Specific Stream Power τv (W/m^2)	Erosion Rate (mm/hr)	
					Tube 1	Tube 2
1	67,733	0.021	2.6	2.6	0.5	
1.5	101,600	0.020	5.6	8.4	0.5	
2	135,467	0.019	9.5	19.0	0.5	
2.5	169,333	0.018	14.1	35.2	1	
3	203,200	0.017	19.1	57.4		1
3.5	237,067	0.016	24.5	85.8		2
4	270,933	0.016	32.0	128.0		3
4.5	304,800	0.015	38.0	170.9		5

Table G.4. Flume testing results.

Sample	Flow (m^3/s)	Flow Depth: Average (m)	Flow Depth: At Velocity Reading (m)	Hydraulic Radius (m)	Reynolds Number	Average Velocity (m/s)	Bed Slope	Energy Slope	Unit Stream Power (m/s)	Shear Stress (Pa)	Specific Stream Power (W/m^2)	Average Bed Erosion (mm/hr)
B1-1-FL	0.0111	0.23	0.222	0.073	60,102	0.23	0.010	0.009	0.002	19.82	4.64	0.63
	0.0234	0.20	0.187	0.069	142,981	0.59	0.010	0.004	0.002	7.10	4.17	0.77
	0.0410	0.22	0.217	0.072	225,834	0.89	0.010	0.009	0.008	18.98	16.89	3.53
	0.0387	0.21	0.213	0.071	213,260	0.85	0.016	0.017	0.015	35.32	30.14	1.91
B2-1-FL	0.0098	0.13	0.139	0.059	68,730	0.33	0.010	0.003	0.001	3.98	1.32	0.33
	0.0206	0.14	0.143	0.060	144,166	0.68	0.010	0.008	0.006	11.50	7.82	2.35
	0.0313	0.17	0.167	0.065	204,245	0.88	0.010	0.002	0.002	3.87	3.42	1.26
	0.0228	0.17	0.158	0.065	154,910	0.68	0.018	0.018	0.012	28.94	19.58	3.12
	0.0214	0.15	0.164	0.063	135,849	0.61	0.025	0.025	0.015	37.81	23.16	1.46
B2-2-FL	0.0097	0.14	0.140	0.061	70,133	0.32	0.010	0.004	0.001	5.64	1.83	0.18
	0.0175	0.16	0.157	0.064	118,621	0.52	0.010	0.003	0.002	4.78	2.50	1.71
	0.0300	0.16	0.158	0.064	202,727	0.89	0.010	0.007	0.007	11.87	10.58	1.43
	0.0236	0.14	0.138	0.060	169,312	0.80	0.018	0.018	0.015	24.22	19.49	4.39
	0.0183	0.11	0.112	0.055	148,561	0.77	0.025	0.026	0.020	28.60	21.88	3.72
B3-1-FL	0.0097	0.20	0.197	0.069	56,750	0.23	0.010	0.009	0.002	18.19	4.22	1.35
	0.0171	0.11	0.109	0.055	142,553	0.74	0.010	0.007	0.005	8.10	5.98	3.74
	0.0286	0.16	0.150	0.064	203,569	0.90	0.010	0.007	0.006	10.82	9.73	2.75
	0.0313	0.14	0.127	0.061	249,284	1.16	0.014	0.013	0.015	17.75	20.61	5.60
	0.0220	0.14	0.116	0.060	186,700	0.89	0.020	0.020	0.018	27.12	24.06	4.98
B3-2-FL	0.0101	0.17	0.152	0.066	72,519	0.31	0.010	0.003	0.001	5.53	1.72	1.38
	0.0189	0.11	0.109	0.055	157,303	0.81	0.010	0.022	0.018	23.80	19.37	1.22
	0.0301	0.19	0.179	0.068	189,902	0.79	0.010	0.008	0.006	14.96	11.81	1.39
	0.0264	0.13	0.119	0.059	215,348	1.04	0.016	0.015	0.016	19.67	20.51	0.97
	0.0191	0.11	0.104	0.055	168,286	0.87	0.018	0.020	0.017	22.02	19.06	3.03
	0.0233	0.10	0.086	0.051	229,318	1.28	0.025	0.025	0.032	23.89	30.51	1.35